Final Report to:

Prairie Adaptation Research Cooperative (PARC), Foothills Model Forest (FMF), and the Sustainable Forest Management Network (NCE-SFMN) (Second Edition: 6 September 2002)

SIMULATING CLIMATIC IMPACTS ON, AND ADAPTIVE MANAGEMENT OPTIONS FOR, BOREAL FOREST ECOSYSTEMS IN WESTERN CANADA

David T. Price[1], Ron Hall[1], Frédéric Raulier[2] Marcus Lindner[3], Brad Case[1], Pierre Bernier[2]

With contributions from

Mike Gartrell[1], Eric Arsenault[1], Marty Siltanen[1] and Jacques Régnière[2],

Collaborators
Mark Johnston[4], Ross Wein[5], Hugh Lougheed[6], Jim Stewart[1], Jing M. Chen[7], Elaine Wheaton[4], Brian Christensen[8]

[1] Canadian Forest Service (CFS), Northern Forestry Centre, 5320–122 Street, Edmonton, AB T6H 3S5. Tel: (780) 435-7249; Fax: (780) 435-7359; E-mail: dprice@nrcan.gc.ca
[2] Canadian Forest Service (CFS), Laurentian Forestry Centre, 1055 rue du PEPS., Ste-Foy, QC
[3] Potsdam Institute for Climate Impact Research (PIK), Telegrafenberg, P.O. Box 601203, D-14412 Potsdam, Germany
[4] Environment Division, Saskatchewan Research Council, 15 Innovation Blvd., Saskatoon, SK
[5] Department of Renewable Resources, University of Alberta, Edmonton, AB
[6] Weldwood of Canada Ltd. Hinton Division, Switzer Drive, Hinton, AB.
[7] Department of Geography, University of Toronto, Toronto. [Formerly of Canada Centre for Remote Sensing, 588 Booth Street, 4th Floor, Ottawa, ON]
[8] Weyerhaeuser Saskatchewan Ltd., Timberlands, P.O. Box 1720, Prince Albert, SK

Start date: 1 September 2000
Completion date: 31 August 2002
Last revised: 9 September 2002

Table of Contents

Table of Figures

Table of Tables

1 Executive Summary

1.1 Process models of forest productivity: the need and the challenge

Given that some impacts of climate warming are being observed across Canada (the current drought in Alberta and Saskatchewan being only one example), and that climate model projections indicate larger, systematic changes occurring within the next 50-100 years, sustainable management of Canada's forest resources will need to take the effects of such changes into account. The most immediately observable impacts are likely to be changes in species productivity, competition and survival. Estimating these impacts will be critical for the development of adaptation and mitigation strategies.

This project attempts to assess these potential impacts on western boreal forest ecosystems using a suite of process models applied to detailed spatial data sets. In principle, the models must first be calibrated and tested by running them with data representative of current climate conditions for the study area. Only when this has been achieved with acceptable results should the effects of possible future climates be investigated using scenario data (ideally derived from global climate model simulations).

Current models of stand productivity generally employ traditional growth and yield (G&Y) modeling based on plot-level measurements of tree growth. Because local climate is a major determinant of environmental conditions at all forest sites, yield forecasts based on such models are likely to be inaccurate if appreciable changes in climate do occur. In the worst cases, the predictions of future yield could be completely incorrect. An alternative approach is to develop *process-based* growth models that use physiological and physical principles to relate stand growth to climate. The Canadian Forest Service's Laurentian Forestry Centre (LFC) is at the forefront in developing and testing this approach. LFC is leading a project termed **ECOLEAP** (Extended COllaboration for Linking Ecophysiology And Forest Productivity) (http://www.cfl.forestry.ca/ECOLEAP), in which forest net primary productivity (NPP) is simulated mechanistically, and then mapped at the landscape scale using spatial data.

The project reported here, and referred to as **ECOLEAP-West**, builds on this initiative for two ecologically-distinct study regions within Alberta and Saskatchewan, respectively. Process-based models to estimate NPP were driven by spatial data sets including digital elevation, soils, satellite remote sensing, and interpolated climate. These NPP estimates were then compared to site-level productivity estimates derived from field measurements at permanent sample plots in the Foothills Model Forest (FMF) study area in Alberta. The aim was to establish an acceptable level of agreement between the different estimates of NPP, and then apply the process-based models to the Saskatchewan study region. The end products should include tools to assess forest productivity under both present-day and plausible future climates, and to investigate the effects of forest management options to adapt to climate change. Preliminary results indicate that forest management can have significant effects on productivity, species composition and carbon sequestration.

1.2 Objectives

This study aimed to assess the possible impacts of a warmer climate on the productivity of representative forests in the Alberta Foothills and southern boreal regions of Saskatchewan. Hence, a key objective of our work was to further develop and test process-based models to estimate forest productivity in these regions and to compare estimates with those obtained using local G&Y data.

Climate has both direct effects on the physiological processes contributing to forest productivity (i.e., photosynthesis and the allocation of photosynthate to plant tissues) and indirect effects on the regeneration and survival of the different species that make up natural forest

vegetation. Our study focuses on these effects, although we also recognize that a warmer and drier climate is likely to increase the risks of serious losses due to fires and pest and disease outbreaks.

The work undertaken in the last two years had two distinct thrusts. The first was the construction of a coherent set of spatial data sets that could be used to apply a range of models of forest responses to climate *at a scale large enough to be useful for operational management*, yet small enough to be manageable with present-day technology and resources. The second thrust was to use these data layers to simulate forest productivity and successional dynamics for the regions using appropriate models. Hence, archived sets of detailed data are extremely valuable for spatial modelling. The methods used to develop the data layers needed to be properly validated and documented, so that they could be made generally available to other researchers, particularly those wishing to apply other models to the same study regions. Models are never finished, and much of the work in applying them requires further development, refinements to their parameterization using local data, and repeated testing.

1.3 Spatial data products

Data sets are substantially completed for the 2700 km^2 Alberta study region, located in the centre of the Weldwood FMA. Progress has been slower for the Saskatchewan study region, mainly because of difficulties in obtaining local PGS plot and inventory data sets. During the study, many sources of data were utilized, including Foothills Model Forest archives, Weldwood Canada proprietary data sets, and databases owned or procured by the Government of Alberta and the Canadian Forest Service. The layers include digital elevation, soils, climatology, Landsat imagery and Alberta Vegetation Inventory (AVI) cover types and densities.

1.3.1 Biomass

Many process models attempt to simulate ecosystem productivity, which is typically reported in biomass terms. A portion of forest biomass is allocated to stemwood production, so field-based measures of merchantable volume should be related to estimates of forest biomass, although this relationship is generally non-linear. Estimates of forest biomass therefore provide an important stepping stone between empirical data and process model output.

Permanent Growth Sample (PGS) plot data obtained from Weldwood in summer 2000 were used to select a subset of sites representative of the range of conditions and forest types found in the region. These data were used in tree biomass models to estimate total above ground forest biomass for each tree. These estimates were found to be well correlated with crown closure and stand height. The tree level estimates were then aggregated to the stand level from which new functions were developed to map forest biomass for the study area. The regression models derived from the PGS plot-level relationships were then applied to crown closure and stand height attribute data for approximately 78,000 AVI polygons classified by species group—thus producing a spatial coverage of forest biomass for the entire study region.

1.3.2 Leaf Area Index

Leaf area index (LAI) is a biophysical indicator fundamental to many important processes in forest ecosystem function. Measurements were made using optical instruments at 27 PGS plot locations distributed across the Alberta study area during the summer of 2000. The data collected were related to estimates of sapwood area derived from tree core data and PGS plot DBH measurements using allometric relationships taken from the research literature. The results showed that LAI could be estimated with reasonable confidence from the PGS data, although the small number of plot locations, probable measurement errors and inherent spatial variability, combined to produce relatively high variances. Plot-level estimates of LAI were then correlated to spectral response data obtained from Landsat-TM imagery, and used to create maps of the distributions of estimated LAI for the entire study region.

Several possibilities emerged for improving LAI estimates, including increasing the number of sampling sites and developing species-specific relationships using local allometric analysis in relatively pure stands, particularly of lodgepole pine. Additional interest in this work has come from the FMF grizzly bear research team, who are attempting to characterize bear habitat based on leaf area measurements. This has led to work being carried out at additional sites in and around the study region. It is anticipated that data resulting from this work will be used to further improve the LAI database and models developed during this study.

1.3.3 f_{PAR}

Related to LAI, f_{PAR} (fraction of incoming photosynthetically active radiation (PAR) absorbed by the vegetation canopy) is a critical input to so-called "Radiation Use Efficiency" models, including the StandLEAP model developed at LFC (see Sections 1.4.1 and 6.1). A map of f_{PAR} for the study region was derived from a Landsat5 satellite image. After image correction, the Landsat data (bands 3 and 4) were used to calculate the "simple ratio" (SR) for 3×3 pixel areas of each AVI stand polygon. These SR values were in turn related to the dominant species identified from the AVI coverage to allow f_{PAR} to be estimated for individual stand polygons.

1.3.4 Soils

Soil texture information (primarily for the upper horizons) is essential to estimate the soil moisture regime for many ecosystem process models. Unfortunately, high quality soils data for extensive regions are notoriously difficult to obtain. In common with many forested regions of Canada, the only generally available information is the modal soil profile texture data for the local Canadian Soil Information System (CanSIS) polygons. This problem was not adequately resolved in the present study, but significant effort was devoted to building a database of soil profile information from several sources, which we anticipate will be useful for a further modelling and mapping exercise to relate soil physical characteristics to topography (elevation, slope gradient, aspect, and slope curvature), basal geology and local climate.

1.3.5 Climate scenario data

J. Régnière at CFS-LFC developed some new routines for his model, BioSIM, to enable it to generate realistic temperature and precipitation regimes for multiple locations across the ECOLEAP study regions. Data produced by this model were used to drive model simulations of forest productivity and succession (Sections 1.4.1 and 6).

1.3.6 Lodgepole pine physiology

J. Stewart and coworkers from CFS-NoFC provided data for parameterizing lodgepole pine growth processes derived from an ongoing study being carried out at a measurement site in the Alberta study area. Additional work was carried out in 2001/2002 to supplement the data set with measurements of photosynthesis sensitivity to temperature and humidity, and additional basal area/sapwood area measurements. These data were then used both to improve the representation of lodgepole pine physiology by the LFC group and the sapwood/leaf area relationships (used in leaf area mapping) for the Foothills study region.

1.4 Spatial modelling

Most of our effort to date has been invested in two models: FORSKA-M and StandLEAP. Work with a relatively new model, 4C, is continuing in collaboration with researchers at the Potsdam Institute for Climate Impacts Research (PIK) in Berlin. Considerable progress has been made in testing both StandLEAP and FORSKA-M and applying them to the Alberta study area.

1.4.1 StandLEAP

StandLEAP is a model of forest productivity based on Landsberg's 3PG, but extensively modified by Raulier and Bernier of CFS Laurentian Forestry Centre (LFC) to simulate NPP in Canadian forests. The model is driven primarily by leaf area index (LAI) and incoming radiation data (actually f_{PAR}), as well as by other climate factors influenced by topography data. StandLEAP was calibrated for lodgepole pine using data obtained from the literature and in some cases, from the BOREAS experiment carried out in southern Saskatchewan. Calibrations for other major species in the area: black spruce, aspen and white spruce, were derived from the literature and data obtained from the BOREAS experiment and from other study sites in eastern Canada.

In general, when tested at the plot scale, StandLEAP tended to overestimate aboveground biomass increment by around 10%, but it still predicted acceptable values of final biomass when the increments were added to the initial plot biomass. Some problems were encountered with the estimation of stand mortality in lodgepole pine, and suggest that the mortality module needs further improvement.

1.4.1.2 Final Product – Maps of NPP

Using the data sets described above, the LFC group performed a simulation of net primary productivity (NPP = photosynthesis – respiration) for approximately 1,000 AVI polygons distributed across the Alberta study area, using the two "modes" available for the model. These representative NPP subsamples were averaged for each of 36 strata, created as a combination of four soil types and 12 forest cover types. Mean values for each stratum were then applied across the study area. This allowed creation of a first approximation for the spatial distribution of productivity derived directly from physically-based inputs (climate, soil conditions, topography) and remote sensing data (estimates of leaf area and species composition). The NPP values estimated in both modes were in the expected range, although an independent validation would be desirable.

At first glance, agreement between the preliminary NPP map product and assessments of productivity based on observations, including the mean annual increment (MAI) of biomass computed from the biomass map reported in Section 1.3.1, seemed relatively poor. The general trend in productivity simulated by StandLEAP ran counter to local observations. On average, many stands appear to support higher stand densities for a given aboveground biomass than the StandLEAP model predicts, pointing to a potential problem with the biomass – stand density relationships used to derive the basic input data.

However, closer examination revealed that although there are some major contradictions at the extreme west and east of the study region, there is substantial agreement between the model and observations for much of the remaining area. The reasons for the contradictions can be traced to two likely sources: (1) NPP does not correlate well to MAI of either merchantable volume or total biomass, and (2) some of the process representation is limited by available spatial data, with soil drainage and nutrition probably being the most poorly resolved. Nevertheless, we believe that this map shows the potential of the approach to predict productivity at the regional scale from physical data and biological principles, and therefore to incorporate the impact of climte change on growth. The work also highlights the problems encountered in scaling up knowledge obtained at the plot scale over short time steps to regions using a coarser time resolution.

1.4.2 FORSKA-M

FORSKA-M is a model derived from the original FORSKA2 of Prentice and coworkers, that simulates competition between boreal species for water and light, and allows effects of climate and forest management on composition and productivity to be investigated. Weldwood PGS plot data were carefully surveyed and a set of 45 sites representative of the range of combinations of ecosystems and soil types selected. Eight of these sites were used to calibrate the

individual species parameters for the model. The remaining 37 sites were then used to test its performance. FORSKA-M was able to replicate both the species composition and height-over-diameter relationships observed at most of the test PSP sites satisfactorily, although aspen growth rates were generally overestimated.

The model was then used to investigate the effects of different disturbance rates, and of changes in climate, at all 45 sites. Mean disturbance intervals (50, 100, 150 and 200 years) were based on those considered typical for the Canadian boreal. The three climate scenarios were representative of the typical range of predictions derived from GCM simulations. In addition, the effect of initializing the simulations with bare patches instead of with PGS plot measurement data was investigated.

1.4.2.1 Effects of climate change and disturbances

In general, FORSKA-M was successful in predicting the occurrence of the dominant species, but it was much more successful when the stand structure and composition was initialized using data observed at PGS plots. When runs were initialized with bare patches, however, the model was generally unable to predict the relative abundances of the less common species (i.e., those other than lodgepole pine). This raises important questions about the model assumptions and/or the parameters used to define species differences. A particular question is whether the spatial distribution of species composition in the study area is due to differences in site characteristics that are not captured by the model (or not present in the soils data). Alternatively, is the poor representation of the real forest distribution due to the assumption in the model that seeds of all species are present at all sites? The latter is a common criticism of gap models and may be quite inappropriate for boreal ecosystems where extensive fires are a frequent occurrence in the natural landscape.

The responses of the model to simulated disturbance regimes were generally consistent with reality when initialized from PGS plot data: i.e., they predicted total biomass densities for individual species consistent with observations. The results for the simulations initialized from bare patches were again less successful: biomass densities were lower and the allocation among species was less realistic. The responses to simulated changes in climate were also contradictory. For runs initialized with bare ground, a 2 ºC increase in mean annual temperature produced slight *increases* in biomass density, relative to current climate, with the greatest increase occurring when future precipitation was assumed to be the same as the 1961-90 mean value. When the runs were initialized with PGS plot data, however, the general response compared to current climate was a small *reduction* in biomass density.

Hence, these simulations suggested that there should be only minor impacts on average biomass production, with a tendency for species composition to shift towards increased occurrence of pine and aspen and reduced abundance of spruces and firs. This interpretation should however be treated with caution: first it is based on the results from only one model, and second it presupposes that there would be no impact of climate change on the natural disturbance regime. Based on these simulations, the most sensitive forest types are spruce-dominated, which suggests that pines and aspen should be favoured in long-term management of the more sensitive sites.

1.5 Further work

Future work could be undertaken in three areas: (1) improvements to spatial data inputs to the statistical models used to estimate the spatial distributions of variables such as LAI, biomass, soil attributes, and stand density; (2) refinements to process model parameters; and (3) the use of different scenarios of future climate to simulate and assess the potential impacts on regional forest productivity. Completion of the data compilation and application of the available tested models to the Saskatchewan study area could also be undertaken.

In particular, StandLEAP was able to predict plot-level biomass increments generally within 10% of the measured increments. However, for both the plot-level and the spatial estimates, this exercise enabled us to identify several gaps in data coverage and the simulation processes. On the simulation side, locally-derived mortality curves are likely needed. We also feel that recurrent, low-level soil droughts may play a major role in regulating self-thinning. Given the predictions of decreased precipitation in the boreal plains ecozone as a result of increased atmospheric CO_2 concentrations, we think that further work should be carried out to better capture this process. At the same time, local soil conditions in general, and profile drainage in particular, influence forest growth in a non-linear but predictable fashion. Better spatial representation of these properties, and proper representation of these processes in the models are therefore likely improve the simulations.

2 Introduction

Current projections of future climate based on general circulation model (GCM) simulations indicate that significant climate warming will occur within the next 50-100 years in the Canadian Prairie Provinces. Increases in mean temperatures, even assuming no changes in inter-annual variability, are likely to cause serious impacts on forest growth, composition and productivity (both negative and positive). A further potential complication is the expectation that inter-annual variability and the occurrence of extreme weather and climatic events may also change, in ways that are as yet impossible to assess. The drought and related incidence of large forest fires in Alberta and Saskatchewan in 2002 are perhaps warnings of the potential for future "surprises". The pine beetle epidemic in northern B.C. also illustrates the consequences of what might at first have seemed to be a relatively benign winter warming. Increased droughts and milder winters are common predictions derived from several GCM scenarios.

The models of stand development and volume productivity, as typically used in present-day yield forecasting and timber supply management, are ultimately based on empirical relationships observed at forest growth sample plots (permanent or temporary). This approach has worked well in the past, because it implicitly assumes that the average climate at each growth sample plot location is unchanging. These traditional growth and yield (G&Y) models will likely fail, however, if changes in climate seriously influence future site conditions. An alternative to the traditional G&Y models is to develop process-based growth models that use physiological and physical principles to relate forest development and productivity to climate. Since 1995, the CFS Laurentian Forestry Centre (in Ste Foy, Québec) has pursued a project called ECOLEAP (Extended COllaboration for Linking Ecophysiology And Forest Productivity, http://www.cfl.forestry.ca/ECOLEAP), where forest net primary productivity[a] (NPP) is simulated mechanistically, and then mapped at the landscape scale using spatial data. A key objective of ECOLEAP is that the models should generate estimates of forest productivity that are both of direct value to forest managers (e.g., site index, merchantable volume production in $m^3\ ha^{-1}\ yr^{-1}$), and can be applied over areas of thousands of square kilometres.

ECOLEAP-West builds on this initiative for two ecologically-distinct study sites within the Foothills and Prince Albert Model Forests in Alberta and Saskatchewan, respectively. The aims were (1) to assess some of the key effects of climate on forest productivity and species composition using mechanistic models driven by detailed spatial data sets (digital elevation, soils, satellite remote sensing, as well as interpolated climatology); and (2) to compare the results to site-level field data derived from field measurements in the study regions. A further requirement was that the results be meaningful in forest industry terms: i.e., they needed to provide sufficient spatial detail to be useful for management purposes over an extensive region (such as a forest management unit in western Canada).

To achieve these aims, it was first necessary to test and refine the models, and to prepare the large-scale data sets needed to drive them. High quality coherent spatial datasets covering large regions are not generally available for forested regions, but there is a wealth of point-based data, and some GIS coverages available from many sources, including company Permanent Growth Sample (PGS) plots, Provincial forest inventories, Federal and Provincial soil mapping projects, climate station records, and ecophysiological research reported in the scientific literature. The challenge was to invest and focus the effort in extracting as much information as possible from all these available data, using remote sensing, GIS and computer modeling, both as methods of extrapolation and as tools for validating the results.

---

[a] Net Primary Productivity is the rate at which plant biomass is produced after accounting for respiratory losses, typically expressed in dry biomass or carbon terms, in units of $g\ m^{-2}\ yr^{-1}$.

This page intentionally blank.

3 Objectives

The primary objectives of this study were (1) to provide spatial data sets needed to develop and test process models of forest productivity and species succession, and (2) to use process models to assess the impacts of plausible changes in future climate on these key forest attributes. The end products would include new tools (models and data) to assess forest productivity and species composition under both present-day and anticipated future climates, and to investigate the potential for forest management to adapt to the effects of climate change (positive as well as negative).

Specific products to be delivered, as outlined in the original proposal were:

- A coherent database of available biophysical and inventory data, in ARC/INFO format, overlaid with topographic and remote sensing data sets.
- A spatially-based forest productivity model calibrated to the extent of the areas included in the study.
- One or more process-based productivity models calibrated for the same areas, and validated against the results obtained from an empirical model.
- Results from the models—in particular, estimates of productivity and accumulations of biomass and wood volume at the stand-level (i.e., treating biomass as a function of stand age), and forecasts of potential impacts of climate change on forest productivity and biomass C accumulation, applied to the study regions.
- Contribution of the results of model simulations to social scientists interested in assessing the impacts of climate change on forests and the communities they support.
- Articles suitable for publication in peer-reviewed journals.

This page intentionally blank.

4 Input datasets

Two study regions were identified and documented (see also: the website for the Earth Observation for Sustainable Development (EOSD) Forest Pilot Regions network at http://www.cfl.cfs.nrcan.gc.ca/ECOLEAP/pilotregions.html). The Alberta region covers about 2,700 km^2 within the Foothills Model Forest while the second extends over about 4,500 km^2 across central Saskatchewan (**Figure 4.1**). The Alberta region was selected for its range of topography and ecological diversity (though most of the forest lies in the Upper and Lower Foothills natural regions). Several other studies were co-located in this region, notably the National Forest Inventory pilot project and a pilot study for the Alberta Biodiversity Monitoring Program. More recently, a research project on grizzly bear habitat overlaps the Alberta study region. The Saskatchewan region was selected primarily because it includes the Prince Albert Model Forest (PAMF) and Weyerhaeuser's FMA, but also because the former BOREAS project (Sellers et al., 1997) and present-day BERMS flux-tower sites lie in this region.

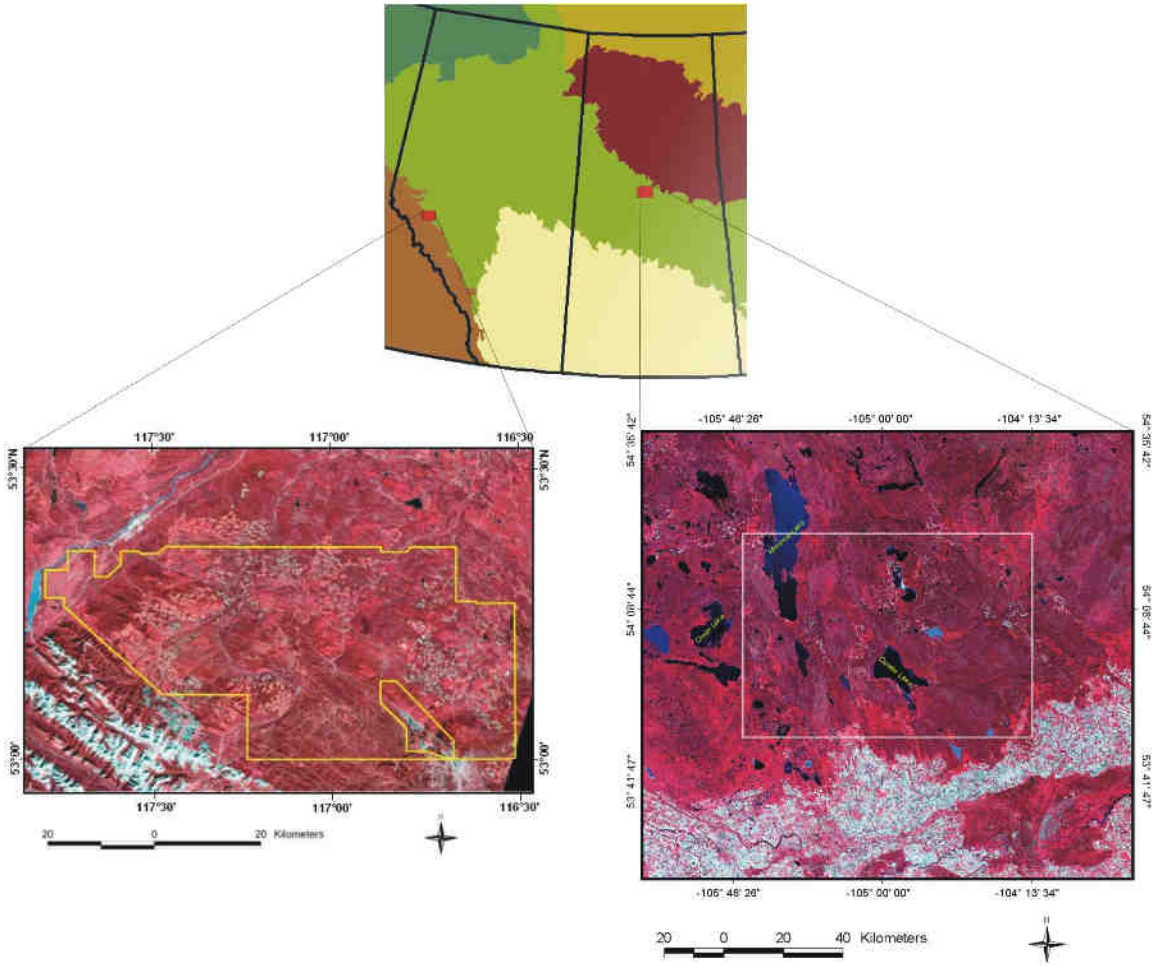

Figure 4.1 Map of Alberta and Saskatchewan indicating the locations of the two study regions, and the two Landsat-TM images used for remote sensing inputs in each region.

Raw data sets for the Alberta study area were obtained from numerous sources, including the Foothills Model Forest archives, Weldwood of Canada – Hinton Division, the Province of Alberta and the Canadian Forest Service (**Table 4.1**). Several comparable data sets have been obtained for the Saskatchewan area (**Table 4.2**). To date, most of the value-added work has been focused on the Alberta data. The work reported here was aimed primarily at manipulating the latter data and using them, or derived intermediate products, to create a coherent spatial database of biophysical and inventory data. The final products include maps of soil attributes, climatology, forest biomass density, leaf area index (LAI), and other forest attributes derived from the Alberta Vegetation Inventory (AVI) data layers.

4.1 Digital elevation models (DEM)

Digital elevation data were available for the study region from Weldwood, but the need for estimating improved soils data within the study area required an extended high resolution DEM for areas outside the study area and FMF boundaries. There is much empirical evidence that soil formation, and basic soil attributes such as texture and depth, will vary as functions of elevation and geomorphology, although little work has been done to assess and quantify these relationships. Most of the detailed soil profile databases available for central Alberta cover areas north of the current study region (**Table 4.1**; note the Weldwood PGS plot soils data set has relatively little detailed information on texture, depth and chemistry). The intention is that these soil profile data be used to establish physically-based relationships between topography and soil characteristics to be incorporated into spatial modelling of water flow and soil properties. Such modelling efforts are dependent on the availability of high-quality topographic data. A DEM is also needed ortho-rectification of remote sensing images, and as inputs for models of biomass and leaf area index (LAI) (see also Sections 5.1 and 5.4). Hence, alternative methods of creating DEMs were explored as a possible means of providing digital topographic data for this and other modelling efforts within and outside the current ECOLEAP-West study regions.

A hydrologically corrected DEM was constructed from point-based elevation data using the Arc/Info TOPOGRID command (ESRI, 1994), derived originally from the ANUDEM program (Hutchinson, 1989; Hutchinson and Dowling, 1991). In general, the TOPOGRID routine calculates grid cell elevations by reading contour data within a cell (maximum of 50 data points) and selecting a representative data point from these to be used as the cell elevation (ESRI, 1994). In our case, elevation data were obtained from contours on the 1:50,000 scale National Topographic Database (NTDB) digital map-sheet 083f03. Contour lines derived from the newly created DEM (**Figure 4.2**a) compared favorably with the original contours, indicating that the TOPOGRID procedure maintained satisfactory terrain definition relative to the original contour data.

In comparison to the TOPOGRID product, the Provincial DEM (**Figure 4.2**b) looks sharper so that valleys and peaks are more discernable. The visual differences in the two DEMs are likely due to both the differences in source data collection and in the methods of DEM construction. The Alberta provincial DEM is derived from an irregular grid of spot-elevations measured photogrametrically on 1:60,000 aerial photographs, interpolated to a regular grid, giving it a relative accuracy of ±5 m in the horizontal plane and ±3 m vertically. In contrast, the NTDB-based DEM is derived from vector-based contours (digitized from 1:50,000 contour paper maps of various dates of origin), interpolated to a regular grid using TOPOGRID. The vertical and horizontal accuracy of the NTDB data are unknown, but it are likely less than those stated for the Alberta data simply because they were created by digitizing hardcopy maps.

Table 4.1 Sources of data used to develop input layers for spatial modelling in the Alberta study area.

Information	Dataset Title	Feature Type	Source	Extent	Description
Elevation	DEM grid	raster	AEP	Study area	Digial Elevation Model: 25m horizontal resolution
	NTDB	point, line, polygon	NRCan	NTS mapsheets for soils	National Topographic Database: 1:50,000 scale contours and point elevations, water lines and polygons
Vegetation	AVI 2.2	polygon	Weldwood	Study area	Alberta Vegetation Inventory: year of origin, 5-level overstory species and percentage, height, crown closure, natural region, volume per ha, year of inventory
Biomass	PGS plot	point	Weldwood	Weldwood FMA	Permanent Growth Sample plots: tree- level species, DBH, height, status
	SINGH	non-spatial	CFS	Praries and NWT	Tree biomass measurements
	MANNING	non-spatial	CFS	Yukon	Tree biomass measurements
Soils	CanSIS	polygon	Weldwood	Weldwood FMA	Derived from Alberta Soil Survey Report. (Dumanski et al, 1972)
	ESIS	point	AEP[a]	West-central Alberta	Ecological Site Information System (ESIS) plot: see **Table III.I**
	PGS plot	point	Weldwood	Weldwood FMA	Permanent Growth Sample plots (PGS plot): see **Table 5.4**, **Table III.1**
	MSE	point	CFS	West-central Alberta	Managed Stand Ecosites: see **Table III.1**
	PLUTH	point	Dr. D. Pluth	Northwest-central Alberta	Soil sample data collected by Dr. D. Pluth: see **Table III.1**.
Access	ACCP	line	AEP	Study area	access areas (airstrips, etc)
	CUT	line	AEP	Study area	cutlines, trails
	FPLY	polygon	AEP	Study area	facilities
	FPT	point	AEP	Study area	facilities
	HYDROPT	point	AEP	Study area	hydrographical points (dams, falls, etc)
	HYDROPY	line	AEP	Study area	water areas
	ROAD	line	AEP	Study area	all roads with class attributes
	RWY	line	AEP	Study area	railways
	SLNET	line, polygon	AEP	Study area	single-line hydrography network
	UTIL	line	AEP	Study area	pipelines and powerlines
Imagery		raster	Weldwood	Study Area	orthophotography flown in 1995
	TM 45/23 - 1999/09/08	raster	CCRS	Central Alberta	Landsat-5 TM acquired 1999/09/08

[a] AEP (Alberta Environmental Protection) now ASRD (Alberta Sustainable Resource Development)

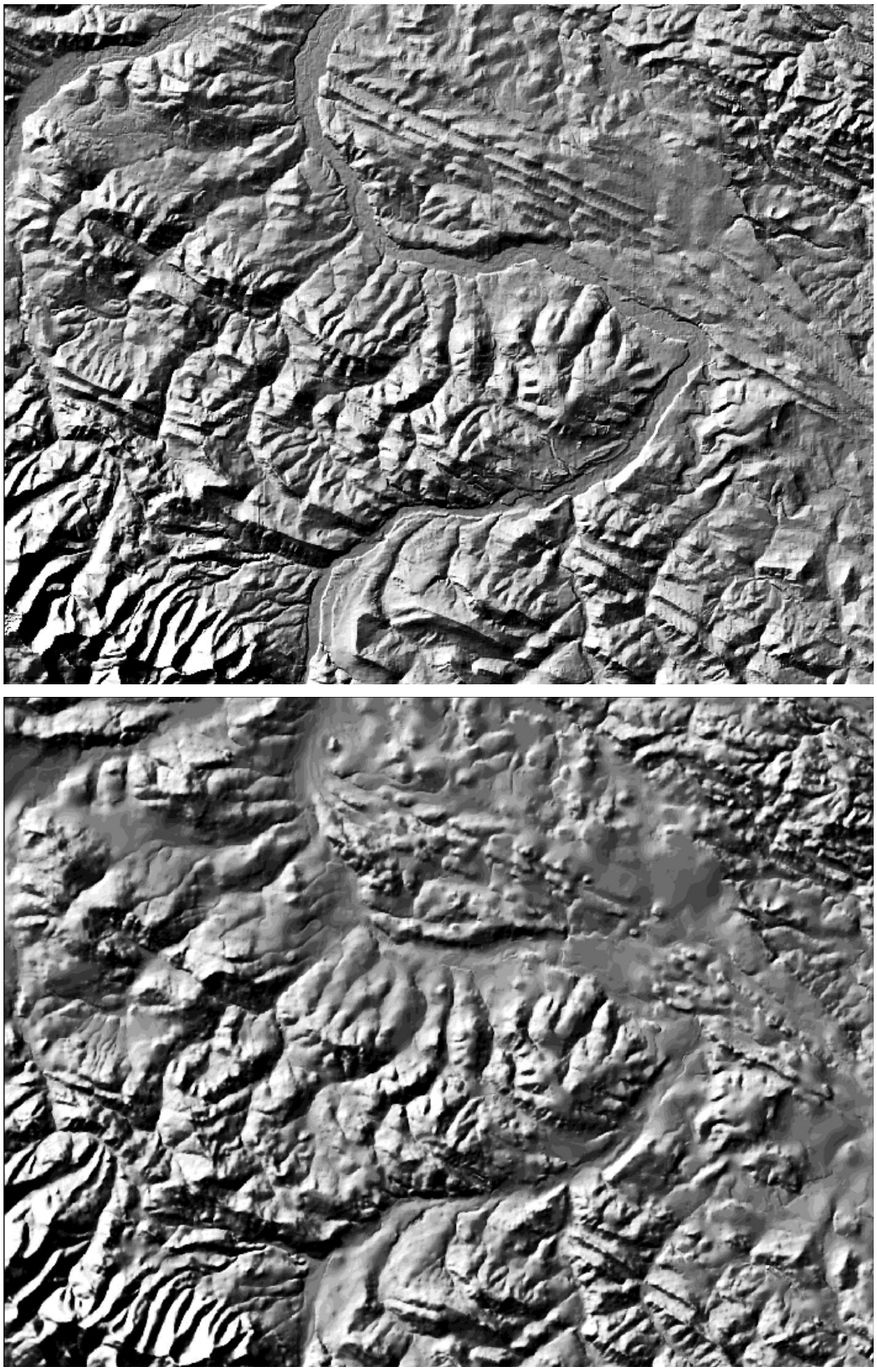

Figure 4.2 Hill-shaded DEMs for mapsheet 083f03. Top: Directly from Alberta digital elevation data; Bottom: derived using Arc/Info TOPOGRID procedure applied to NTDB contour data:

Table 4.2 Spatial data layers obtained and processed for the Saskatchewan study area.

Information	Dateset Title	Feature Type	Source	Extent	Description
Elevation	DEM grid	raster	SERM	Province of Saskatchewan	Digital Elevation Model at 100 m horizontal resolution
Vegetation	Sakatchewan Forest Inventory	polygon	SERM	Study Area	Vegetation: dominant species, 5 m height class, crown closure, stand origin, disturbance type, moisture
Soils	CanSIS	polygon	SERM	Study Area	Derived from CanSIS data
Access	Roads	line	SERM	Study Area	Extracted from Sask. Forest Inventory: primary and secondary road network
Rivers	Rivers	line	SERM	Study Area	Extracted from Sask. Forest Inventory
Water	Water Areas	polygon	SERM	Study Area	Extracted from Sask. Forest Inventory, includes: lakes, treed muskeg, flooded land.

Frequency histograms of elevation values for the two grids suggest that the overall range and distribution of elevations are very similar. Further, a strong relationship exists for a subset of elevations sampled from each grid for 270 PGS plot locations (**Figure 4.3**). On average, the elevation difference between the two DEMs was less than 10 m, though a few points showed differences as large as 80 m. It is not clear whether these differences are indicative of errors in the Provincial DEM, or result from problems in TOPOGRID interpolation, though the greater sharpness of the Provincial DEM suggests the NTDB contour data are of inherently poorer resolution.

Figure 4.3 suggests that the magnitudes of the differences increase with increasing elevation. In this study region, terrain ruggedness generally increases as elevation increases and may cause greater discrepancies in interpolation of elevation values from contours. Similarly, both contour and spot-height values will likely be less well-defined in areas of greater relief, such as on steeply sloping areas. Hence, the largest discrepancies generally occur at high elevation peaks, and are unlikely to have major impact on most results from process models.

The TOPOGRID procedure will ultimately be used to provide DEM coverage for the extended soil modelling area. The digital map sheets were edge-joined using GIS to create an input coverage for TOPOGRID covering most of southern Alberta (see also **Appendix III**).

4.2 Soils coverage

Many ecosystem models require at least a representation of surface soil texture (top 15 cm) to simulate seasonal or annual water balances and the availability of soil moisture to vegetation. The soils coverage obtained from the Canadian Soil Information System (CanSIS) database (via Weldwood), however, did not contain a soil texture attribute. Instead, soil texture codes were derived for the Hinton data set by combining the association (Assoc1) and first variant (Var1) polygon attributes. A texture code was assigned to each Association/Variant combination based on profile descriptions found within the soil survey manual for the Hinton/ Edson area (Dumanski et al. 1972). In those cases where a soil texture could not be derived, a value of 999 was assigned. Examples of such cases include: an unknown soil association; an unknown variant within a series; no soil series or profile information at all; or classification as "miscellaneous" land units (such as river banks). In the final data set, 134 of 437 soil polygon records contain missing texture values, although the majority of these are in alluvial river valley areas where texture is highly variable and not easily assigned. Polygons were dissolved based on the new soil texture codes to produce the final soil texture coverage (**Figure 4.4**).

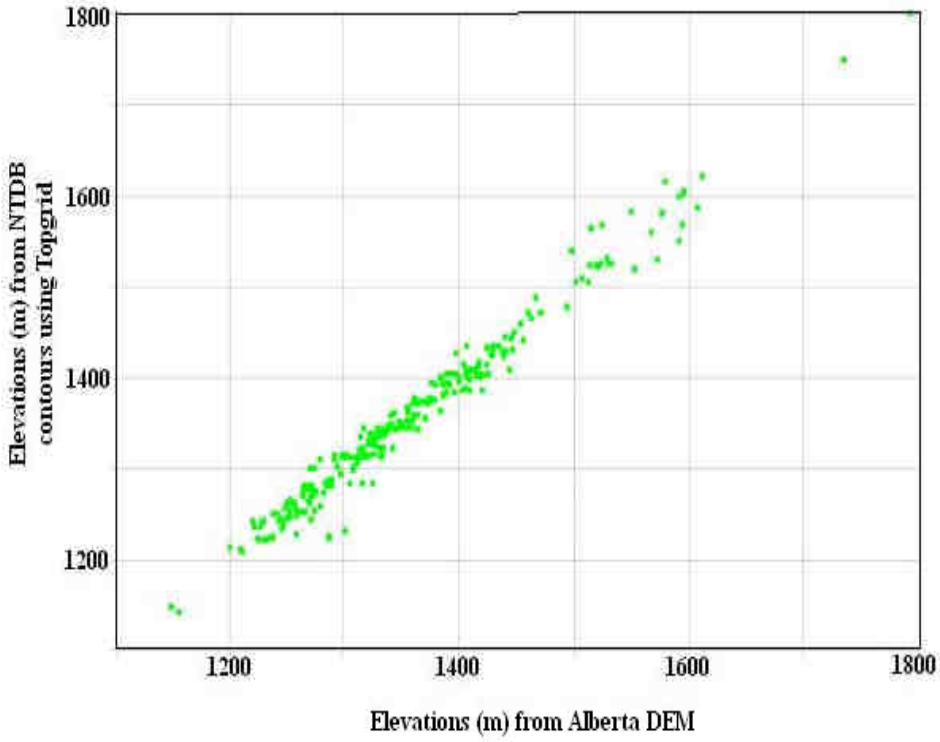

Figure 4.3 Scattergram showing a strong agreement between a sample of elevations taken from both the Alberta 25m DEM and one derived from NTDB contour data using the TOPOGRID ArcInfo command. Sample points are for active PGS plot locations within NTDB mapsheet 083f03 in the study region.

Because soil textures were derived from generalized soil association profiles, the accuracy of the texture information in the present soils coverage is almost certainly poor and should be used with caution. Additionally, several main soil associations identified in the Hinton area soil survey report are classed as Luvisolic with finer textured clayey soils underlying the coarse-to-medium textured surface soils. At present, soil polygons with these associations are assigned the coarse-medium texture codes of the top 15 cm, but in reality, the underlying clay soils will likely have an impact on vertical and lateral soil drainage.

These limitations are the primary motivation for investigating the relationship between detailed soil profiles and digital elevation data (as mentioned in Section 4.1). We are attempting to create a more detailed map of soil physical and chemical attributes as functions of elevation and soil depth, using four different sets of soil profile data (i.e., including those from Weldwood's Permanent Growth Sample plots, **Table 4.1**) (see also **Appendix III**). A similar soils modelling and mapping approach is planned for the Saskatchewan study region, for which copies of the modal soil profile information used to characterize the CanSIS polygons were obtained from the University of Saskatchewan (Glen Padbury, personal communication, 2002).

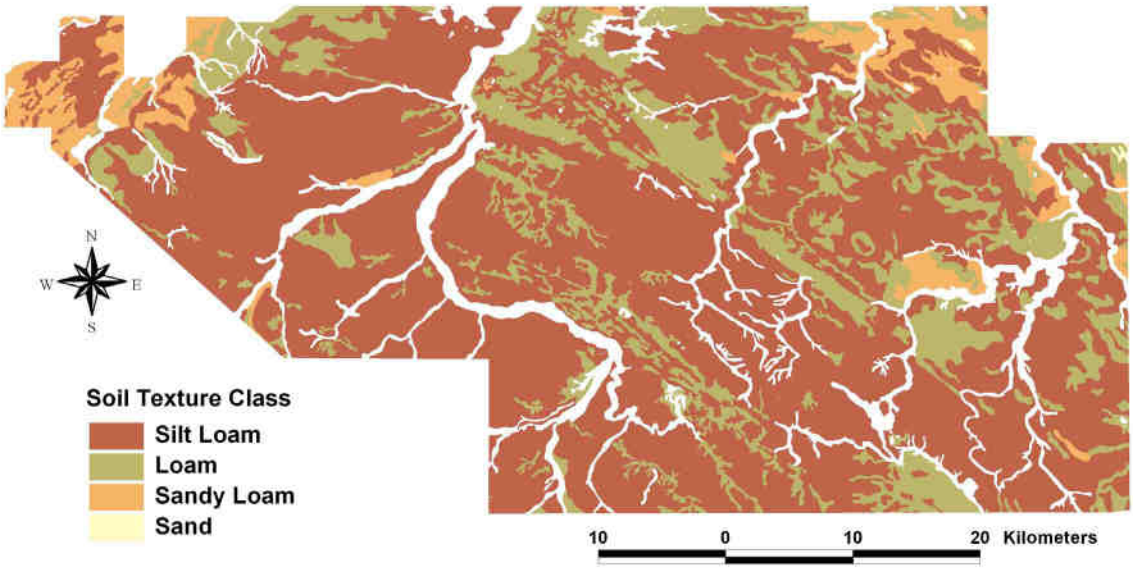

Figure 4.4 Map of soil texture for the study region.

4.3 Climate surfaces

Climate surfaces for the Alberta study area were derived using a new implementation of the daily weather generation algorithm described in Régnière and St-Amant (2002, in prep), originally developed as a component of the BioSIM, Pest Management Planning Decision Support program (Régnière et al. 2001). The climate generator program is a Microsoft *Windows* application that interpolates monthly climate statistics (means and variances) for a series of point locations within the domain of interest, using a database of 1961-90 Canadian climate "Normals" (e.g., Environment Canada, 1994). Input data consist of latitude, longitude and elevation, with slope and aspect derived from DEM data (Section 4.1) using Arc/Info. The output is a representation of the observed temperature and precipitation regimes for any number of multiple locations across the study regions. For the purposes of this study, a 100 m resolution grid was set up over the study region, and the climate generator used to simulate a set of daily values for each variable for a one-year period based on the 1961-90 monthly climate statistics observed at local stations. After completing the interpolation, the daily values for each variable were averaged to create monthly statistics for each 100 m pixel and imported back into Arc/Info GRID to create individual climate surface grids. The output variables for each month include extreme and mean daily maximum and minimum temperatures, total rainfall and total precipitation.

Data produced by the climate generator were used by Lindner in his simulations of species succession and productivity in the Alberta study area using FORSKA-M (Section 6.2). Similar routines are embedded in the StandLEAP productivity model (Section 6.1). In a related project funded by the Climate Change Action Fund (CCAF), data from the Canadian Coupled General Circulation Model (CGCMII) were used to develop high resolution scenarios of future climate under the IPCC IS92A greenhouse gas emissions scenario (Price et al. 2001). These and similar data could be used to drive the climate generator to create detailed local climate scenarios—ultimately to simulate impacts of projected climate change at the stand level.

4.4 Inventory data

4.4.1 Alberta Vegetation Inventory (AVI)

The forest stands in the study region were previously mapped to Alberta Vegetation Inventory (AVI) version 2.1 standards (Resource Information Division, 1991) based on aerial photographs flown during 1988 and 1993. The spatial forest stand data were subsequently mapped to a UTM Zone 11 NAD27 projection in an Arc/Info coverage with an accompanying INFO data table keyed by stand identification numbers (STAND-ID).

Individual AVI map-sheets were joined and reprojected to NAD83 to match the data layers received from the Province. The coverage was clipped to the study region and then dissolved by STAND-ID to remove map-sheet boundaries. The dissolving operation primarily removed the administrative boundaries that were causing spurious fragmentation of vegetation polygons, affecting 11% of the forested portion of the study area (**Figure 4.5**). The overstory vegetation attributes that were of interest for this research were then selected: moisture regime, crown closure, height, species and percentage composition designations, stand structure coding, year of origin, timber productivity rating, non-forest area coding, yield group, site index, timber volume (m^3 ha^{-1}), by softwood, hardwood and all species; year of inventory; and natural region.

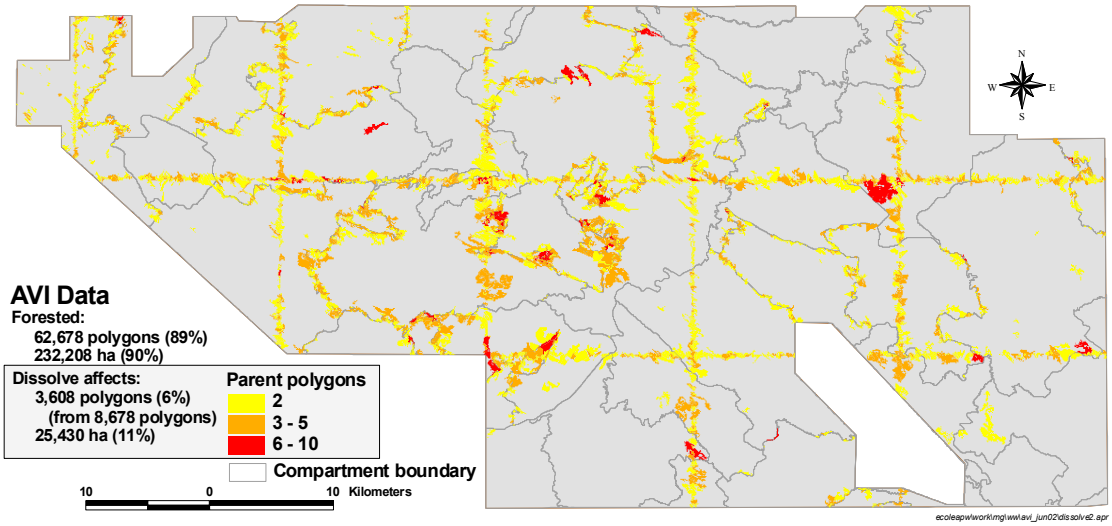

Figure 4.5 Polygons affected by dissolving the administrative boundaries in the AVI map sheets.

Types of adjacent stands dissolved by this process included:

- stands split by an administrative boundary
- stands possessing different STAND-ID, but no differences in other AVI attributes
- stands where the only attributes that differed were not relevant to this study. Examples include clearcuts recorded as 1962 and 1963 in adjoining stands, but the reported year of origin was the same; or stands where the year of the most recent field check differed.

In a few rare instances, adjacent polygons occurred with similar AVI characteristics, but the boundaries were not dissolved. These included:

- stands with differences in the reported year of inventory (which was used to estimate stand age)

- stands reported to lie in different natural regions (used for preliminary stratification)

The resulting AVI coverage was used to investigate and display the location and spatial distribution of stand characteristics across the study region. For forested areas, stand-level polygon data were first classified by species composition, year of origin, stand height, and crown closure. Beyond familiarization with the AVI dataset for this region, these initial queries were important in determining the most effective use of the AVI data for both empirical and process-based model development and application.

4.4.1.1 Initial AVI queries: height, crown closure, and age structure

The AVI database was queried to derive area statistics for the recognizable land cover types and occurrences of unique species combinations. The total area of the study region according to this analysis was found to be 261,142 ha, of which 235,384 ha (90%) were classified as forested land. Approximately 67% of the total study area consisted of stand polygons where the dominant species contributed at least 80% of stand composition (**Table 4.3**).

Stand heights were allocated to three classes: 1-10, 11-20, and 21+ metres (**Figure 4.6**). The spatial distribution of stand heights is characterized by shorter stands in the northwest, and broad patches of both taller and shorter stands to the southeast. Interestingly, the largest extent of tall stands occurs in proximity to the mine area in the southeast of the study region.

Table 4.3 Summary of results of AVI queries for proportions of FMF study area where the dominant species occupies more than 80% of total forest cover (canopy closure basis).

Dominant species group	Code	Area (ha)	Fraction of forested area (%)
Deciduous	Aw	10,052	3.8
White birch	Bw	13.9	0.0
Alpine fir	Fa	70.4	0.0
Balsam fir	Fb	182.5	0.1
Tamarack larch	Lt	3,167	1.2
Balsam poplar	Pb	1,092	0.4
Lodgepole pine	Pl	109,742	41.3
Black spruce	Sb	35,622	13.4
Engelmann spruce	Se	1,055	0.4
White spruce	Sw	17,112	6.4
Subtotal		**178,109**	**67.**
Other forest land[a]		57,275	21
Non-forest (water)		1,252	0.5
Non-forest (other[b])		24,606	11
AVI total land area		**261,142**	**100**

[a] forested area not dominated by a single species
[b] human-cleared, or naturally non-vegetated

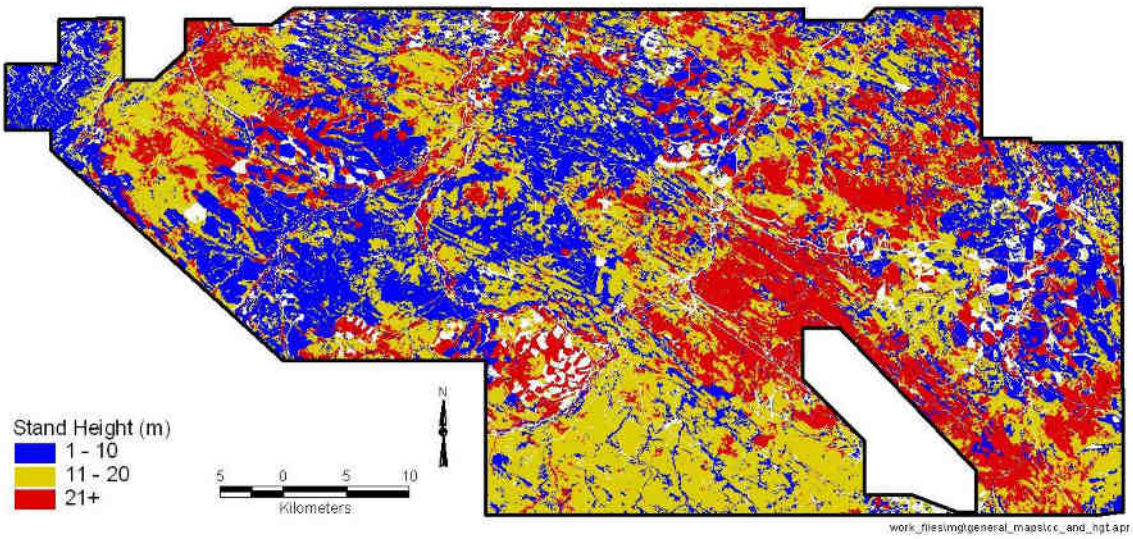

Figure 4.6 Stand height distribution over the study area as derived from a reclassification of the AVI dataset.

The results of the height mapping shown in **Figure 4.6** can be compared to the four crown closure classes recorded in the AVI database: A: 6-30%, B: 31-50%, C: 51-70%, and D: 71-100% (**Figure 4.7**). Low density stands occur in the Subalpine and Montane ecozones in the extreme northwest of the study region. Elsewhere, a few alternating bands of denser and lighter coverage run northeast/southwest.

Forest stands in the study area are relatively mature as evident from the height and crown closure class distributions for each of the species groups shown in **Figure 4.8**. The black spruce-larch species group that occurs primarily on relatively wet sites consists of generally shorter and more open stands than other species or species groups. Further evidence of the relatively mature state of most stands in the area was observed in the height-over-age curves generated from available data for each species group (see **Figure 4.11**).

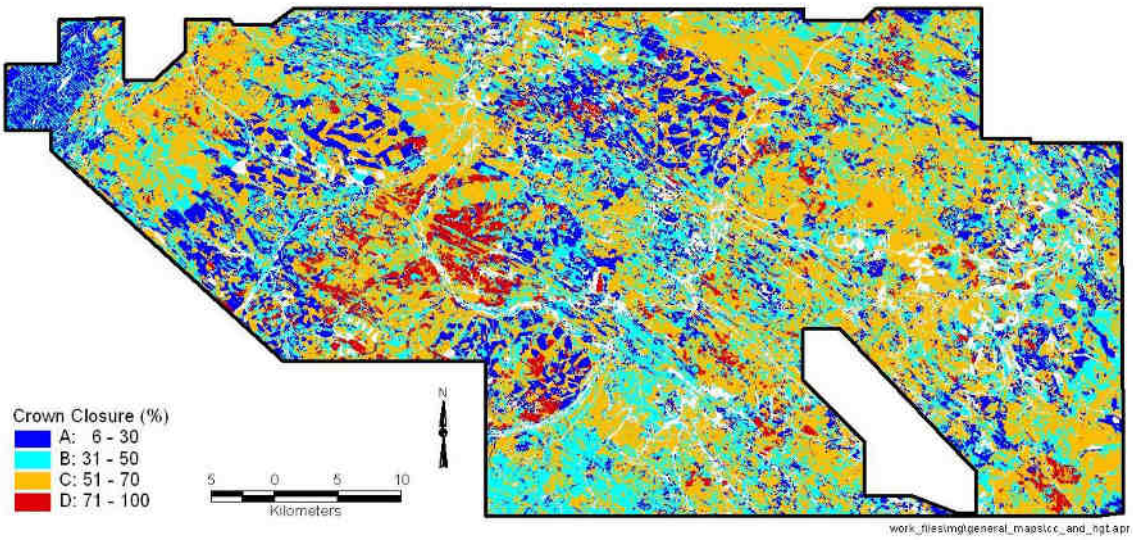

Figure 4.7 Crown closure distribution for the study area taken from the AVI database.

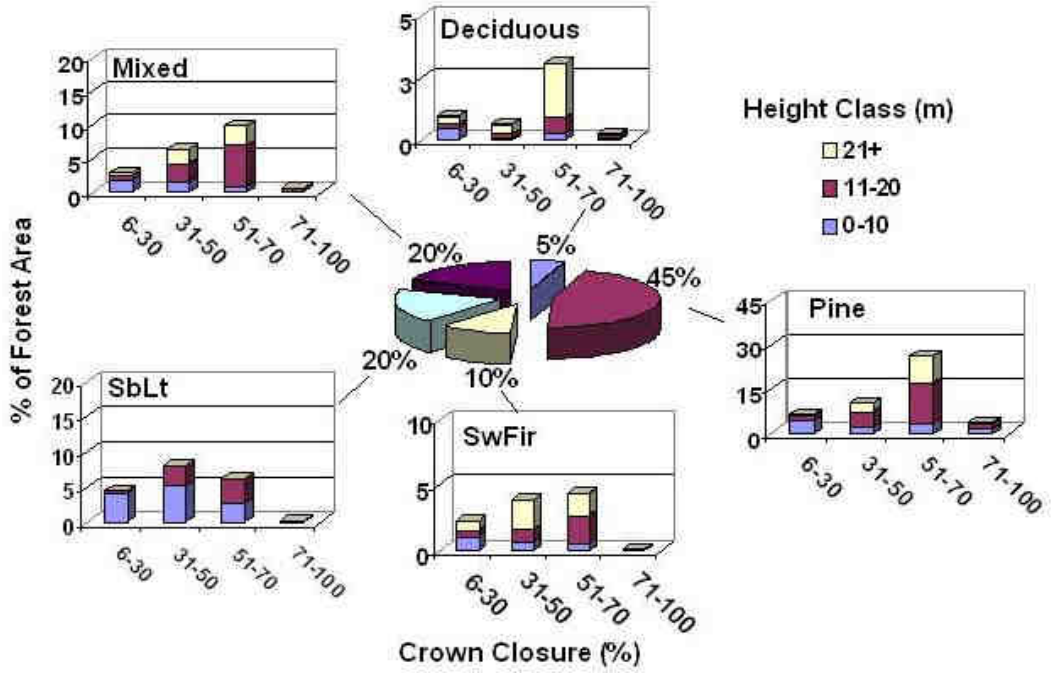

Figure 4.8 Distribution of height by crown closure class and species group across the study area.

4.4.1.2 AVI species classification for biomass modelling

A strategy for mapping total standing biomass (Mg ha^{-1})[b] for a series of pilot regions across Canada, including the ECOLEAP-West Alberta study area, was developed as part of the Earth Observation for Sustainable Development of Forests (EOSD) project. EOSD is a joint effort between the Canadian Forest Service and the Canadian Space Agency (Wood et al., 2002). Hence, the creation of a map of forest biomass, served not only as a data input and validation layer for the present study, but also contributed to the requirements of the EOSD project.

In summary, mapping the forest biomass in the Alberta study area was achieved by deriving a set of species-specific stand-level empirical models that were then applied to the AVI data (see Section 5.1 for further details). The initial stage was to simplify the AVI classification down to five species classes: Pine (lodgepole pine), SbLt (black spruce/larch), SwFir (white spruce/balsam fir/subalpine fir), Deciduous (trembling aspen/balsam poplar) and Mixed species (**Figure 4.9**).

Of the five classes, the first four "pure species" classes were defined as those stands where the dominant species or species group comprised at least 80% of stand composition by species (expressed in crown closure terms). Any other stand for which the dominant species contributed less than 80% of stand composition was assigned to a fifth species class termed "mixed". Because lodgepole pine was prevalent across the study region and occurs mainly in relatively pure stands, it was assigned to its own species class. Black spruce and larch tended to occupy the wetter and less productive ecosites and were therefore aggregated. White spruce and subalpine fir generally occupy similar ecosites in the study region, and were also aggregated, together with balsam fir (because Fb was not particularly widespread and, of the species present, was most similar to subalpine fir, Fa). Trembling aspen and balsam poplar were the dominant deciduous species in the study region possessing broadly similar ecological characteristics, and were therefore grouped into a single "deciduous" class. Nineteen percent of the total forested area was classified as "mixed". The remaining 2% of the polygons classed as "regeneration" were

[b] 1 Mg, Megagram = 10^6 g = 1000 kg = 1 metric tonne

recently harvested sites with no species composition label. Overall, this procedure resulted in a complete classification of the forested portion of the study region expressed in terms of only the dominant species (**Figure 4.9**).

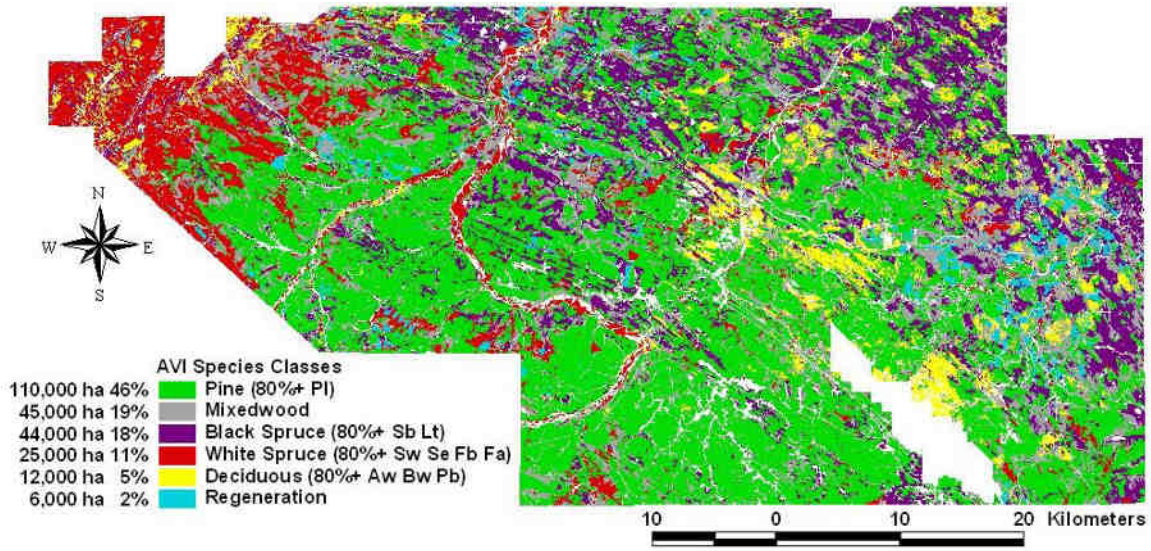

Figure 4.9 Species classes derived from AVI data for 1996, as used for estimating the spatial distribution of forest biomass across the Alberta study area.

4.4.1.3 Classification of species for StandLEAP modelling

The StandLEAP simulation model was used to produce spatially-explicit estimates of forest productivity for the study region (Section 6.1). This modelling effort required as input, a GIS coverage of the major forest cover types found in the study region. To improve the representation of the forested area with more explicit species groupings, the AVI database was further queried to identify all stands where the occurrence of the two most dominant species (SP1 and SP2, respectively) occupied at least 80% of the stand (based on canopy closure estimates). This resulted in twelve species classes, with an additional class 0 used to designate water or non-forest. The 12 classes account for approximately 84% of the study area overall and 95% of the forested area. Some additional species and/or species combinations were grouped to form single classes, derived from the SP1 proportions combined with the most commonly occurring combinations of SP1 and SP2 (**Table 4.4**). For example in Class 4, species Pb (balsam poplar), AwPb and PbAw did not occur frequently in the study area so they were grouped to form a composite deciduous species (Aw) group. Although the species groupings analyzed in this study were a simplified representation of the species proportions reported in the AVI, they account for about 95% of the forested area in the study region. Overall, this classification (**Figure 4.10**) corresponded closely to the five class scheme used for biomass modelling (**Figure 4.9**), with the main exception that the "Mixed" class was expanded into eight more explicit groups (represented in **Table 4.4** with codes 5-12).

Table 4.4 Species classes for forested portion of the study area, derived from AVI database queries. Species codes as in **Table 4.3**.

Code[a]	Species class	Count	Area (ha)	Fraction of forest area (%)	Fraction of study area (%)
1	Pl	22925	109742	46.6	41.2
2	Sb, Lt, SbLt, LtSb	16299	43820	18.6	16.4
3	Sw	7300	17112	7.3	6.4
4	Aw, Pb, AwPb, PbAw	4925	11522	4.9	4.3
5	AwPl, AwSw	1325	3320	1.4	1.2
6	SbPl, SbSw	2048	4756	2.0	1.8
7	PlAw, PlPb	1489	5264	2.2	2.0
8	PlSb	3741	13291	5.6	5.0
9	PlSw	2255	7468	3.2	2.8
10	SwAw, SwPb	644	1497	0.6	0.6
11	SwPl	1488	4381	1.9	1.6
12	SwSb	694	1225	0.5	0.5
	Total species classes 1-12	65133	223398	94.8	83.8

[a] Code attribute was added to the AVI coverage, for each of the above species classifications.

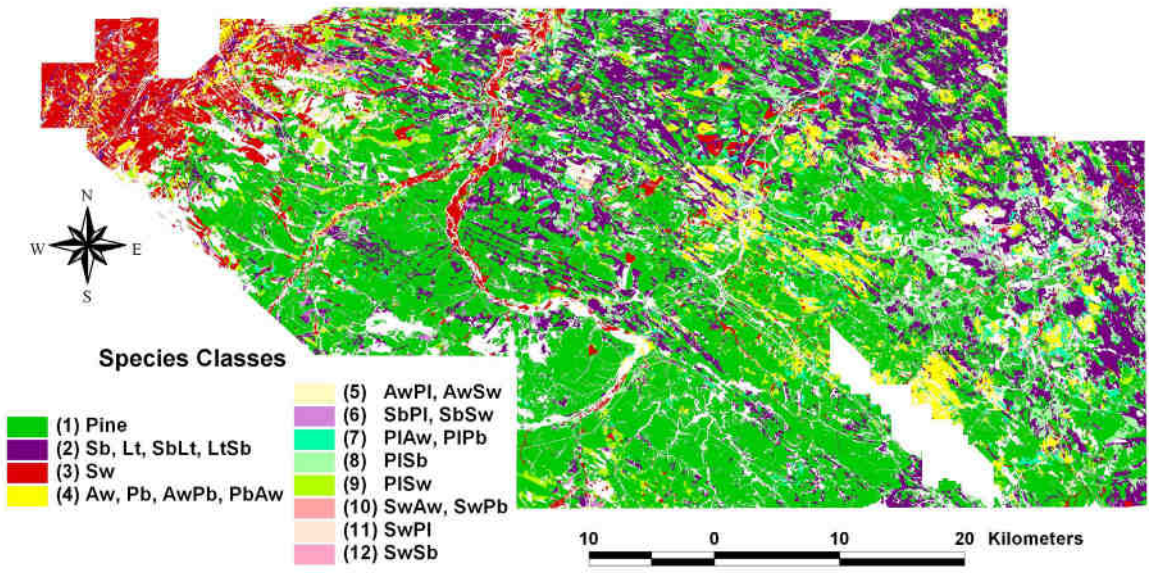

Figure 4.10 AVI species classification used as input to the Standleap model, as outlined in **Table 4.4**.

4.4.1.4 Derived height over age curves

Scatterplots of the height-over-age relationships for each of the five major species groups were created from all the available data in the AVI (**Figure 4.11**). Some spurious data points were evident where some young stands were reported to have exceptional (one might say impossible!) heights. These outliers led to a few impossibly high estimates of biomass productivity (Section 5.2.2) because the modelling approach used the reported stand height as an independent variable. Nevertheless, these height-over-age relationships are generally very plausible, in both absolute and relative terms (note for example the lower rate of height growth in the SbLt species group compared to the others). Hence these results provide confidence that estimates of biomass and

volume productivity obtained from the AVI data set are a good basis for assessing the results of process models.

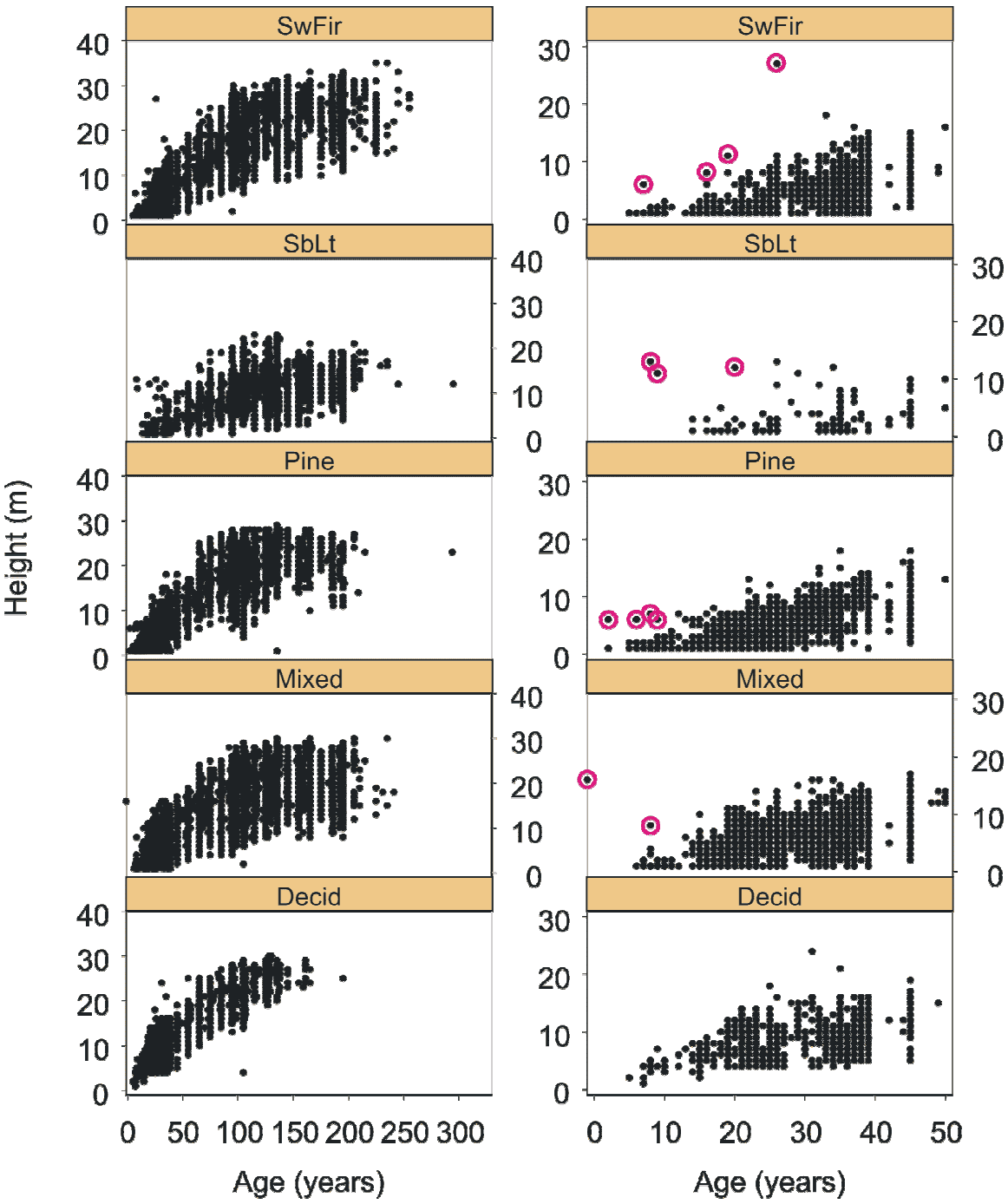

Figure 4.11 Scatterplots of the distribution of stand height by stand age for all AVI data (left panel) and for the first 50 years only (right-hand panels). Outliers highlighted by red circles were considered to be spurious, and therefore omitted from productivity estimates.

4.4.2 Permanent Growth Sample (PGS) plot dataset

The traditional purpose of PGS plots is to provide periodic measurement data (typically 5-10 year intervals, depending on stand growth rates), to be used for the development of growth and yield tables. The Weldwood FMA has a particularly well-developed grid of PGS plots. At each plot location, subplots are arranged in clusters of four around a plot center and are generally 1/10 acre (0.04 ha) or 1/5 acre (0.08 ha) in size. A subplot is the location where tree measurements are actually taken; hence for most purposes in this report, the term "plot" or "PGS plot" actually refers to a subplot.

The PGS plot data are maintained in a relational database, with georeferencing information stored in a separate, relational spatial database. GPS coordinate collection began in 1997 to improve on the coordinate precision previously obtained by reading from forest company maps and air photos. For some purposes, only plots that can be spatially referenced are useful. In other cases, only actively maintained plots can provide useful information (**Table 4.5**).

Tree measurements are recorded within the subplots for all live and dead free-standing trees above 1.3 m height, excluding willow and alder. Measurements include diameter at 1.3 m (DBH), stem height to top of live foliage (entire height for dead standing trees, adjusted for leaning trees). Site Indices (SI) are estimated from top heights calculated as the average height of the tallest 100 DBH live trees per hectare (i.e., 8 tallest trees and tallest 4 trees for 0.08 and 0.04 ha plots respectively), which are of good form. Age measurements are taken by coring selected site trees at 1.3 m.

The PGS plot data were used for four distinct purposes: (1) calculation of PGS plot-level biomass from allometric tree biomass functions prior to mapping at the AVI stand level (Section **5.1.2**); (2) estimation of sapwood basal area based on tree basal area in estimation of leaf area index (Section **5.4.2.3**); (3) validation of StandLEAP estimates of plot-level growth; and (4) for parameterization and validation of FORSKA-M (Sections **6.2.1** and **6.2.2**).

Table 4.5 Summary of subplot status in Weldwood FMA and those available for research use in the Alberta study area (as of December 2001).

	Number of Plots	Active Plots
Total PGS	3208	1440
Geocoded	3128	1400
Study area	1037	481

4.4.3 f_{PAR} data

The fraction of incoming photosynthetically active radiation (PAR) absorbed by the vegetation canopy (denoted f_{PAR}) is a critical input to radiation use efficiency (RUE) models such as StandLEAP. The Landsat-5 TM image of the Hinton study area (TM45/23), acquired on 8 September, 1999 was used to estimate stand-level f_{PAR}. A correction algorithm developed by the Canadian Centre for Remote Sensing (CCRS) was applied to the raw image to obtain a top-of-atmosphere reflectance image. Further pre-processing included ortho-rectification based on ground control points identified from 1:50,000 scale NTDB digital maps, and on elevation data collected from the Alberta Provincial DEM (25 m horizontal resolution).

A simple ratio (SR) equation was applied to bands TM4 (NIR (near infra-red) band) and TM3 (PAR band) for the entire study area. Based on modeling work of Goudriaan and van Laar (1994) and Bernier et al. (2001), theoretical reflectance values of the canopy-soil system in the two wavebands were estimated for different species and a range of LAI values using a simple two-stream radiative transfer model (Goudriaan and Van Laar 1994).

With these theoretical canopy-soil reflectance values, a generalized cubic relationship was built between the simple ratio (SR = NIR/PAR) and modelled f_{PAR}. The equation was parameterized for each of lodgepole pine, aspen, black spruce and balsam fir (as a substitute for

white spruce), assuming a solar zenith angle of 50.1º and soil reflectances of 0.14 and 0.19 in the PAR and NIR wavebands, respectively (**Figure 4.12**). The resulting equations were not satisfactory for all species (note particularly, the equation in **Figure 4.12**c for aspen, where a linear equation was adopted). However, it would seem that SR always converges quickly towards the saturating value of 5, almost independently of LAI.

AVI stand polygon data were used as complementary input for this process. Values of SR were first obtained from the ratios of the pixel values in bands TM4 and TM3. The AVI coverage (Section 4.4.1) was then overlaid on the resulting SR image and the average SR value extracted for a 2×2 pixel window centered on each polygon. The appropriate species-specific equation and coefficients were determined for the dominant species (SP1) reported in the AVI attribute table for the same stand polygon. This equation was then applied to the SR pixel values to estimate f_{PAR}. In the particular case of white spruce, where adequate stand-level data were unavailable, the relationship determined for balsam fir was used instead. Finally, each polygon was labeled with the newly calculated f_{PAR} value. The resulting data layer could then be used as input to the StandLEAP model (see Section 6.1).

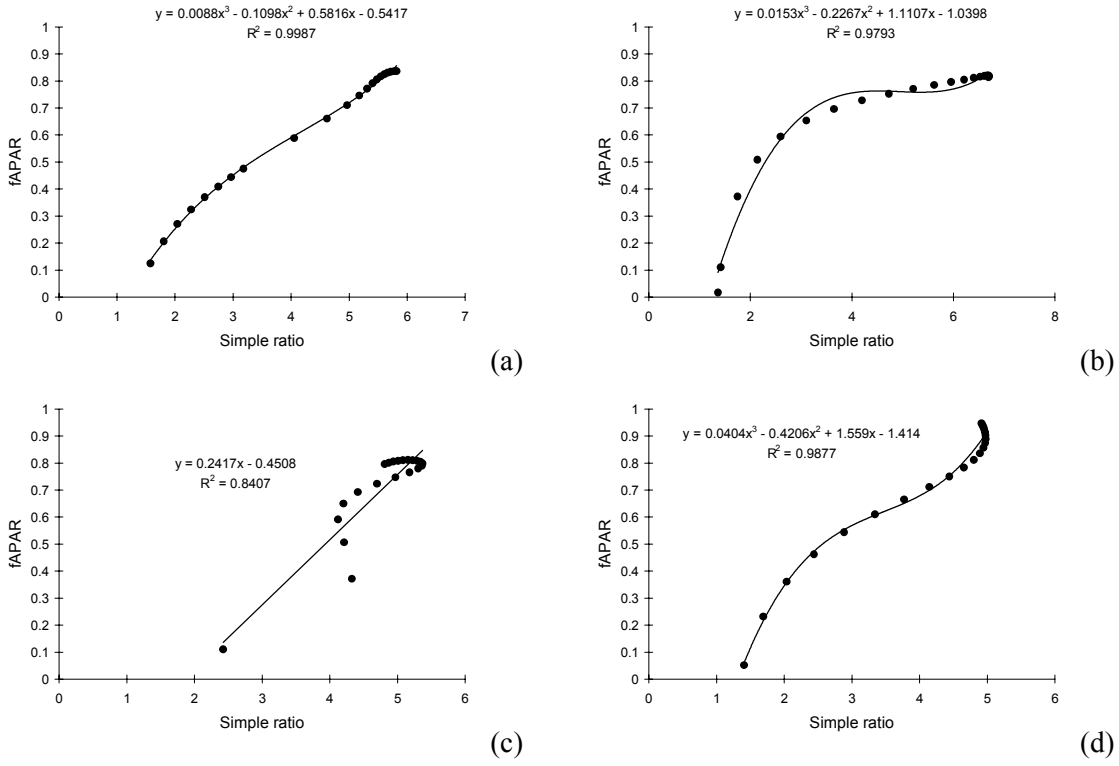

Figure 4.12 Relationships between simple ratio, SR, and f_{PAR} for major species in the Alberta study area, derived for Landsat image TM45/23 - 1999/09/08 used in the StandLEAP simulations. (a) lodgepole pine; (b) black spruce; (c) trembling aspen; and (d) balsam fir (used as a substitute for white spruce).

5 Spatial data products

5.1 Biomass map

5.1.1 Background

Forest biomass is the dry mass of live plant material (trees and understory species) found in all forest ecosystems. Accurate estimation of forest biomass, though challenging, is needed for studies of ecosystem productivity, and in models for calculating and forecasting carbon budgets (Kurz and Apps, 1999; Price et al., 1997, 1999; Parresol, 1999; Penner et al., 1997).

Depending upon the level of accuracy required, field-based methods for estimating forest biomass over extensive areas are costly, time-consuming and location-specific. Scaling the results of site-level measurements up to larger scales (FMA, region, Province, national) will involve modelling, and the challenging exercise of dealing with factors such as ecological differences, variation in inventory systems, and the scattered sources of measured biomass data.

There has been an increasing demand for spatially-explicit methods of forest biomass estimation that could be implemented nationally. Bonner (1985) compiled Canada's first national forest biomass inventory from wood volume data reported in the 1986 Canadian forest inventory (CanFI) database. Penner et al. (1997) attempted to improve on this using the 1991 CanFI data set. These efforts are the primary sources of Canadian biomass data currently reported at national scale, and for various reasons the spatial resolution is necessarily limited to that of 10 km township units. There is, however, a demand for forest biomass data at finer spatial resolutions. The lack of accurate spatial forest biomass data has been considered one of the most serious uncertainties in calculating the C budgets of forests (Harrell et al., 1995). Accurate high resolution forest biomass maps are also required if Canada is to benefit from including forest carbon sinks to offset its fossil fuel emissions of greenhouse gases under the terms of the Kyoto Protocol. To meet these needs, the methods developed will need to be robust, and the resulting estimates independently verifiable.

The Earth Observation for Sustainable Development of Forests (EOSD) project, a joint effort between the Canadian Forest Service and the Canadian Space Agency (Wood et al., 2002), has been tasked with mapping Canada's biomass at the forest stand level using Landsat Thematic Mapper (TM) data (30 metre pixel resolution). The EOSD strategy outlines a combined forest inventory-based method for biomass mapping, expansion of the method to several pilot regions, and implementation at the national level (Luther et al., 2002).

The ECOLEAP-West project study area in the Foothills Model Forest was selected as a test site to develop a validated method of estimating spatial biomass data for EOSD. The map of biomass distribution produced in this way could then serve both as an input data layer and to validate modelled estimates of forest productivity. The objectives of this work were: (1) to estimate stand-level biomass using both Alberta Vegetation Inventory (AVI) and Landsat-TM data; and (2) to identify and explore data and method implementation issues relevant to their application to Alberta.

5.1.2 Estimating tree and stand-level biomass

Weldwood Canada (Hinton Division) provided a copy of their database for approximately 3,200 PGS plots, distributed across the Foothills Forest Management Agreement (FMA) area. The database was queried to determine the most recent plots that were still under a periodic remeasurement program. Tree data attributes queried included: plot ID, tree ID, species, diameter at breast height (DBH), tree height, and tree status (i.e., live, snag, log, missing). Tree data were filtered to remove all dead or fallen trees and any records missing both DBH and height measurements. For records missing either DBH or height, the missing value was estimated from

the other using a provincial height-diameter equation specific to the natural subregion in which the plot was located (Huang et al. 1994). After sorting and filtering, tree data for 1,382 PGS plots were retained for further analysis.

5.1.3 Biomass calculations

In summary, forest biomass for the Alberta study area was estimated by: (1) deriving species-specific allometric tree biomass functions from previously published tree stem analysis and biomass data; (2) applying derived functions to PGS plot trees in the study area to estimate tree biomass; (3) aggregating tree biomass to a stand-level biomass density (Mg ha^{-1}) at each PGS plot location; (4) deriving functions relating stand-level biomass to stand structural characteristics; and (5) applying stand-level functions to the AVI polygons to map biomass density (**Figure 5.1**).

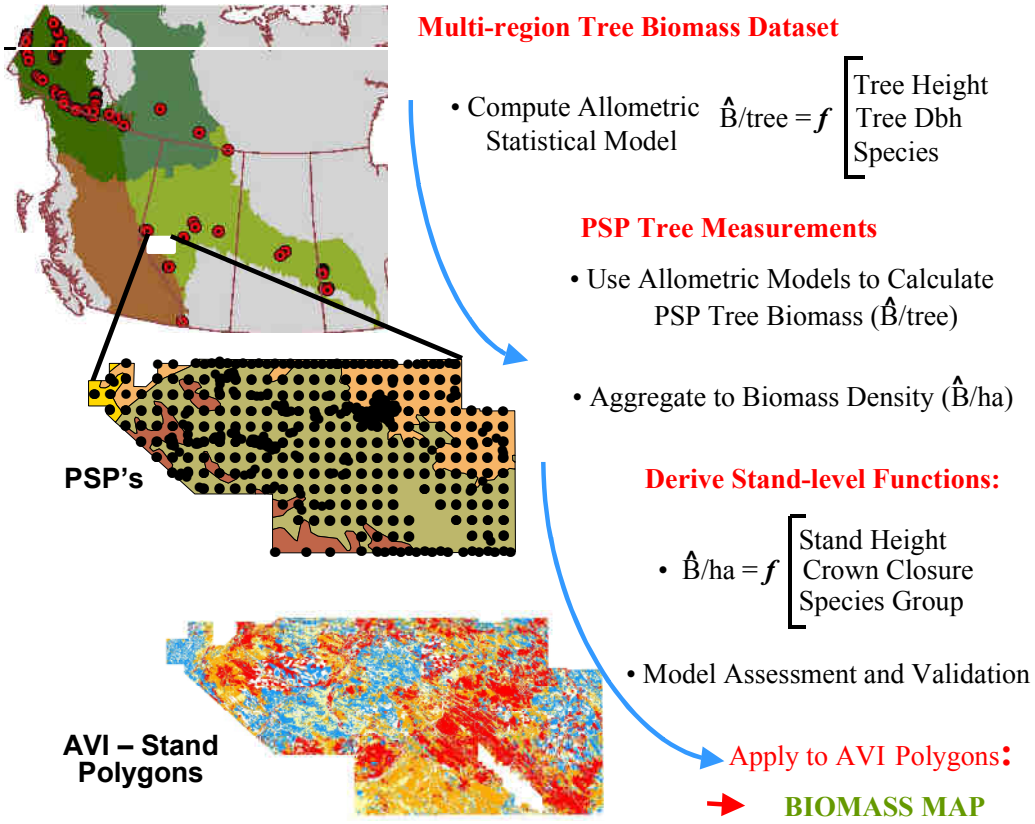

Figure 5.1 Diagram showing the flow of biomass calculation, modelling, and mapping for the ECOLEAP-West Alberta study area.

Biomass allometry data collected in the boreal forest regions of the Prairie Provinces and Northwest Territories (Singh 1982, 1984), and the Yukon (Manning et al. 1984), were pooled and used to develop allometric functions relating DBH and height to above-ground total tree biomass (kg $tree^{-1}$) for the four "pure" species groups. The pooling of the allometric data created a larger sample size from which to establish general relationships. Seventy percent of the data were used for model fitting and the remainder for model validation. Three functions selected from the literature were explored using non-linear regression analysis, with each assessed on the basis of adjusted R^2 and Root Mean Square Error (RMSE) (Payandeh 1981; Crow and Schlaegel 1988). The equation of best-fit was selected for each species group, based on the model of tree biomass $(Y) = b_0(D^2H)b_1$, and was used to estimate the biomass of each tree at each PGS plot. The

individual tree biomass values were totalled for each plot and divided by the plot area to estimate stand level biomass density for each plot (Mg ha^{-1}).

A stand level model of biomass was also developed to estimate biomass density as a function of AVI stand attributes of height and crown closure. Mean tree heights were first calculated for each PGS plot, using the individual measurements reported for all standing live trees. Crown closure class (A: 5-30%, B: 31-50%, C: 51-70%, D: 71-100%) was also obtained from the PGS plot database. Following the simplified classification adopted for the AVI database (Section 4.4.1.1), PGS plots were classed into one of four "pure" species classes if the dominant species (SP1) formed at least 80% of the stand (in terms of AVI species composition): Decid (Deciduous: aspen, balsam poplar), Pine (lodgepole pine), SbLt (black spruce/larch), and SwFir (white spruce/fir). Otherwise they were classed as Mixed (mixed species) (**Figure 4.9**; see also Section 4.4.1.2).

The AVI stand attributes were used to assign a given PGS plot to a species group. Thirty percent (316) of the 1,382 PGS plots were randomly selected and withheld for model validation. The stand-level estimates of biomass density for each species group were then correlated to stand height and crown closure (mid-value) measurements reported at the remaining 70% (966) of the PGS plots, using both multiple linear and non-linear regression procedures. The models were validated using a paired *t*-test between predicted and "observed" biomass density and an examination of the prediction bias across sets of five species groups for each of low, mid-range and high biomass density classes.

A biomass density value was estimated for each polygon in the AVI coverage of the study region by applying the best stand-level regression model to the height and crown closure attributes. Subsequently, a thematic map of estimated biomass density was created. As a further validation, the trends in the modelled biomass estimates were compared to independently calculated volume estimates within the AVI coverage, by species group.

5.1.4 Biomass modelling results

5.1.4.1 Tree-level biomass estimates

The pooled tree measurement data from the published reports for the two independent data sources (Singh 1982, 1984; Manning et al. 1984) showed strong, overlapping relationships with D^2H (i.e., DBH squared times tree height) for all four "pure" species groups (**Figure 5.2**). Non-linear allometric regressions were strong and highly significant, with low RMSE (**Table 5.1**). Scatterplots of the validation data for predicted biomass with the biomass data from the literature also suggests the model predictions were excellent given the input source data used (**Figure 5.3**).

Table 5.1 Results, by species group, for regressions between tree biomass and D^2H for pooled biomass dataset. Model: $y = b_0(D^2H)^{b1}$

Species Group	R^2	RMSE	Reg. Coeff.	
			b_0	b_1
Pine	0.97	23.1	0.048	0.903
SwFir	0.98	27.4	0.060	0.870
SbLt	0.98	14.7	0.028	0.962
Decid	0.96	34.0	0.017	1.005

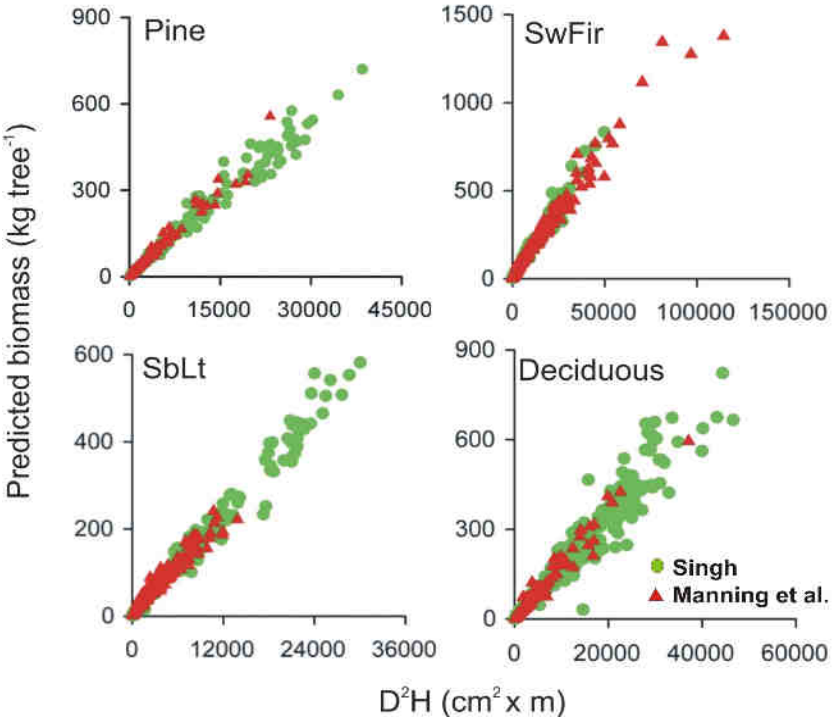

Figure 5.2 Relationships between tree biomass (kg tree^{-1}) and D^2H for trees from both the Manning et al. (1984) and Singh (1982, 1984) datsets, for the four "pure" species groups.

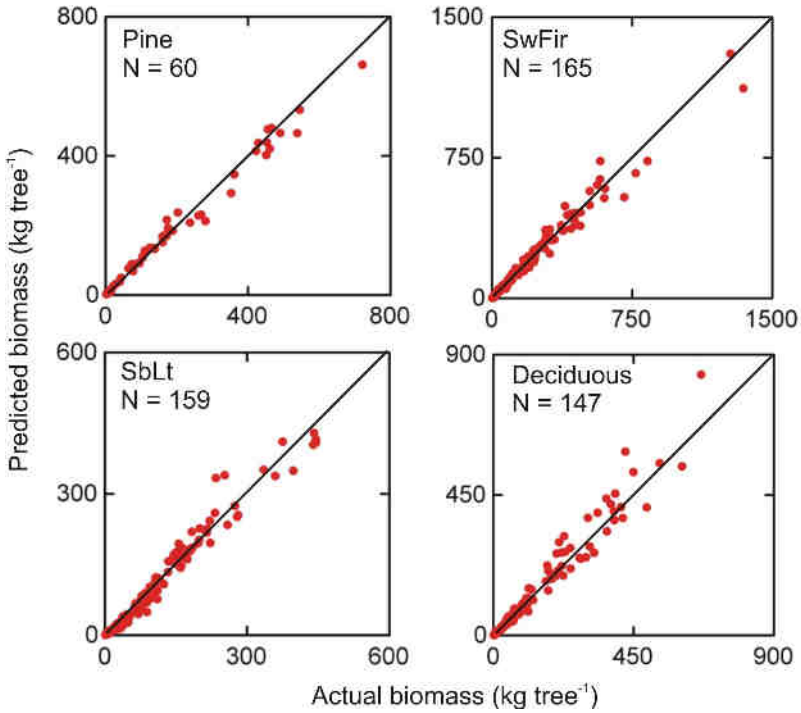

Figure 5.3 Scatterplots showing the relationships between observed and predicted biomass data for the four "pure" species groups.

5.1.4.2 Stand-level biomass estimates

The five species groups were distributed across the study area as: Decid: 5%, Pl: 46%, Mixed: 19%, SbLt: 18%, SwFir: 11% (fractions estimated from crown-closure attributes). Mean biomass densities calculated for PGS plots varied by species group, in the following decreasing order of Decid > Pl > SwFir > Mixed > SbLt (**Table 5.2**). Biomass variability was relatively consistent in its distribution among all species, although data for SwFir were more positively skewed than for the other species groups.

Table 5.2 Descriptive statistics for aboveground biomass density (Mg ha^{-1}) by species groups.

Species group	Range	Mean	Median	S.D.[a]	Skewness
Decid	0.00-362.23	131.74	133.00	86.14	0.34
Pl	0.00-359.91	108.30	96.60	77.51	0.50
Mixed	0.00-325.83	98.78	93.57	73.63	0.57
SbLt	0.03-230.81	63.30	58.09	47.69	0.51
SwFir	0.00-287.17	106.09	104.94	70.45	1.13

[a] S.D.: standard deviation of the mean

Based on tests of different statistical models of the relationship between biomass density (B) and stand height (H) and crown closure (CC), the overall best-fit model was found to be of the general form:

$$(B)^{1/3} = b_0 + b_1(\ln H) + b_2(CC) \quad [5.1]$$

The transformations of the B and H terms served to increase model fit and decrease heteroscedasticity of variance in the data. The model fits attained by species groups were (R^2, RMSE): Decid (0.77, 41.2), Pl (0.77, 37.1), Mixed (0.72, 38.8), SbLt (0.60, 31.7), and SwFir (0.62, 43.5).

5.1.5 Validation of biomass density estimates

The results of paired *t*-tests between the fitted statistical models and the validation datasets suggested there were no statistical differences in estimations of stand-level biomass for Decid ($p = 0.25$), Pl ($p = 0.35$), Mixed ($p = 0.42$), and SwFir ($p = 0.57$). The only exception was for SbLt ($p = 0.03$). I.e., the stand models predicted biomass density values that were statistically equivalent to the observed data for four out of the five species.

Over the range of predicted biomass values, comparisons of observed and predicted data indicate that the greatest prediction bias occurs at the highest biomass densities (**Figure 5.4**), where the statistical model consistently underestimated the observed data with errors up to 80 Mg ha^{-1}. For low and medium biomass densities, there was no consistent prediction bias, though the magnitude of the error ranged from 0 to as much as 30 Mg ha^{-1}.

A comparison of AVI merchantable volume density (m^3 ha^{-1}) and modelled aboveground biomass density showed an obviously positive, though highly scattered, relationship for all species groups (**Figure 5.5**). The difficulty associated with estimating biomass for the SbLt group is illustrated by the more scattered relationship between volume and biomass for this species (although even in this case, the R^2 was 0.6).

The estimates of aboveground biomass at the stand level were applied to the individual AVI polygons to create a map of biomass spatial distribution across the study area (**Figure 5.6**). This map shows that average biomass density generally increases from west to east, suggesting that mean annual productivity is higher towards the east (but particularly north of the mine area).

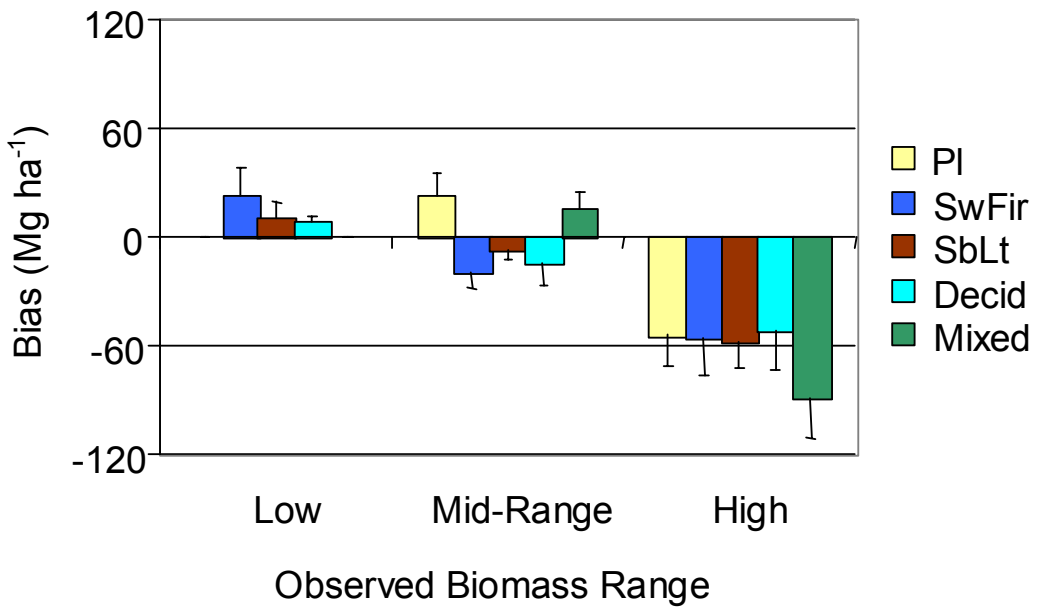

Figure 5.4 Prediction bias between observed and predicted biomass estimates for the five species groups for PGS plots selected from each of the lowest, highest, and mid-range observed biomass density classes-sized biomass values by species group.

5.2 Productivity estimates

We tried to confirm the hypothesis that the biomass data shown in **Figure 5.6** suggested an east–west gradient in productivity. Biomass density data, and merchantable volume estimates taken directly from the AVI data set, could each be divided by stand ages reported in the AVI, to produce maps of estimated average productivity (in terms of m^3 ha^{-1} yr^{-1} and Mg ha^{-1} yr^{-1}, respectively). It should be recognized, however, that the ratio of biomass to age can vary appreciably, with the highest values typically occurring in semi-mature stands and lower values occurring at younger and older stages. At best, this remains a crude estimate of bioproductivity.

5.2.1 Volume productivity

Volume density data were available directly from the AVI database, together with information on the "stand origin" year and the inventory date. Subtracting stand-origin year from the inventory date allowed the stand age to be estimated at the time of inventory. Hence, it was possible to generate an approximate map of stand productivity (Mean Annual Increment, MAI) expressed in m^3 ha^{-1} yr^{-1}. Volume productivity was estimated in this way for approximately 80% of the forested area—after removing records that were missing age or volume information (**Figure 5.7**).

5.2.2 Biomass productivity

Similarly to the estimation of volume productivity (Section 5.2.1), the biomass data presented in **Figure 5.6** were divided by the estimates of stand age developed for each AVI polygon, to create a map of biomass productivity (**Figure 5.8**). These estimates were used subsequently to assess the results of productivity modelling. The overall spatial distributions of biomass density and estimated productivity appear quite similar, indicating that the age-class distribution is broadly similar across the region and across forest types—and supporting the earlier inference obtained from AVI maps of height and crown closure (Section 4.4.1.1). **Table 5.3** presents a summary of the area-weighted averages for stand age, stand height and the

estimates of volume, biomass and productivity derived from the AVI data. These are useful both as a general guide to the stand characteristics in the region and as bases for assessing the results obtained from process modelling (see Section 6).

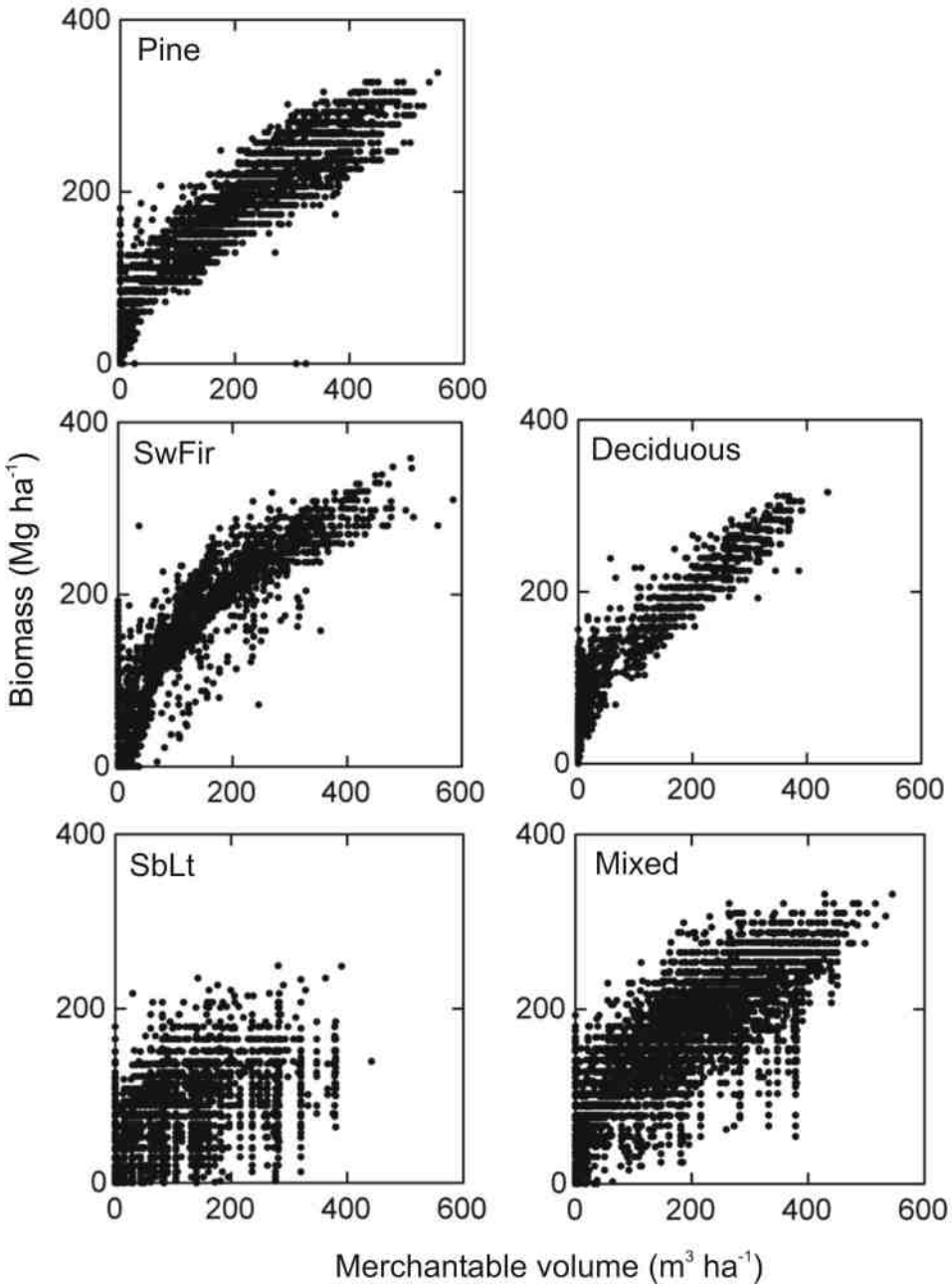

Figure 5.5 Relationships between estimated aboveground biomass density (Mg ha^{-1}) and merchantable volume (m^3 ha^{-1}) for AVI forest inventory polygons in the Alberta study area.

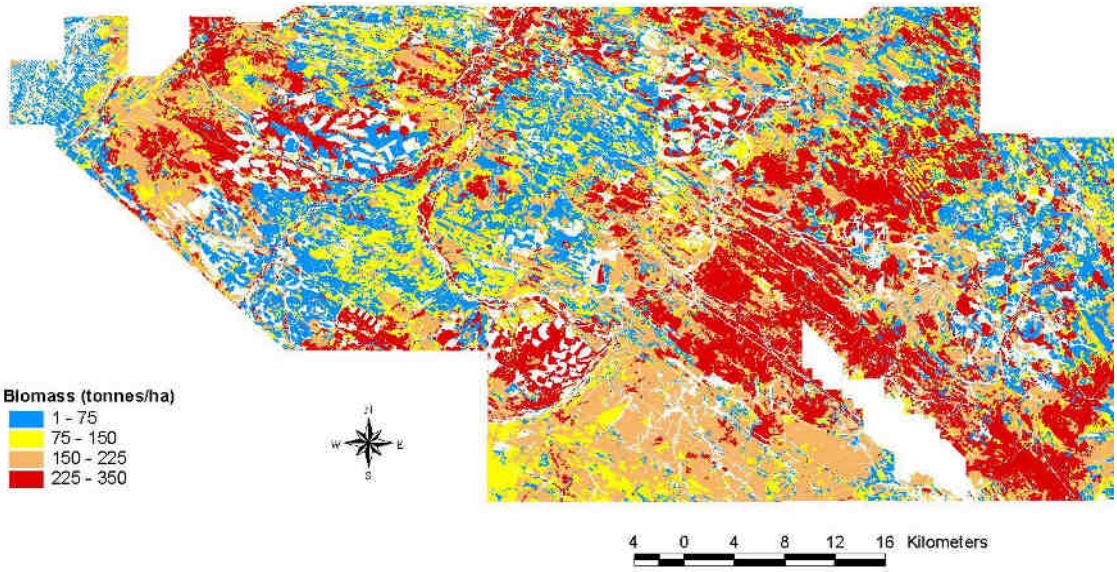

Figure 5.6 Biomass map obtained from stand-level regression models relating biomass (Mg ha^{-1}) estimated from allometric relationships at PGS plot locations to the crown closure and height attributes in the AVI.

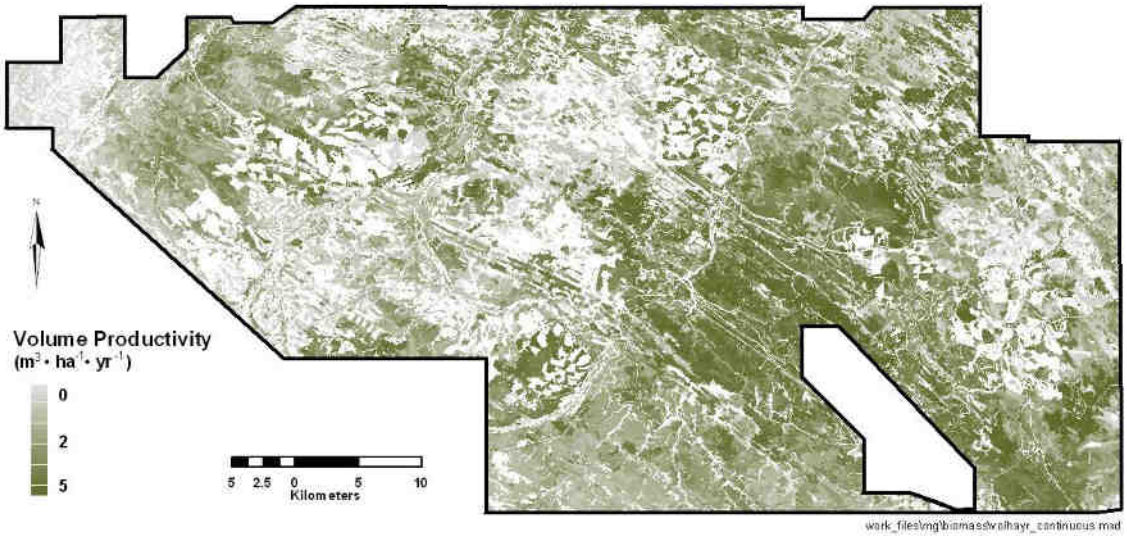

Figure 5.7 Distribution of stand productivity expressed in merchantable wood volume terms (m^3 ha^{-1} yr^{-1}), using data derived from stand volumes reported in the AVI divided by the stand age estimated as the difference between year of inventory and year of origin reported in the AVI.

Table 5.3 Area-weighted average AVI stand-level productivity descriptors by species group.

	Deciduous	Mixed	Pine	SbLt	SwFir
Age	81	96	82	110	109
Height	18.9	16.1	15.9	9.2	17.5
Standing volume (m^3 ha^{-1})	226	213	240	97	178
Volume productivity (m^3 ha^{-1} yr^{-1})	2.3	1.9	2.4	0.8	1.5
Biomass density (Mg ha^{-1})	187	162	176	63	179
Biomass productivity (Mg ha^{-1} yr^{-1})	2.3	1.6	1.9	0.5	1.5

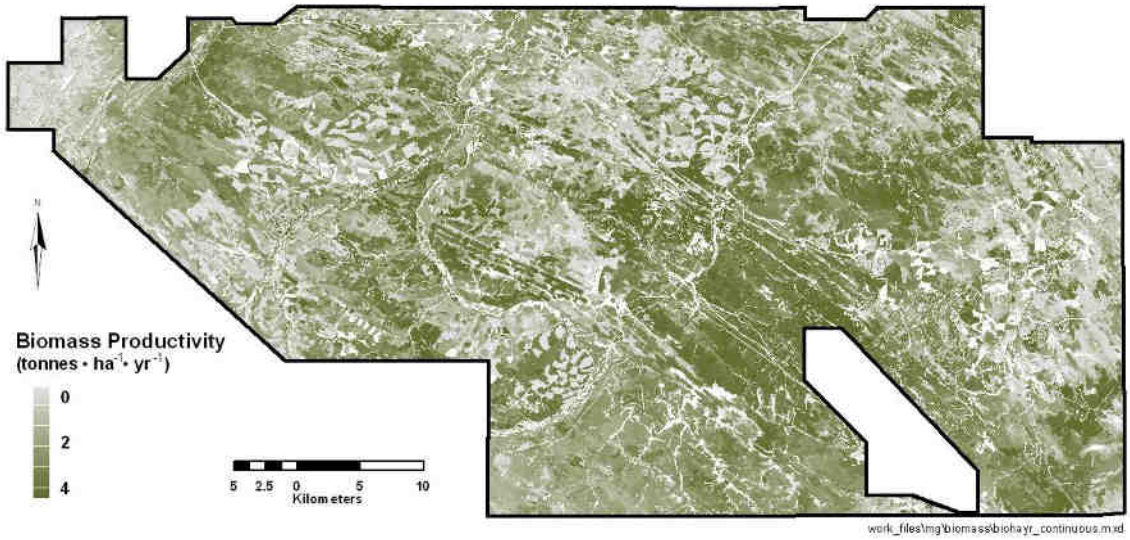

Figure 5.8 Distribution of stand productivity expressed in aboveground biomass terms (Mg ha^{-1} yr^{-1}). Data were estimated from the dry biomass values shown in **Figure 5.6** divided by the stand age (the latter estimated as the difference between year of inventory and year of origin reported in the AVI).

5.3 Stand Density Modelling

5.3.1 Background

Stand density data (stem ha^{-1}) are useful for a range of purposes, including forest management and assessments of biodiversity and wildlife habitat. Density data are also needed for process modelling studies, either as input (as in StandLEAP) or to validate output (as in FORSKA-M). Within the Alberta study area, stand density data were available from the AVI database, but only for about 6% (4,900 of 78,000) of the forest stand polygons. These data were entered from air-photo interpretation carried out by Pearson Timberline in a trial project for Weldwood. An alternative source of stand density data would be to compile them from the PGS plot database, relating them to other stand structural characteristics. Hence, to derive an estimate of stand density for each AVI polygon, a set of predictive functions was needed that would define the relationship between plot-level stand density to attributes of stand structure that were also available for all stand polygons from the AVI.

5.3.2 Methods

Total numbers of trees in 1,278 PGS plots were converted to stand density values (stem ha^{-1}). Stand density was correlated to stand height and crown closure class mid-point values for each of the five species groups (as used for biomass modelling—Section 5.1). Regression R^2 and RMSE were used to assess model fit, and the resulting equations of best fit used to calculate stem density for each polygon in the AVI coverage. Values of stand density reported for the 4,900 trial AVI polygons were correlated to the regression model estimates to assess the level of agreement.

5.3.3 Results and Discussion

Stand density statistics were compiled and summarized for the five species groups (**Table 5.4**). Lodgepole pine (Pl) stands were the most dense. In the Foothills region, pure lodgepole pine stands frequently develop following fire or harvesting, and are often characterized by high stocking densities of 10,000 stem ha^{-1} or greater (Farrar 1995). Such high densities therefore result in wide variation in density among stands, although the coefficient of variation (C.V.), was

not remarkably high compared to other species groups in the Alberta study area. Deciduous stands (dominated by aspen) were the most variable (C.V. of 86%) but not remarkably dense. Peterson and Peterson (1992) report that young, regenerating aspen-dominant stands may achieve stand densities above 100,000 stem ha^{-1}, particularly if developing from suckers. Most deciduous stands reported in the database were older than 10 years, however, so the stand density estimates reported here likely indicate the significant self-thinning that typically occurs before this stage (Peterson and Peterson, 1992). Stands dominated by black spruce were the least dense and the least variable (C.V. of 53%), presumably related to the relatively poor quality sites usually occupied by this species. The white spruce-dominated and mixed stands were of intermediate density and variability.

Table 5.4 Summary statistics, by species group, for PGS stand density data.

	Species Group				
Statistic	**Pl**	**SwFir**	**SbLt**	**Deciduous**	**Mixed**
Sample Size	510	147	114	142	365
Mean	2398.40	1560.01	2065.63	1651.80	1817.59
Standard Deviation	1812.03	1238.77	1084.47	1422.64	1365.61
Coeff. of Variation	0.76	0.79	0.53	0.86	0.75
Minimum	506.17	222.22	86.42	185.18	49.38
Maximum	16987.62	6814.82	5555.57	6987.65	8049.38

Stand density generally displayed an exponential relationship with height, decreasing rapidly at first, but generally levelling off for heights over 10 m. The greatest variation occurred in young and newly regenerated stands (age < 5 years), of 1–5 m height. In a few PGS plots, stand densities were also low (< 500 stem ha^{-1}), however, and therefore inconsistent with the overall trend. Such data points were treated as outliers and omitted from the regression analysis. The low stand density-height values at these plots may in fact reflect high moisture or low nutrient conditions that remained unaccounted for in the models. Stands dominated by black spruce occupy a wide range of ecosites, from upland to wetland areas, which were not adequately captured using only height and crown closure structural attributes.

As might be expected, crown closure was positively related to stand density, although the trends were weak overall, with a high variation in stand densities in each crown closure class. In combination, stand height and crown closure were statistically significant predictors of stand density ($p<0.001$), although the regression results suggested that these variables alone could account for only 14 to 41 % of the variation in stand density by species (**Table 5.5**).

For the 4,900 AVI polygons originally assigned stand density values, there were low to moderate, yet significant ($p<0.001$) correlations with modelled stand density (r values were: Pl 0.56, SwFir 0.64, SbLt 0.71, Decid 0.41, and Mixed 0.38). In general, the regression functions overestimated stem density relative to the reported AVI values at the lower stem density range for all species, and underestimated values at the upper range when compared to the AVI stand density estimates. It should be noted, however, that these correlations are more indicative than reflective of their actual associations and not necessarily an observation of poor prediction. The AVI stand density data were themselves interpreted from aerial photographs and are therefore somewhat subjective estimates.

The data for the PGS plots were compared to the AVI stand density estimates for the polygons in which they were located (**Table 5.6**). Strong and statistically significant correlations were found only for lodgepole pine and for all species—the latter presumably because many of the polygons were dominated by lodgepole pine. Hence it appears that this method of estimating stand density performs reasonably well, if adequate samples are available. It should be noted that

stand attributes (species composition, stand height, crown closure) for the PGS plot often do not agree closely with those reported in the AVI for the corresponding stand polygon. For example, the dominant species found in the PGS plot frequently differed from the dominant species group reported in the AVI. Potential reasons for this poor agreement include: inaccurate location data for the PGS plot centroid; digitizing inaccuracies in the AVI coverage; recent disturbance events (primarily logging); and, of course, spatial variability in stand composition.

Table 5.5 Results for regressions of PGS plot stem density on stand height and crown closure for five species groups. [Model: $(\text{stem ha}^{-1})^{1/3} = b0 + b_1(\text{Height}) + b_2(\text{Crown Closure})$]

				Coefficients		
Sp. Class	**N**	**R^2**	**RMSE**	**b_0**	**b_1**	**b_2**
Pl	510	0.25	1574.94	13.58	-0.281	0.053
SwFir	147	0.30	1042.65	13.08	-0.303	0.035
SbLt	114	0.14	1009.97	13.07	-0.250	0.044
Decid	142	0.41	1072.36	12.59	-0.354	0.071
Mixed	365	0.28	1164.66	12.99	-0.297	0.043

Table 5.6 Summary statistics for comparison of stand density derived from PGS plot data with stand density estimated from AVI crown closure and height in the corresponding stand polygon.

Species	**N**	**r**	**P level**
Lodgepole pine	247	0.59	<0.001
SbLt	34	0.06	0.74
SwFir	36	0.30	0.08
Deciduous	25	0.15	0.49
Mixed	115	0.12	0.21
All species	457	0.48	<0.001

An attempt was made to validate the AVI stand density estimates obtained from air-photo interpretation, by overlaying the PGS plots on top of the 4,900 AVI polygons and comparing the values. Only 28 AVI polygons were found to contain a PGS plot site. There was no significant correlation for these observations (r = 0.02)—which could be due to the small sample size. It is also possible that the locations of the PGS plots are not always representative of average conditions existing in the stand polygons.

Comparison of the air-photo interpretation estimates to those derived here (N = 4,900) showed only a weak, statistically significant relationship, which suggests that at least one of these methods gives inferior results. Because the stand density estimates derived from AVI stand height and crown closure data and relationships obtained from the PGS data, compare more favorably to the PGS data set, it seems reasonable to conclude that these estimates are also superior to the stand density data previously estimated from air-photo interpretation.

As a first-approximation, this work provides an approach to modelling stand density for the entire study region. However, since stand density is determined by many factors including: site moisture and nutrient conditions; stand species composition, structure, and age; competition; and disturbance factors, a more detailed ecological framework is really needed for future density modelling efforts.

5.4 Leaf Area Index (LAI) mapping

5.4.1 Background

Leaf area index (LAI) is an important measure of canopy structure that influences many biological and physiological processes associated with the terrestrial biosphere (Welles, 1990), including: canopy interception of rain and snowfall, evapotranspiration, photosynthesis, and the exchanges of radiant, sensible and kinetic energy between vegetation and atmosphere (Pierce and Running, 1988; Gholz, 1982; Gower and Norman, 1991). Although LAI has been defined in various ways, the generally preferred definition now follows that of Chen and Black (1992), who proposed that LAI be reported as *one half the total intercepting area per unit ground surface area*. LAI has also been recognized as the most important variable for characterizing the structure of vegetation canopies over large areas at broad spatial scales using satellite remote sensing data (Running and Coughlan, 1988). Thus, LAI information is often a key input to many terrestrial ecosystem models (Running and Coughlan, 1988; Running and Hunt, 1993; Liu et al., 1997).

Optical, allometric, and satellite remote sensing methods can all be employed to estimate LAI. Optical methods typically estimate LAI based on the proportion of beam radiation intercepted by the canopy. Allometric methods estimate LAI from statistical models that relate leaf area to other measures of tree structure. A particularly common method derives from the pipe model theory (Shinozaki et al. 1964a,b), which proposes that the cross-sectional area of conductive xylem in tree sapwood is strongly correlated to the actively transpiring foliage area. Sapwood area can often be related to basal area calculated from DBH measurements. As a component of the present study, tree basal area – sapwood basal area functions were derived by species and used to estimate tree sapwood basal area and, subsequently, leaf area at several selected PGS plots within the study region. The satellite remote sensing method is based on the relationship between ground-based optical LAI measurements, and their associated image-based reflectance values. This relationship could then be used to assign an LAI value to each image pixel, and thence to construct an LAI map for the entire study region. The objectives of this work were:

1. Estimate and compare LAI estimates using optical, allometric, and satellite remote sensing methods; and
2. Produce a local map of stand-level LAI for the study region (derived from Landsat-TM imagery) to be used in productivity modelling efforts.

5.4.2 Methods

Briefly, the steps involved in measuring and mapping LAI were as follows:

1. Collect and process optical LAI measurements at a sample of PGS plot locations.
2. Collect tree core samples for lodgepole pine, white spruce, trembling aspen and black spruce species, and derive the best regression models relating total basal area to sapwood basal area estimated from these tree core samples.
3. Estimate leaf area for each PGS plot tree using allometric sapwood basal area to leaf area relationship coefficients compiled from the literature, and aggregate the tree leaf areas to a plot-level LAI value.
4. Compare allometric LAI estimates with optical LAI measurements.
5. Relate the optical LAI measurements to satellite spectral response values and use the relationship to produce a satellite-image based LAI map of the study area.

5.4.2.1 Collect and process optical LAI measurements

The optical method of estimating LAI used in this study was a rapid, non-destructive approach that employs field-portable electronic light sensitive instruments. In simple terms, these

instruments base their measurements on the percentage of solar radiation transmitted through the canopy. Two optical instruments were employed: the Li-Cor LAI-2000 Plant Canopy Analyser and the TRAC ("Tracing Radiation and Architecture of Canopies"). The LAI-2000 measures beam radiation penetrating the canopy with five sensors arranged in concentric rings to measure light levels at mean zenith angles of 7^0, 23^0, 38^0, 53^0 and 67^0 (Li-Cor Inc., 1991). LAI-2000 readings were obtained at 1.3 m above ground and at 10 locations within the stand at each selected PGS plot location (located at 10 m intervals along two parallel 50 m transects). The TRAC measures LAI of "clumped" canopies typical of stands that are either dominated by conifers or contain mixtures of species (Chen and Cihlar, 1995). Correct estimation of the "shoot agglomeration" factor, or "foliar clumping index" is an essential input for estimating absorbed PAR, and hence canopy photosynthesis. The theory of the TRAC is that it measures canopy gap sizes, and hence the fraction of the canopy that is *not* occupied by foliage (the "gap fraction"), to provide an estimate of the clumping index. Once this has been established, the effects of non-random spatial distribution of foliage on LAI measurements can be quantified, and thus used to correct the optical LAI measurements made with the LAI-2000 (Chen et al. 1997). Combining the LAI measurement of the LAI-2000 with the canopy clumping index derived from of the TRAC has been shown to produce significantly more accurate estimates of LAI than the use of the LAI-2000 alone, particularly in conifer-dominated forest canopies (Chen et al. 1997).

A sampling approach was created to select a subset of active PGS plots at which LAI would be measured in the field. Initially, the forest stands mapped in the AVI were reclassified to produce a simple map based on a structure of four dominant species (lodgepole pine, white spruce, black spruce, deciduous) in two height classes (<15 m, >15 m) for three ecoregions (Upper Foothills, Lower Foothills, and Montane natural regions). The active PGS plots were overlaid on this map and a subset selected for field sampling based on accessibility and the desire to sample as broad a range of forest types as possible within the study area. During summer 2000, optical LAI measurements were carried out at 27 PGS plots distributed across the study area as illustrated in **Figure 5.9**. Additional fieldwork included locating the plots and recording GPS coordinates, and remeasuring the trees in these plots.

5.4.2.2 Tree core sampling and derivation of total to sapwood basal area relationships

While the optical measures of LAI provided a rapid means of sampling LAI non-destructively, they were limited by sample size and needed some means of validation. Allometric methods were the only means of deriving LAI values that could be compared to the optical methods other than destructive sampling (which was neither feasible nor permitted in the PGS plots). During the summer of 2001, tree cores were extracted from trees outside the buffer zones of PGS plots for the four species (lodgepole pine, N = 77; white spruce, N = 29; black spruce, N = 33; and trembling aspen/balsam poplar, N = 45). Tree diameters were measured and used to compute basal area including bark thickness. Provincial tree outside bark and inside bark models were used to compute basal area excluding bark (Huang 1994). Sapwood basal area was computed as the difference between the basal area inside bark and the inner basal area of the wood located at the zone of the sapwood transition to the pith.

Scatterplots of tree basal area against sapwood basal area were created for each species to explore potential relationships. A simple linear regression, a non-linear allometric power function, and a non-linear square root transform function, based on the "Transform Both Sides" methodology (Ryan, 1997), were employed for each species. The latter method aims to correct for non-homogeneity of variance by transforming both sides of the equation by some factor. Model results were compared by assessing the R^2/RMSE statistics. These models were then applied to the Weldwood PGS plot database to compute tree sapwood basal areas. The resulting allometric functions could then be applied to estimate tree-level leaf area.

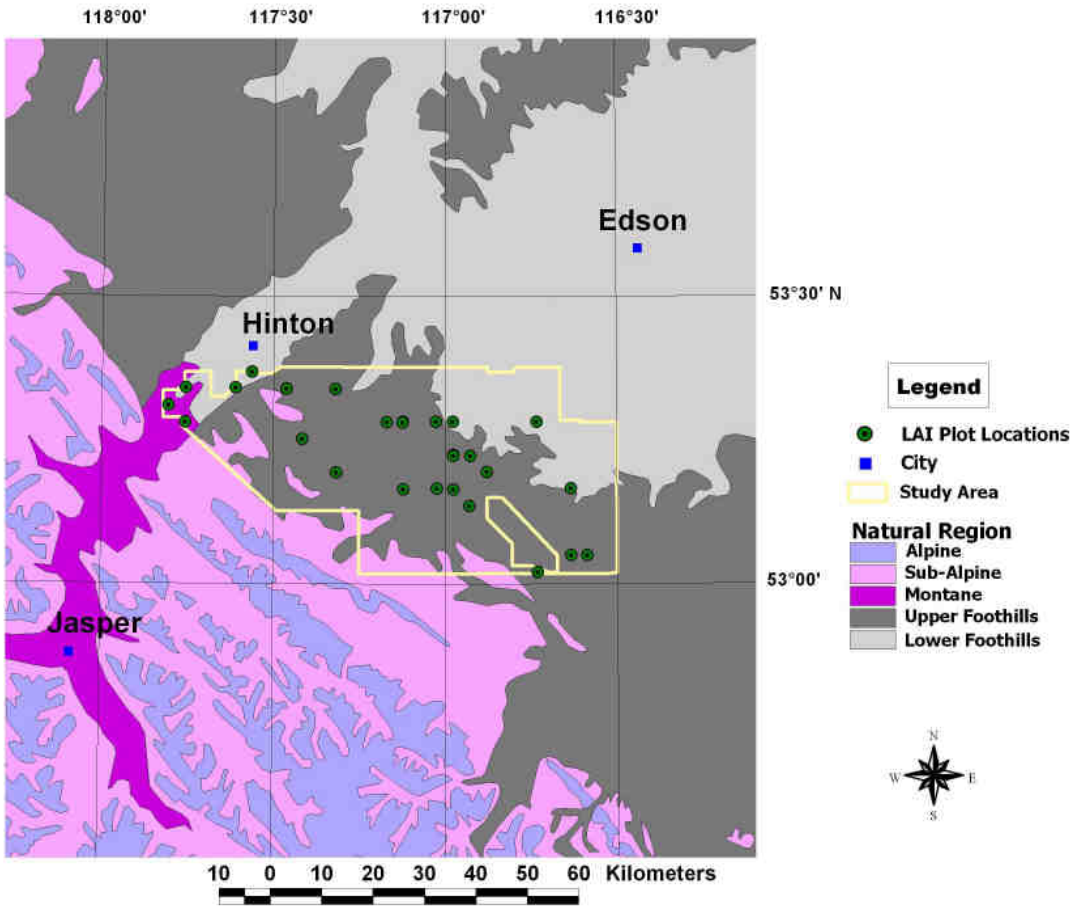

Figure 5.9 Map of study area depicting location of optical LAI measurements.

Tree data were obtained from the Weldwood PGS database for the 27 plots selected for optical LAI measurement. Other than the plot ID and area, only the most recent tree measurements were used, including: species, DBH, height, age, tree status, and mortality code attributes. The data were filtered to remove all dead or missing trees from the database records.

The overall best-fit regression model was used to calculate sapwood basal area from tree basal area for each species. Tree core data were not available to derive functions for certain species. As a result, functions for Aw, Sw, and Sb were used for PbBw, Fa, and larch species, respectively. There were a total of 978 Pl, 164 Sw, 844 Sb and 521 Aw trees at the 27 PGS plots for a total of 2,507 tree records for which individual tree leaf area could be calculated.

5.4.2.3 Estimating LAI at PGS plot locations

A search of the research literature was undertaken to obtain suitable Leaf Area:Sapwood Basal Area linear proportion coefficients, which could then be used to estimate leaf areas for each tree. Plot-level LAI was then derived by dividing the total leaf area for all trees in the plot by the PGS plot area.

5.4.2.4 Comparison of allometric LAI estimates with optical LAI measurements

The allometrically-derived LAI values were compared statistically to the optically-derived LAI dataset (i.e., for 27 data pairs). Both datasets were tested for normality and were determined to display non-normal distributions. Non-parametric Kruskal-Wallis comparisons were therefore carried out, for each of three species groups (Deciduous, Coniferous, and Pl). It

was possible to keep Pl separate because a much larger sample was available than for the other species. Subsequently, LAI values derived from both methods were also tested for a relationship by computing a non-parametric Spearman's rank correlation coefficient.

5.4.2.5 Derivation of LAI map from satellite data

The satellite remote sensing approach to leaf area was employed to create a map of leaf-area index (LAI) by relating the ground-based optical measurements of LAI at the 27 PGS plot locations to vegetation indices derived from remote sensing imagery using a statistical model. Commonly, the *simple ratio* (SR) or the *normalized difference vegetation index* (NDVI) are used for this type of operation. However, the vegetation index values over open forest canopies obtained from these indices tend to be overestimated because of underlying vegetation, such as grasses, that contribute greatly to the measured signal. Hence, these high image-based vegetation index values do not correlate well with the low LAI ground-based optical values over open canopies. For our study, we used the *reduced simple ratio* (RSR) developed by Brown *et al.* (1993). This method is based on the SR but introduces a correction factor for open canopies based on their short-wave infrared (SWIR) response. The RSR was derived from the 8 September 1999 Landsat-TM reflectance image (after orthorectification and top-of-atmosphere correction) using:

$$RSR = \frac{NIR}{RED} * \left[1 - \frac{(SWIR - SWIR\min)}{(SWIR\max - SWIR\min)} \right] \qquad [5.2]$$

where *RED*, *NIR*, and *SWIR* terms represent the pixel reflectance values in the red, near and middle infrared portions of the electromagnetic spectrum, respectively. *SWIRmin* and *SWIRmax* are the median infrared reflectance values from completely closed and open canopies respectively. Careful attention must be given when extracting these two values from the scene as they tend to occur over water bodies and exposed rock or roads. Previous studies applying the RSR suggest using ancillary forest crown closure data (e.g., inventory data) to locate open and closed canopies on the image in order to retrieve the minimum and maximum SWIR values (Nemani *et al.*, 1993; Brown *et al.*, 2000). When ancillary crown closure data are not available, visual interpretation of composite imagery (e.g., TM5 [red], TM4 [green], TM3 [blue]) may be used to discriminate between open and closed canopy stands to select the minimum and maximum values. In our case, the PGS plot data were available and the SWIR (TM5) image layer was sampled for each crown closure class at a total of 481 plot locations.

After applying equation 5.2 to the remote sensing data, the resulting RSR image layer was then sampled for the 27 locations where field optical measurements existed. For each location, the average of a 3×3 window of pixels was extracted. The average RSR values were then plotted against the optical LAI values measured in the field. The resulting relationship was then applied to the pixel values to generate the complete map.

5.4.3 Results

5.4.3.1 Optical LAI measurements

Based on the measurements from the LAI-2000 and the TRAC, LAI values ranged from 0.8 in a young regenerating stand of balsam poplar to a maximum of 8.1 in a mature, dense, upland black spruce stand (**Table 5.7**).

5.4.3.2 Relationship between total basal area and sapwood basal area

Tests of various regression functions relating total basal area (TBA) to sapwood basal area (SBA) suggested that fits using non-linear power functions were marginally superior (**Table 5.8**). In particular, b_2 coefficients and scattergrams for Pl and Sw data displayed a non-linear trend that was best represented using the allometric relationship—possibly because TBA and SBA are geometrically related. Trends for Sb and AwPb were closer to linear (b_2 coefficients

close to 1.0), which was likely due to lack of samples at larger tree sizes. In addition, the use of a simple linear function assumes a normal data distribution, but coefficients of variation for TBA and SBA indicated that these distributions were in fact highly skewed to the right (**Table 5.9**)— which precluded the correct use of least-squares analysis for this dataset. The "Transform Both Sides" non-linear approach employs a square root transformation of both TBA and SBA and uses non-linear regression to fit the model. This approach provides comparable regression results to the other two methods, but increases variance homogeneity, so may be a superior alternative for future modelling.

Table 5.7 Computed optical LAI measurements at sampled PGS PLOT locations.

Plot	LAI	Weldwood AVI photo	AVI field call
1	2.95	C23AW7SW2PB1 - 1890	B22Sw6Aw4/A14Sw7Aw3
2	2.93	C9SB9SW1 - 1870	C9Sb6Pl3Aw1
3	2.81	B11PL10 - 1968	B9Pl10/B4Pl5Sb5
4	6.24	C23PL10 - 1880	C23Pl10
5	1.77	C23AW10 - 1907	C23Aw10
6	3.13	C23AW7PL2SW1 - 1890	C22Aw7Pl2Sw1
			B21Aw7Pl3/B16Sw6Aw2Pl2 (plot)
7	6.44	B22PL9PB1 - 1920	B24Pl10
8	8.10	C14SB10 - 1867	D16Sb10
10	4.28	B5PL8AW2 - 1970	B9Pl6Aw4
11	5.28	C22PL10 - 1880	B24Pl5Sw3Aw2/C7Fb7Sw3 (Plot)
12	5.37	C25PL10 - 1830	C28Pl9Aw1/A15Sw10
13	4.27	B18PL8SB1SE1 - 1880	B18Pl10/A12Pl9Sb1
14	3.63	B23SW9PL1 - 1870	B23Pl10/B10Sw6Pl4
15	3.18	C23PL10 - 1870	C22Pl10/A6Sw10
16	4.44	C11PL9AW1 - 1962	C12Aw6Pl4/B5Aw7Sb2Pl1
17	3.32	B13SB10 - 1800	B14Sb10/A8Lt5Sb5
18	2.54	B4SW9PB1 - 1961	B10Sw9Pb1
20	1.68	B6SW8BW1PB1 - 1960	B12Sw5Pb3Bw2/A4Sw6Pb4
			A6Sw6Pb4 (plot)
21	0.79	A6PB10 - 1970	A6Pb10/A2Sw6Pb4
			(A15Sw in overstory)
25	3.27	C18PL10 – 1896	B15Pb6Sw2Pl2/B10Sb8Pb1Pl1
29	2.88	B15SB10 – 1800	B14Sb9Pl1/B8Sb10
33	4.35	D12PL8SB2 – 1950	D15Pl10/C8Sb10
36	5.58	B19PL8SW2 – 1900	A19Pl10/B8Sb10
37	6.62	B19PL9SW1 – 1900	B21Pl9Sw1/B12Sw10
41	6.24	C11PL9AW1 – 1962	C16Pl9Aw1/B10Sb7Aw2Pl1
43	3.35	C25Aw7Pl2Pb1 – 1930	C26Aw8Pl2

A summary of research studies providing linear coefficients relating tree leaf area (LA) to SBA is presented in **Table 5.10**. Additionally, Gower et al. (1997) presented allometric functions for calculating LA from tree DBH, for Aw and Sb, but to remain consistent, we used the literature search to provide the best linear coefficient estimates available for all species in our dataset. The LA:SBA coefficients adopted were: Aw/Pb/Bw: 0.10, Pl: 0.24, Sb/Larch: 0.29, Se/Sw/Fb: 0.35.

Table 5.8 Statistical results from modeling SBA as a function of TBA by species.

Species group/ Sample size	Model [a]	R^2	RMSE	Coefficients b_0	b_1	b_2
Pl	1	0.86	38.07	25.26	0.40	
N = 77	2	0.88	35.54	-9.28	3.31	0.69
	3	0.86	39.40	13.15	0.44	
Sw	1	0.87	52.83	31.65	0.38	
N = 29	2	0.9	47.10	-25.58	5.17	0.64
	3	0.86	55.76	13.56	0.43	
Sb	1	0.93	10.20	16.58	0.26	
N = 33	2	0.93	10.28	12.18	0.45	0.92
	3	0.93	10.26	15.02	0.27	
AwPb	1	0.85	55.21	-1.40	0.60	
N = 45	2	0.85	55.86	-0.28	0.57	1.01
	3	0.85	56.49	5.54	0.56	

[a]Model 1: $SBA = b_0 + b_1*TBA$
Model 2: $SBA = b_0 + b_1*(TBA)^{b2}$
Model 3: $SBA^{0.5} = (b_0 + b_1*TBA)^{0.5}$

Table 5.9 Descriptive statistics for total basal area (TBA) and sapwood basal area (SBA) derived from tree core data.

Variable	Statistic	Species Aw	Pl	Sb	Sw
	N	45	77	36	29
TBA	**Mean**	306.5	239.7	181.3	263.1
	Min	11.2	7.7	23.4	13.1
	Max	1,097.8	1,002.5	1,220.6	1,398.0
	S.D.	220.9	240.1	230.8	353.6
	C.V.	0.7	1.0	1.3	1.3
SBA	**Mean**	182.4	119.7	60.9	132.4
	Min	8.2	6.7	13.0	8.8
	Max	590.0	447.4	289.6	485.8
	S.D.	143.3	102.8	54.7	145.0
	C.V.	0.8	0.9	0.9	1.1

Table 5.10 Literature sources of allometric functions to estimate leaf area by species.

Study	Location	Species	Comments	Coefficients
Gower et al. 1999	BOREAS: Saskatchewan and Manitoba	Aw, Sb, Pj	Reported as allometric equations LA = f(Dbh)	none stated
White et al. 1997	Montane ecosites in Montana	Various	Used published LA:SA ratios in calculations	none defined
Long and Smith 1988	S.E. Wyoming	Pl	Found non-linear LA:SBA relationship; attributed to differences in stand conditions (stem density, site quality etc.	0.084 (Pl) on average
Gower et al. 1987	Subalpine/ Montane in Washington	Pl, Larch, Douglas-fir	Used Log-Log regressions between LA and SBA	0.14 (Pl), 0.29 (Lt)
Keane and Weetman 1987	Williams Lake, BC	Pl	Increase in LA:SBA coefficient from high (100,000) to low (5000) density Pl stands	0.15 to 0.07(Pl) *
Hungerford 1987	Montana	Pl	Found that stand density did not affect LA:SBA relationships.	0.14 (Pl) *
Dean and Long 1986	N. Utah	Pl	Relationships differed between sapling and mature stands of Pl (ie. age difference)	0.18 (mature Pl) 0.10 (sapling Pl)
Marchand 1984	N. Vermont/ New Hampshire	Fb	Only article found for balsam fir	0.67 (Fb)
Pearson et al. 1984	S.E. Wyoming	Pl	Highest ratios for old growth/low density stands and *vice-versa*	0.15 to 0.28 (Pl)
Waring et al. 1982	W. Oregon	Se, Pl	Found linear LA:SBA relationships; cautioned that ratios will likely be less linear and different with breast height SBA measures relative to crown sapwood measurements	0.35 (Se) 0.15 (Pl)
Kaufmann and Troendle 1981	Subalpine Colorado	Se, Pl, Fa, Aw	Found linear LA:SBA relationships	0.29 (Se), 0.18 (Pl), 0.75 (Fa), 0.08 (Aw)

5.4.3.3 Comparison of allometric and optical LAI estimates

Non-parametric comparisons indicated no significant differences between allometric and optical estimates of LAI for both deciduous (N = 7) and coniferous (N = 8, i.e., excluding lodgepole pine) species groups with p values of 0.91 and 0.82 respectively. The estimates for "pure" lodgepole pine stands differed significantly (N = 11; p = 0.04). Comparisons for all samples combined also indicated a significant difference (N = 26; p = 0.03).

Overall, allometric and optical LAI were positively correlated (Spearman's r = 0.55). Based on the distribution of basal area by species (**Table 5.11**), plots were classified further into one of six species groups (aspen, lodgepole pine, black spruce, white spruce, mixed conifer, mixed deciduous) for graphical comparison (**Figure 5.10**). The plots for Pl display the greatest variation, with the allometric estimates generally underestimating the optical measurements. This lack of close agreement, particularly for Pl stands, may be due to the use of the linear LA:SBA coefficients drawn from the literature. Further, the relationship between SBA and LAI in lodgepole pine has been shown to vary significantly (and often non-linearly) among stands, due to their wide variation in age, stem density, canopy position and site quality (Dean and Long 1986; Hungerford 1986; Keane and Weetman 1986; Long and Smith 1988). Given that sites were selected to account for the range of conditions found in the study area, it was inevitable that these

factors will have varied in our samples (**Table 5.12**), but the relatively small sample size makes it difficult to explore the possible effects of stem density and age by species on LAI estimation. Further, some of the variation in the results is likely due to limitations in applicability of the allometric functions from the literature to the study area. Another possible factor is the limited sampling precision of the optical measurements. Clearly, both the allometric and optical methods are indicators more than absolute measures of leaf area.

Table 5.11 Distribution (%) of basal area by species for Alberta study area LAI sample plots.

	Species								Classified	
Plot	**Aw**	**Bw**	**Fb**	**Lt**	**Pb**	**Pl**	**Sb**	**Sw**	**Species group**	**AVI field call**
1	33				3			65	Conif. mixed	B22Sw6Aw4/A14Sw7Aw3
2	9					91			Pl	C9Sb6Pl3Aw1
3						88	12		Pl	B9Pl10/B4Pl5Sb5
4						95	5		Pl	C23Pl10
5	100								Aw	C23Aw10
6	53					40	2	5	Decid. mixed	C22Aw6Pl2Sw1 B21Aw7Pl3/B16Sw6Aw2Pl2 (plot)
7						100			Pl	B24Pl10
8						9	90	1	Sb	D16Sb10
10	9					91			Pl	B9Pl6Aw4
11	15		7			48		30	Conif. mixed	B24Pl5Sw3Aw2/C7Fb7Sw3 (plot)
12	15		0			82	2	1	Pl	C28Pl9Aw1/A15Sw10
13						96	4		Pl	B18Pl10/A12Pl9Sb1
14	5		3			88	3		Pl	B23Pl10/B10Sw6Pl4
15						98	1	1	Pl	C22Pl10/A6Sw10
16	58					38	3		Decid. mixed	C12Aw6Pl4/B5Aw7Sb2Pl1
17				9			70	21	Sb	B14Sb10/A8Lt5Sb5
18					6			94	Sw	B10Sw9Pb1
20		29			29			42	Decid. mixed	B12Sw5Pb3Bw2/A4Sw6Pb4 A6Sw6Pb4 (plot)
21					100				Aw	A6Pb10/A2Sw6Pb4 (A15Sw in overstory)
25					50	13	32	5	Decid. mixed	B15Pb6Sw2Pl2/B10Sb8Pb1Pl1
29						3	97		Sb	B14Sb9Pl1/B8Sb10
33						95	5		Pl	D15Pl10/C8Sb10
36						69	31		Conif. mixed	A19Pl10/B8Sb10
37						95	5		Pl	B21Pl9Sw1/B12Sw10
41	13		3		1	71	12	1	Conif. mixed	C16Pl9Aw1/B10Sb7Aw2Pl1
42						100			Cutover	C2Pl9Aw1/B1Sw5Aw5
43	100								Aw	C26Aw8Pl2

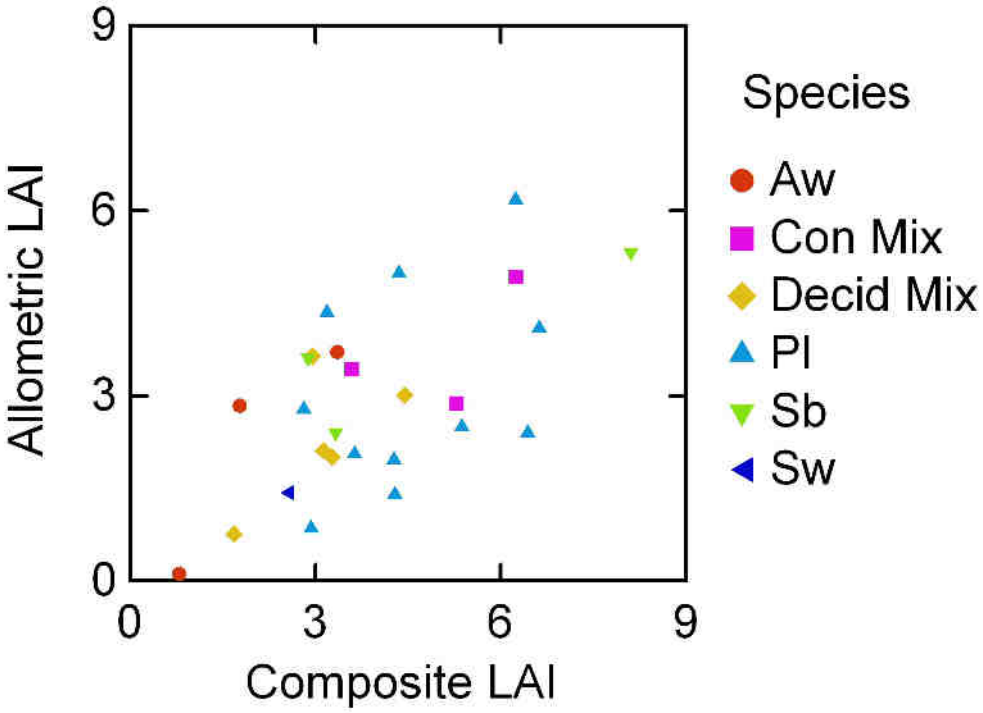

Figure 5.10 The relationship of allometrically-derived LAI with optically-measured composite LAI (a composite of Li-Cor LAI 2000 and TRAC measurements), organised by species group for 27 sites in the Hinton study region.

5.4.3.4 Satellite-derived LAI map.

There was a statistically significant relationship between optical LAI and the satellite remote sensing model based on Landsat-TM RSR ($r = 0.68$, $p < 0.0001$) with a resulting model fit that was used to produce an image map of LAI for the study area ($R^2 = 0.47$, $p < 0.0001$, **Figure 5.11**). The relatively low R^2 and small sample size (27 PGS plots) suggests that further improvements to model prediction and LAI mapping of the study area would be obtained by increasing the sample size and spatial distribution of the field measurements collected. The LAI map (**Figure 5.12**) rendered a spatial pattern of high and low values that compare favorably with the biomass and volume productivity maps (**Figure 5.7** and **Figure 5.8**).

Use of the allometric method to estimate LAI was intended as a means of increasing the number of field samples that could be used. Comparison of the LAI at the PGS plots and their associated estimates from the satellite remote sensing model using Spearman's rank correlation, showed the results differed among species (r values were: Pl 0.15, Sw 0.36, Sb 0.54, Deciduous 0.64, Mixed 0.34). The poor results for lodgepole pine were consistent with the results obtained using the allometric method—which suggests more attention is needed to account for stand structure and site conditions in LAI estimation. These results are not intended to validate one method against another but they emphasize that the challenge in estimating and mapping leaf area lies in the need to create and employ allometric functions based on local data. It suggests an opportunity to pursue further work to improve the mapping of LAI across the study region.

Table 5.12 Stand characteristics and LAI estimates taken from 27 PGS plots in the Alberta study region during summer 2000.

Plot	Area (m^2)	Mean DBH	Mean Height	Stand Age	Density (stem ha^{-1})	Optical LAI	Allometric LAI	Species Group
1	810	22.8	18.4	98	691	2.95	3.64	Conif. mixed
2	405	7.1	5.5	28	1086	2.93	0.85	Pl
3	405	8.8	7.5	33	2370	2.81	2.78	Pl
4	810	19.1	20.3	93	1654	6.24	6.18	Pl
5	810	23.0	21.3	101	1074	1.77	2.84	Aw
6	810	18.3	15.2	100	790	3.13	2.11	Decid. mixed
7	810	31.4	22.5	89	309	6.44	2.40	Pl
8	810	11.2	11.3	94	3901	8.10	5.32	Sb
10	405	7.1	5.4	16	1877	4.28	1.39	Pl
11	810	18.2	13.0	105	617	5.28	2.87	Conif. mixed
12	810	26.2	19.1	99	432	5.37	2.49	Pl
13	810	18.9	14.2	90	531	4.27	1.97	Pl
14	810	20.6	14.8	90	457	3.63	2.06	Pl
15	810	16.1	16.2	126	1457	3.18	4.35	Pl
16	405	7.9	9.3	38	4963	4.44	3.00	Decid. mixed
17	810	14.5	11.5	226	988	3.32	2.40	Sb
18	405	8.6	5.7	34	1012	2.54	1.43	Sw
20	405	6.8	5.5	35	1358	1.68	0.75	Decid. mixed
21	405	7.5	5.6	25	420	0.79	0.11	Aw
25	810	14.3	10.0	99	1062	3.27	2.00	Decid. mixed
29	810	11.3	9.6	187	2457	2.88	3.61	Sb
33	405	9.1	8.9	51	4000	4.35	4.98	Pl
36	810	14.1	11.3	101	1494	3.58	3.43	Conif. mixed
37	810	17.6	16.2	90	1222	6.62	4.10	Pl
41	405	8.7	8.4	38	4617	6.24	4.93	Conif. mixed
42	405	3.3	2.5	6	25			Cutover
43	810	27.5	23.6	107	951	3.35	3.71	Aw

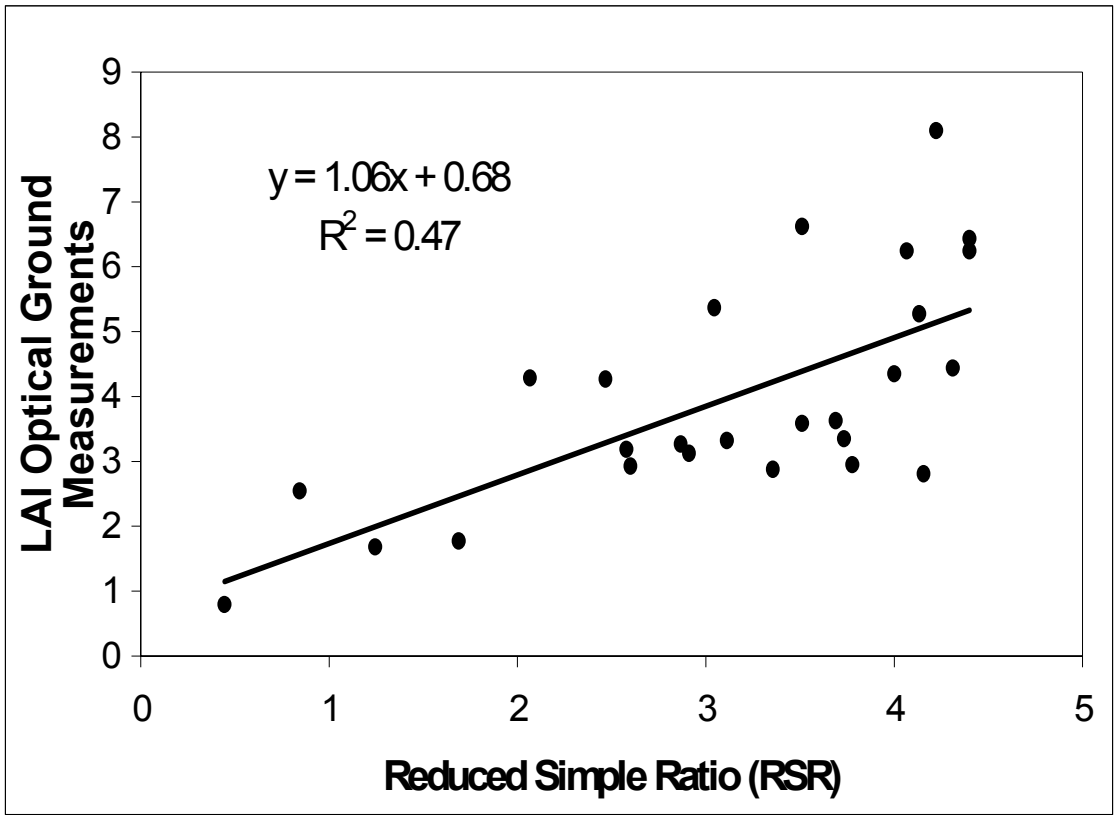

Figure 5.11 Linear regression model relating optical LAI values to image-based RSR values.

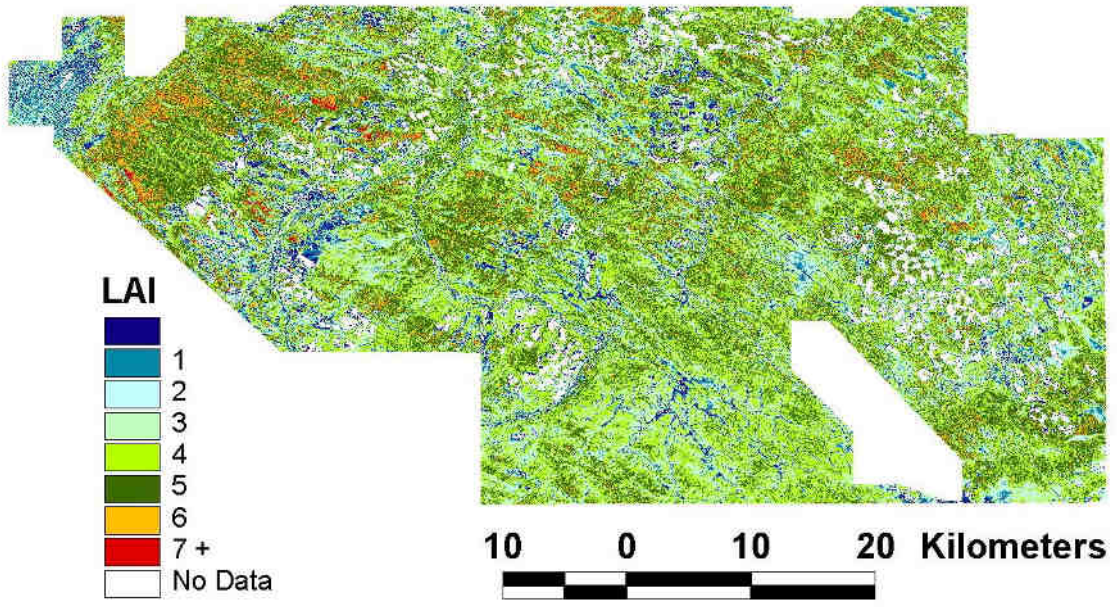

Figure 5.12 Map of Leaf Area Index (LAI) for Alberta study area, derived from Landsat TM imagery.

6 Process Modelling

Parameterizations and tests have been performed for three different models of forest ecosystem processes. Briefly, these models are StandLEAP, FORSKA-M and 4C. StandLEAP is a physiologically-based radiation use efficiency (RUE) type model, developed directly from Landsberg's 3PG model, which estimates forest NPP based on LAI, incoming radiation, topographic data and other climate variables. FORSKA-M is a version of the succession (gap) model first developed by Prentice et al. in Sweden, modified by Marcus Lindner to account for management practices that may compensate for effects of a changing climate. Though less mechanistic in its representation of tree growth than StandLEAP, it is able to simulate competition between species and stand development. The newest model is called "4C" (originated by Bugmann and colleagues), and is still undergoing active development at the Potsdam Institute in Germany. 4C is also a succession-type model, but contains more detailed representations of plant physiology and also accounts for soil decomposition processes. Although our intention is to work with this model in the future, relatively little has been tackled so far, and it will not be discussed further in this report.

6.1 Spatial simulation of Net Primary Productivity using StandLEAP

StandLEAP is a top-down radiation-use-efficiency (RUE) model that computes net primary productivity (NPP) of a forest stand from the fraction of absorbed photosynthetically active radiation (f_{PAR}) (see **Figure 6.1**). Derived from the 3-PG model of Landsberg and Gower (1997), it uses many of the same modifiers to constrain NPP as a function of specific limiting environmental conditions and stand properties including air temperature, soil water content and stand developmental stage. Transpiration is estimated via a water-use-efficiency (WUE) model (Dewar 1997) and is also constrained by limiting environmental conditions in a similar fashion to that of the RUE model. The time step is monthly and the results are summarized on a yearly basis. In order to validate results against permanent sample plots, StandLEAP also simulates stand dynamics through the computation of self-thinning and accrual of standing biomass.

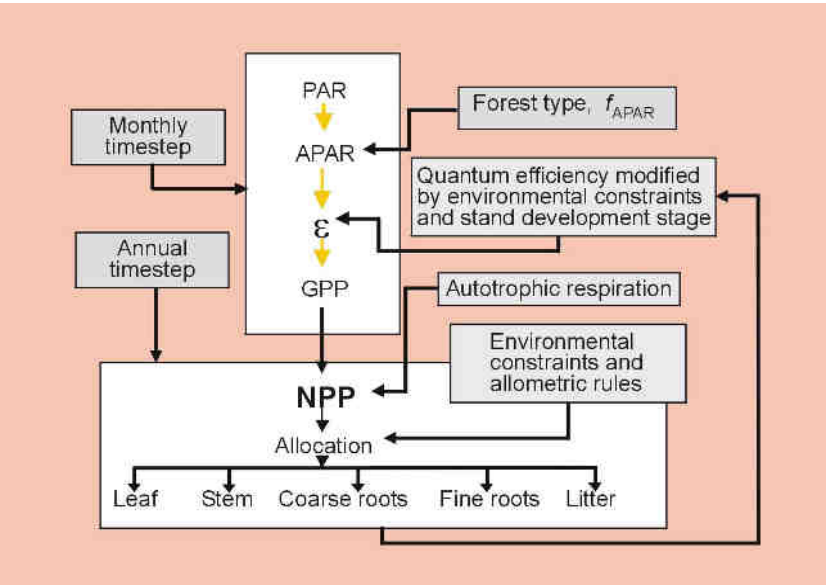

Figure 6.1 StandLEAP schematic description. PAR: photosynthetically active radiation, APAR, PAR absorbed by the canopy, f_{APAR} (= f_{PAR} elsewhere in text): APAR fraction, ε: radiation use efficiency (RUE), GPP: gross primary production, NPP: net primary production.

6.1.1 StandLEAP calibration

StandLEAP is defined to operate at the canopy level and on a monthly time step. These spatial and temporal scales differ greatly from those at which direct and diffuse light are absorbed by the canopy elements (leaves, shoots, branches and stems) to drive photosynthesis. Hence, the process of *scaling up* from the leaf-level and hourly timesteps to the canopy and monthly intervals involves prior use of a more detailed process model (FineLEAP, Raulier et al. 2000, Bernier et al. 2001b), parameterized from field measurements of growth processes. The choice of tree-level processes to be used in StandLEAP, the shape of the functions representing them, and the value of the parameters used in these functions, are all derived from simulations carried out with FineLEAP. A general description is provided here on how StandLEAP was calibrated for three major species in the FMF study area: lodgepole pine, black spruce and aspen, including the data sources used.

6.1.1.1 Shoot-level photosynthesis and transpiration

FineLEAP is a multi-layer canopy gas exchange model in which the layers correspond to classes of foliage of similar photosynthetic characteristics assumed to be subject to a similar average light environment. Shoot needle mass per unit area (specific leaf area, SLA) is used as a covariable to link the shoot photosynthetic properties (mainly photosynthetic capacity and STAR) to the average light environment. The representation of gas exchange is based on the model of Farquhar et al. (1980). Stomatal conductance is simulated using Leuning's (1995) model, which links conductance to shoot net photosynthesis and accounts for the influence of atmospheric humidity (vapour pressure deficit, VPD). Leaf energy balance is taken into account with the iterative procedure of Leuning et al. (1995).

Calibration of StandLEAP from FineLEAP simulations required a complete set of gas exchange measurements (sensitivity of shoot photosynthesis to PAR, temperature and VPD; and characterization of shoot physiological and light-capturing properties with age and its surrounding average light environment). Such a complete set of photosynthetic data was not available for lodgepole pine, so photosynthetic measurements made during the BOREAS campaign (Sellers et al. 1997) on jack pine (*Pinus banksiana* Lamb.) by Dang et al. (1998, BOREAS study TE-09), were used to estimate RUE and WUE and their corresponding modifiers needed for StandLEAP. Unlike balsam fir (*Abies balsamea* (Mill.) Lamb.), but similarly to lodgepole pine, SLA and STAR of jack pine are relatively insensitive to the light environment surrounding the shoots (BOREAS studies TE-09 and TE-12 SSA). This allowed the convenient assumption that the light environment of individual pine shoots was unaffected by their position in the canopy. The shoot clumping index was derived from the work of Chen (1996; see also Section 5.4.2.1). No data or references were found to characterize the shoot boundary layer conductance for jack pine, but information for lodgepole pine (Smith 1980) was used instead.

Prior to the commencement of this study, Stewart (CFS-NoFC) collected a set of photosynthetic measurements on lodgepole pine within the Foothills Model Forest at the site of a thinning trial (1956 Gregg River fire), which, by coincidence, also lies within the ECOLEAP-West study area. These data did not include a sensitivity analysis of shoot photosynthesis to temperature and vapour pressure deficit (VPD), but they were useful to determine whether the Farquhar model parameterized with data for jack pine could adequately predict Stewart's measurements. A relatively good relationship was obtained (**Figure 6.2**), but lodgepole pine photosynthesis was overestimated by 28%. This led to two weeks' of fieldwork at Stewart's study site in summer and fall 2001, with follow-up laboratory analysis. The results of this effort provided the data needed to properly parameterize lodgepole pine photosynthesis responses to temperature and vapour pressure deficit (humidity).

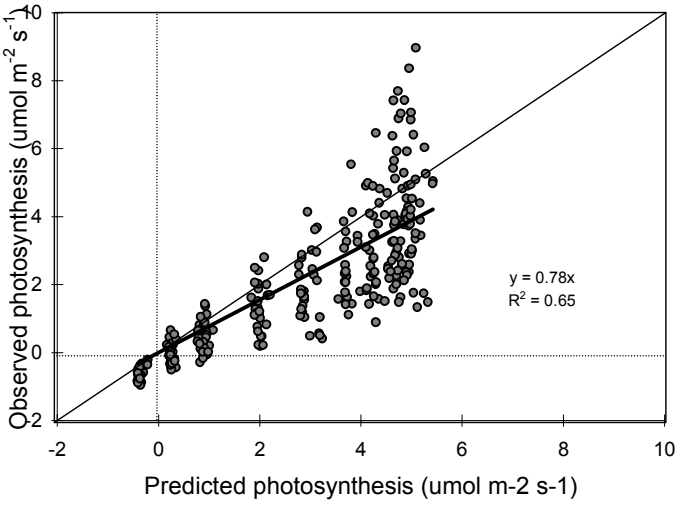

Figure 6.2 Relationship between values of photosynthesis predicted by the Farquhar model parameterized using the jack pine data set (BOREAS TE 09 study) and measurements of net photosynthesis on lodgepole pine (Stewart, 2000).

Laboratory measurements of photosynthesis made on black spruce and trembling aspen during the BOREAS campaign (study TE-09; Dang et al. 1998) were used to estimate RUE and WUE factors for these two species. For black spruce shoots, SLA and STAR were considered constant through the canopy. The leaf boundary conductance for aspen was derived as described by Leuning et al. (1995, their equation E1) and requires the average leaf width, derived from Middleton et al. (1997, their Table 3). No data or references were available to characterize shoot boundary layer conductance for black spruce but measurements of Landsberg and Ludlow (1970) on Sitka spruce (*Picea sitchensis* (Bong.) Carr.) were used instead.

6.1.1.2 Absorption of photosynthetically active radiation (PAR)

The value of the Beer-Lambert light extinction coefficient, when considered at the monthly time scale, depends on leaf area index (LAI) (e.g., Raulier et al. 2000). The values of the parameters used in the function relating extinction coefficient to LAI were derived using FineLEAP. Values for the optical properties of forest canopies (mainly the shoot clumping index and the mean Shoot-to-Area Ratio, "STAR") required by FineLEAP were first derived from Oker-Blom et al. (1991) and Sampson and Smith (1993). Driven by hourly climate data, FineLEAP was then used to simulate the monthly PAR absorption of pure canopies of the major tree species for LAI in the range 2 to 8 m^2 m^{-2} (expressed on a hemi-surface area basis). Three years of hourly climatic records (1994-1996) from the Northern and Southern Study Areas of the BOREAS project (Newcomer et al. 2000) were used for this purpose.

6.1.1.3 Plant respiration

The original respiration submodel in 3-PG was inappropriate for the cold winters typical of central Canada, which tend to decouple respiration rates from photosynthesis. Respiration in StandLEAP is divided into maintenance and growth respiration. Growth respiration was assumed to be independent of temperature and proportional to biomass growth (McCree 1970). Maintenance respiration was predicted using the relationship derived by Ryan (1991), but also modified to account for effects of tissue nitrogen content and temperature. As this last relationship is established at an hourly time-scale, it is numerically integrated over a 24-hour period (Ågren and Axelsson 1980). Nitrogen contents of stem sapwood, foliage and fine and

coarse root compartments for lodgepole pine were found in the literature and averaged (Fahey 1983; Pearson et al. 1987; Prescott et al. 1989; Schoettle 1994).

6.1.1.4 Shoot phenology and frost effects on NPP

Frost delimits the season during which conifer photosynthesis is active and at its optimum. In StandLEAP, the effect of frost is modelled as in PnET II (Aber et al. 1995), where NPP diminishes once the minimum monthly temperature goes below 6°C, independently of the species considered. The phenology of bud burst and shoot elongation in lodgepole pine has evidently received little attention (no reference was found) but Burton and Cumming (1995) indirectly estimated the heat sum required for lodgepole pine buds to burst on the basis of the mean number of frost-free days weighted across its range in British Columbia. Their estimation was used to predict the phenology of bud burst in StandLEAP. The phenology of bud burst was derived from Hogg (1999) for aspen and from Frolking et al. (1996) for black spruce.

6.1.1.5 Allocation and allometry

NPP allocation in StandLEAP is essentially derived from 3-PG and, except for fine roots, depends on allometric relationships established between diameter at breast height (DBH) and the tree biomass compartments (stem, branches, foliage and coarse roots). Fine root allocation is represented as in 3-PG.

For lodgepole pine and aspen, allometric data on trees harvested for ENFOR project P-92 (Singh 1982) were used to calibrate the relationships between DBH, foliage and aboveground woody biomass. Data obtained in ENFOR project P-236 by Ouellet (1983) in Quebec were used to calibrate similar allometric relationships for black spruce. A relationship developed by Comeau and Kimmins (1989) was used to estimate coarse root biomass from DBH and height for the lodgepole pine measured in Singh's (1982) ENFOR project. A similar relationship established by Perala and Alban (1984) for black spruce and aspen was used to estimate coarse root biomass from DBH and height for the trees of these species sampled in the ENFOR projects. These estimates were used in turn to calibrate allometric relationships between DBH and coarse root biomass. Also for black spruce and aspen, ratios between fine root and leaf biomass were derived from data gathered by the BOREAS TE-06 team (Steele et al. 1997; Gower et al. 1997).

Stem sapwood biomass is needed in order to estimate stem respiration. Equations of Ryan (1989) were used with the ENFOR lodgepole pine data to estimate stem sapwood volume and to convert volume to biomass. Data collected by BOREAS team TE-06 (Gower et al. 1997) were used to this effect for black spruce and aspen. Stem sapwood biomass was added to the measured branch biomass without bark to estimate the aboveground sapwood biomass. An allometric relationship could then be derived between DBH and aboveground sapwood biomass.

6.1.1.6 Self-thinning and stand developmental stage effect on NPP

Self-thinning is expressed in StandLEAP, as in 3-PG, through the relationship between average aboveground biomass and stand density (stem ha^{-1}). For lodgepole pine, all PGS plots in the Alberta study area (including those marked in the database as inactive), containing more than 80% lodgepole pine (expressed in basal area terms) were used to calibrate the self-thinning relationship. Similarly, all temporary sample plots (TSP) in Québec, containing more than 80% aspen or black spruce in basal area terms, were used to calibrate the self-thinning relationships for these species. As explained in Section 6.1.1.5, aboveground biomass for each species was estimated using the allometric relationships established by Singh (1982) and Ouellet (1983).

Empirical self-thinning relationships were derived using data from the plot databases constructed for each species. Plots were first subdivided into stand density classes. Within each density class, the 5% of plots with the highest biomass were retained for the analysis. Classes with fewer than five selected plots were dropped from the analysis. The selected plots were then used to estimate the parameters of the self-thinning relationship.

The phenomenon that tree growth decreases with increasing tree size is well captured in growth and yield tables, but it has yet to be well-explained from a process perspective (e.g., Ryan and Yoder, 1997). In 3-PG, this effect was taken into account by tracking the ratio of age to maximum age—although "maximum age" is a vague concept. Instead, in StandLEAP, the effect of ageing is activated after aboveground biomass growth of the average tree has passed its maximum. Determination of aboveground tree biomass corresponding to maximum growth is based on the empirical evidence contained in site index (SI) curves for the dominant trees in the stand. The SI curves of Cieszewski and Bella (1989) were used to develop relationships between total height and aboveground biomass, using the Singh (1982) relationships. Similarly, for black spruce and aspen, the SI curves of Pothier and Savard (1998) were used to establish a relationship between total height and aboveground biomass derived from Ouellet (1983).

6.1.2 StandLEAP validation against Weldwood sample plot data

6.1.2.1 Selection of Permanent Growth Sample Plots

The ecological classification system adopted for West-Central Alberta (Beckingham et al. 1996) subdivides its territory into (1) *regions* and *subregions* (areas characterized by distinctive regional climates as expressed by vegetation); and (2) *ecosites* within subregions (ecological units that develop under similar environmental influences – i.e., climate, soil moisture and nutrient regime). According to the ecological classification of the PGS plots, four subregions and 12 forest ecosites occur within the Weldwood FMA (**Table 6.1**).

Table 6.1 PGS plots in the Weldwood FMA, classified by ecological subregions and forested ecosites. Values are percentages of the total number of PGS plots.

	Ecosite												Total
Subregion	**B**	**C**	**D**	**E**	**F**	**G**	**H**	**I**	**J**	**K**	**L**	**M**	**ecosites**
Lower Foothills	0.1	4.0	3.4	10.8	6.4		2.6	1.7	3.3	1.0	3.0	0.4	36.7
Upper Foothills	0.7	8.0	7.7	15.9	8.0	0.4	4.3	5.2	0.7	2.0	3.0	0.5	56.3
Montane	0.4	1.8	0.3		0.1	0.1							2.7
Subalpine	0.1	0.7	2.4	0.1	0.3	0.5		0.3					4.3
Total subregions	1.3	14.4	13.7	26.9	14.7	1.0	6.8	7.2	3.9	3.0	6.1	0.9	100.0

The ecological classification presented in **Table 6.1** was too detailed for an initial validation of StandLEAP in the Alberta study area, however, because forest cover-types also needed to be considered. A simplification was therefore carried out based on two factors: water regime and spatial extent. Since water regime is generally considered the most limiting factor for tree growth in the Foothills, ecosites within the Lower and Upper Foothills subregions were regrouped into mesic (C to F ecosites) and hygric (G to L) "ecotypes" (Beckingham et al. 1996, pp. 7-2 and 8-2). The database contained about 300 randomly selected PGS plots, representing approximately 15% of the total number of plots that were classified as forested ecosites. Random sampling assured that the most important types were represented in approximate proportion to their true area representation across the FMF. Consequently, any of the regrouped types with samples fewer than 30 plots were discarded (30 being a reasonable number for a trustworthy estimation of confidence intervals). In addition, the Montane and Subalpine subregions, and "B" ecosites (**Table 6.1**) within the Upper and Lower Foothills subregions, were also rejected for the initial validation of StandLEAP. These adjustments led to a greatly simplified ecological classification that still accounted for 88% of the PGS plots but provided an excellent discrimination of the main forest types (**Table 6.2**). The dominant species are black spruce in the

hygric type and lodgepole pine in the mesic type. Aspen and white spruce mostly appear in the mesic types while tamarack appears only in the hygric types.

Table 6.2 Simplified ecological classification considered for StandLEAP validation. Values are percentages of a random sample of 300 PGS plots located throughout Weldwood's Forest Management Agreement area.

	Ecotype		
Subregion	**Mesic**	**Hygric**	**Total**
Lower Foothills	23.8	11	34.8
Upper Foothills	38.9	14.5	53.4
Grand Total	62.7	25.5	88.2

Cover types for the PGS plots were grouped following the AVI classification using an approach similar to that presented in **Figure 4.10**:

- when the dominant species contributed 80% or more of canopy cover, the stand was considered monospecific;
- when the dominant species contributed less than 80% of canopy cover, mixed forest types were defined by the first two species in the AVI classification;

This simplified forest type classification (**Table 6.3**) only recognizes four species (aspen, lodgepole pine, black spruce and white spruce) but still accounts for 81% of the total number of active PGS plots.

6.1.2.2 Validation of StandLEAP calibration for lodgepole pine

Table 6.3 summarizes the classification of the Weldwood PGS dataset for all active PGS plots in the FMA. Of these, 272 located in the study area fell into the lodgepole pine forest type (i.e., more than 80% lodgepole pine in basal area terms), and were used to validate the StandLEAP calibration for lodgepole pine. Validations were limited to 10 simulated years because StandLEAP does not account for changes in stand structure and composition due to forest succession. Initially, StandLEAP was used to estimate growth in PGS plot aboveground biomass between the first (1957-1959) and second (1962-1966) measurements (a period that varies between 5 and 8 growing seasons). Of these plots, 92 were discarded, either because there was evidence of significant disturbance between the two measurement dates or because large numbers of new stems appeared in the second measurement. In this last case, the criterion for exclusion was an error of prediction in biomass increment falling outside the interval defined by the average prediction error for the entire PGS plot data set, plus or minus 3 times the standard deviation.

The validation runs were initialized with values of aboveground biomass (Mg ha^{-1}) and stand density (stem ha^{-1}) taken from the PGS plot data. Simulated changes in these variables were then compared with the changes observed between the two measurement dates for each plot.

The average *observed* aboveground biomass increment of lodgepole pine was 1.69 ± 0.16 Mg ha^{-1} yr^{-1} with a prediction error (PE) of 0.16 ± 0.15 Mg ha^{-1} yr^{-1} (9.5%). The aboveground biomass increment predicted by StandLEAP was within the PE, but on average biomass growth was overestimated by about 10% (**Figure 6.3**a). StandLEAP greatly underestimated stem mortality (**Figure 6.3**b).

Table 6.3 Simplified ecological classification of active Weldwood PGS plots developed for StandLEAP validation. Values are numbers of PGS plots falling in each class. This classification was also used in the selection of PGS plots for calibrating and validating FORSKA-M (Section 6.2).

Simplified forest types	Simplified ecotypes				Total	Cumulative percentage
	LFh	LFm	UFh	UFm		
Pl	13	143	65	540	761	33.1
Sb	147	4	192	7	350	48.4
AwPl	1	83	3	61	148	54.8
PlSb	22	31	34	54	141	60.9
Sw	16	58	17	44	135	66.8
AwPl	1	92		31	124	72.2
PlSw	1	39	8	56	104	76.8
SbSw	17	9	14	3	43	78.6
AwSw	1	33		9	43	80.5
AwSb	2	3		1	6	80.8
All types	221	495	333	806	1855	

Simplified forest type codes	
Aw	Trembling aspen
Pl	Lodgepole pine
Sb	Black spruce
Sw	White spruce

Simplified ecotype codes	
LFh	Lower Foothills - hygric
LFm	Lower Foothills - mesic
UFh	Upper Foothills - hygric
UFm	Upper Foothills - mesic

The approximate equivalence between observed and predicted biomass increments results in a strong correlation between predicted and observed plot biomass density (**Figure 6.3**c), when used in conjunction with initial plot biomass measurements. Most of the stands used for validation are situated within the mesic Upper Foothills (193 plots out of 272) and no significant relationship appears when considering the PE as a function of five ecotypes (**Figure 6.4**b; note the Subalpine ecotype was included here for easier assessment of PE). Model predictions of stand density were evidently biased (**Figure 6.4**a), although the absolute importance of this bias is small given the small number of plots in high-density stands. Compensating errors may cause the lack of large bias even when mortality is underestimated.

The exact causes of the observed bias, and of the overall errors, are difficult to identify, but are likely linked to the interaction between known uncertainties in the modelling process. The first of these uncertainties is the biased representation of canopy photosynthesis for lodgepole pine resulting from the absence of gas exchange data on lodgepole pine for model calibration (**Figure 6.2**). The second is the obvious shortcoming in the prediction of mortality (**Figure 6.3**b) resulting from a common, but simplistic representation of the self-thinning rule in stands. The third uncertainty lies with the canopy-light interaction, and is caused by the absence of a coherent dataset on the geometric properties of lodgepole pine canopy that would include shoot properties such as STAR These uncertainties influence values of WUE and RUE obtained from FineLEAP, as well as the computation of growth and mortality processes in StandLEAP. Although there are presumably other sources of uncertainty, these three (and particularly the first two) are likely to be the major contributors to the observed error.

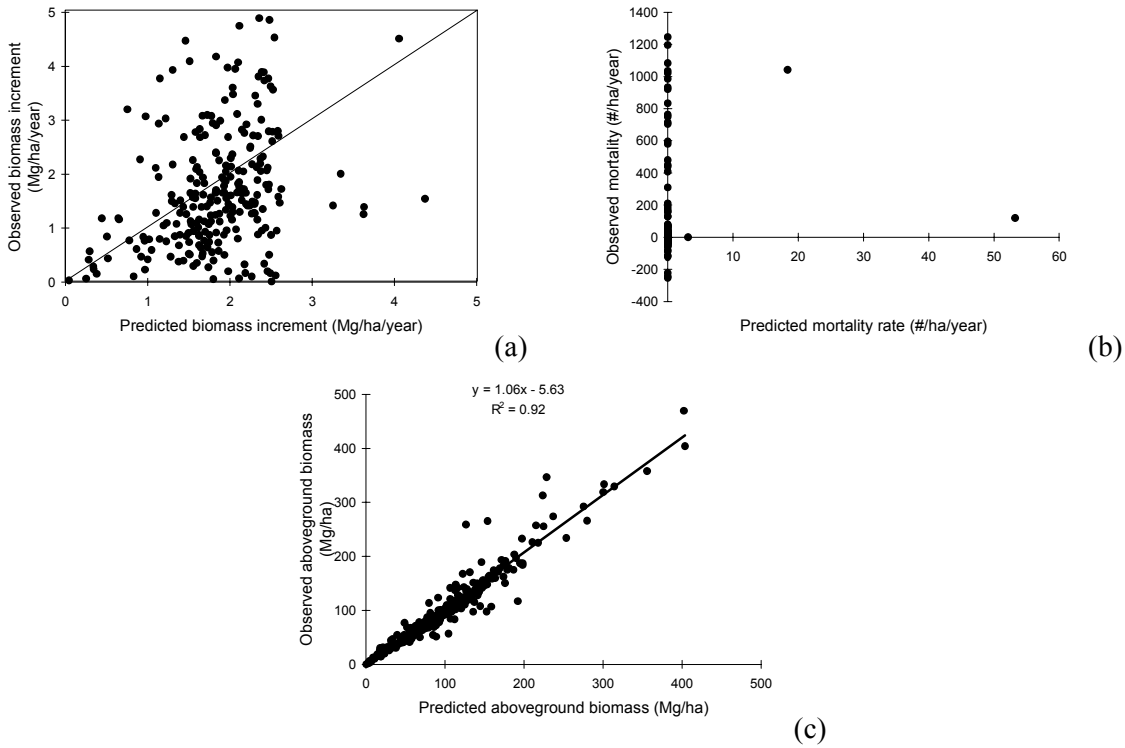

Figure 6.3 Comparison between predicted and observed aboveground biomass increment, stem mortality and aboveground biomass in undisturbed PGS plots in lodgepole pine-dominated stands (>80% of total basal area) between the first and second PGS plot measurement campaigns.

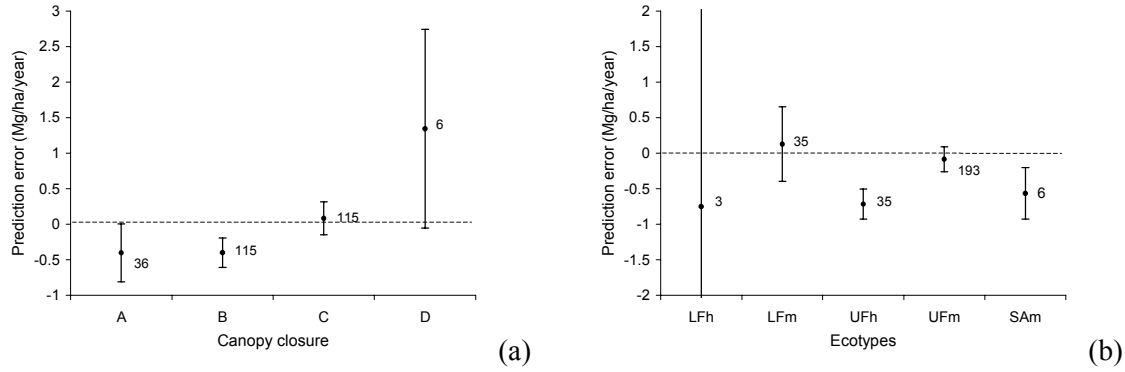

Figure 6.4 Relationship between (a) stand canopy closure (A=6 to 30%, B=30 to 50%, C=50 to 70% and D=70 to 100%) or (b) the simplified ecotype classification (see Table 3) and the prediction error of aboveground biomass increment. The number of observations is given with the confidence intervals.

6.1.3 Application of StandLEAP

Once StandLEAP has been calibrated and validated, relatively few input data sets are required to run it for an extensive area. The model can be used in two different modes, depending on the method by which PAR absorbed by the canopy (APAR) is to be estimated. In real mode, APAR is estimated directly from f_{PAR} calculated from remote sensing data or other sources (Section 4.4.3). In potential mode, APAR is estimated from simulated foliage characteristics. These are derived from changes in aboveground biomass density and stand density, which are initialized from observed data (Sections 5.1 and 5.3). The remaining input data requirements included latitude, elevation, slope and aspect, soil texture, and forest type (species classes). The GIS coverages described in Sections 4.2 and 4.4 were used for this purpose:

1. soil polygon coverage re-classified by texture codes [Section 4.2];
2. AVI polygon coverage re-classified and dissolved into simplified forest types, covering as much of the forested area as possible [Section 4.4.1.3];
3. for each forest polygon, estimated total aboveground biomass density [Section 5.1];
4. for each forest polygon, estimated average stand density [Section 5.3];
5. for each forest polygon, estimated value of f_{PAR} [Section 4.4.3].

StandLEAP also requires daily climate data to estimate seasonal photosynthesis, respiration and evapotranspiration. The routines of Régnière and St-Amant (2002; see also Section 4.3) are called by StandLEAP to create a realistically varying daily climate record for each set of stand coordinates, based on the 1961-90 normals observed at surrounding climate stations.

6.1.3.1 Soil texture

The soil texture data layer derived from the Hinton area soil survey report (Dumanski et al. 1972) and CanSIS modal profiles was used (Section 4.2). The caveats concerning texture of alluvial and underlying clayey soils apply here and may need to be accounted for in the future, depending on the sensitivity of the model to soil texture effects on moisture availability.

6.1.3.2 Simplified AVI classification of forest types

The composition of each stand polygon in the AVI coverage can be comprised of up to five different species, resulting in a very large number of possible species combinations. As such, only stands where the two most dominant species summed to more than 80% of the stand's crown closure were used to classify the AVI into 12 meaningful species types, as described in Section **4.4.1.3**. These 12 groupings proved not completely satisfactory, however, because StandLEAP simulations could sometimes cause the proportions of the major species to adjust to the point where they would classify into a different undefined class. Two classes were added (SbPl and AwSw) to ensure that this could not occur. The final set of species classes used in StandLEAP simulations is given in **Table 6.4**.

In the current simulations, therefore, a forest type the occupying a stand polygon or map pixel is assumed to consist of either one, or a mixture of two dominant species. These forest types are used to access a table of species-specific parameters (such as those used for calculating f_{PAR}; see Section **4.4.3**). Parameters were available for lodgepole pine, black spruce and trembling aspen, but not for white spruce (which was therefore represented by the parameter set for balsam fir). For species other than lodgepole pine, parameter values were obtained mostly from the intensive study site in Montmorency Forest in southern Québec (Bernier et al. 2001).

Table 6.4 Species classes used for StandLEAP simulation of NPP and biomass increment for forest stands in the Alberta study area. Species codes as in **Table 4.4**.

Species class	Code	gFracMin[a]	gFrac_int[b]
Non-forest/water	0	0	0.0
Pl	1	0.8	0.2
Sb	2	0.8	0.2
Sw	3	0.8	0.2
Aw	4	0.8	0.2
AwPl	5	0.5	0.3
SbSw	6	0.5	0.3
PlAw	7	0.5	0.3
PlSb	8	0.5	0.3
PlSw	9	0.5	0.3
SwAw	10	0.5	0.3
SwPl	11	0.5	0.3
SwSb	12	0.5	0.3
SbPl	13	0.5	0.3
AwSw	14	0.5	0.3

[a] gFracMin: minimum fraction of basal area of the most dominant species
[b] gFrac_int: domain of amplitude of variation of the basal area percentage for the dominant species

6.1.3.3 Aboveground biomass, stand density and f_{PAR}

As reported in Sections 5.1 and 5.3, biomass and stand density values were derived from the AVI data, using allometric relationships applied at individual PGS plots. Section 4.4.3 explains the importance of f_{PAR} and how it was estimated from AVI data and the LandsatTM-5 remote sensing image data.

6.1.4 Results

6.1.4.1 Real mode

In real mode, APAR is estimated directly from the f_{PAR} value, computed in turn from the Simple Ratio obtained from satellite imagery (adjusted for sun angle). In this mode, StandLEAP provides only NPP estimates, as further processing of the NPP to compute allocation to the stand biomass compartments (stems, branches, foliage, fine and coarse roots) would require an estimate of the mean tree size. The results presented here come from a sample of 3,000 stand polygons randomly selected across the pilot region. The simulated NPP fell within the expected range (but compare these with the results obtained by running StandLEAP in potential mode, Section 6.1.4.2).

Results showing the response of NPP to LAI immediately indicated that the sensitivity of the relationship obtained between the Simple Ratio (SR) and f_{PAR} was too low for trembling aspen, so that almost all aspen stands were "locked" at the maximum f_{PAR} (and hence at "maximum" LAI) (**Figure 6.5**c, **Figure 6.5**d and **Figure 6.6**b). The effect is however not too important given the apparently low sensitivity of NPP to high LAI for this species (**Figure 6.5**c), as compared to black spruce, for instance (**Figure 6.5**b), which exhibits an almost linear increase for LAI up to 8.

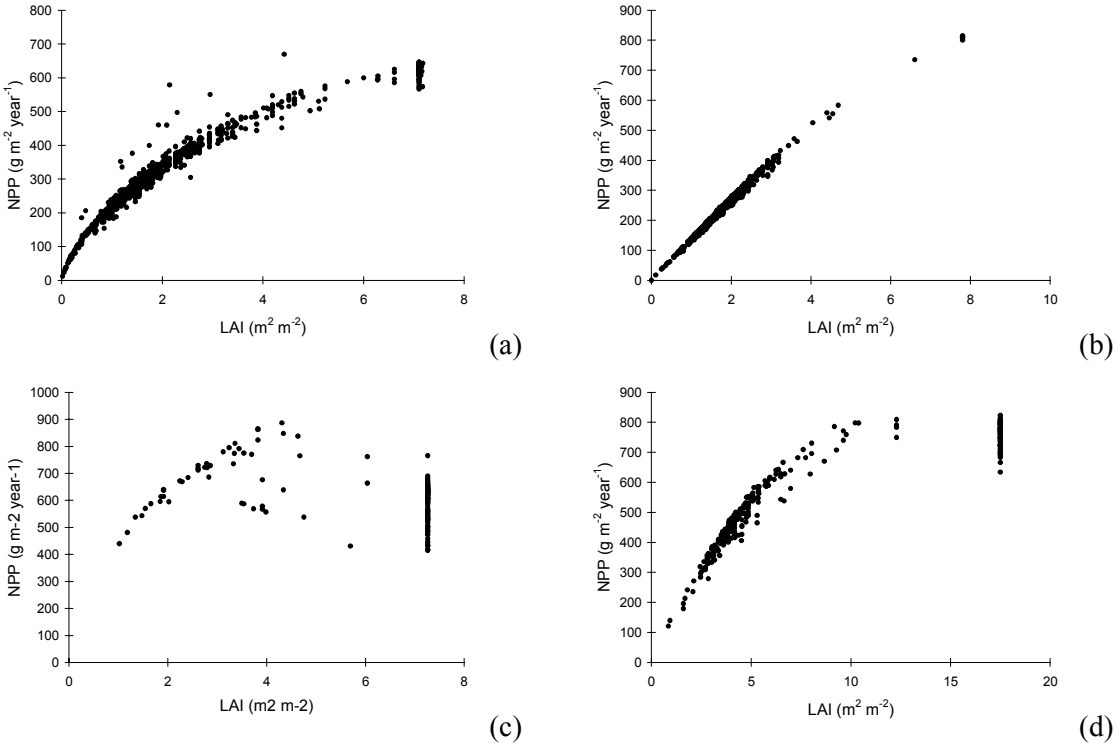

Figure 6.5 Relationship between NPP prediction and the LAI value derived from f_{PAR} for: (a) lodgepole pine, (b) black spruce, (c) aspen and (d) balsam fir.

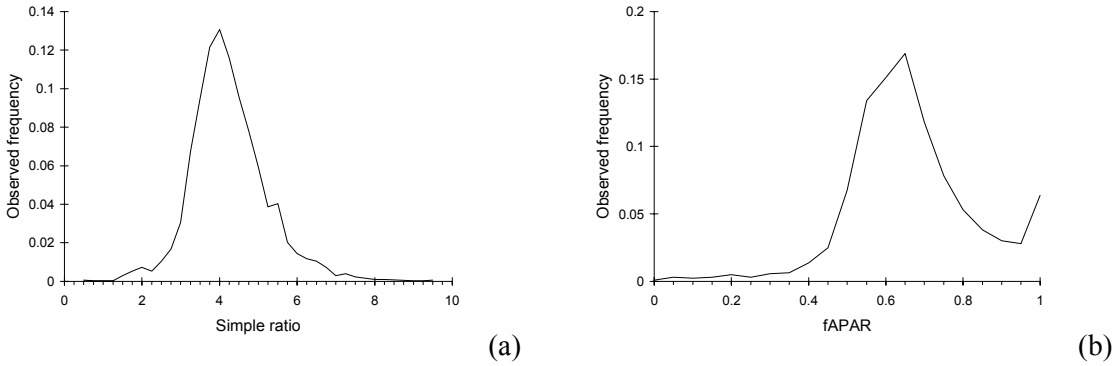

Figure 6.6 Observed frequency distributions of: (a) Simple Ratio, and (b) estimated f_{PAR} for the Alberta study area (based on a sample of 3000 stand centroids).

6.1.4.2 Potential mode

In potential mode, APAR is estimated from the initial aboveground biomass and stand density specified in the inputs. Before any calculations are performed, a procedure in StandLEAP verifies whether the biomass and stand density are reasonable compared to species-specific self-thinning lines. For the simulations reported here, these self-thinning lines were calibrated from PGS plot data for lodgepole pine in the Alberta study area and from temporary sampling plot (TSP) measurements in Québec for black spruce, aspen and balsam fir. The results showed that in many stands, the mean tree biomass exceeded the maximum allowed by the self-thinning line (**Figure 6.7**). As a consequence, the verification procedure reduced simulated stand density to the point where it fell below the self-thinning line.

Total and aboveground NPP estimates were in the range of expected values (**Figure 6.8**; see also Comeau and Kimmins 1989; Prescott et al. 1989; Gower et al. 1997; Goetz and Prince 1998; Smith and Resh 1999; Kimball et al. 2000).

Some estimated LAI values were too high compared to what could be expected for the Foothills Model Forest (**Figure 6.9**), although as noted previously, the tendency for NPP to saturate at high LAI, means that in general this would not result in greatly exaggerated estimates of NPP. No major differences between the leaf biomass to DBH relationships reported by Singh (1982) for Alberta and those by Ouellet (1983) for Québec for black spruce and balsam fir can be found to explain such high values of LAI (**Figure 6.10**). As an alternative explanation, it is possible that the characteristics of self-thinning differ significantly between Quebec and the FMF for both species—and perhaps even for aspen. This strongly suggests that the self-thinning lines need to be recalibrated using more local data.

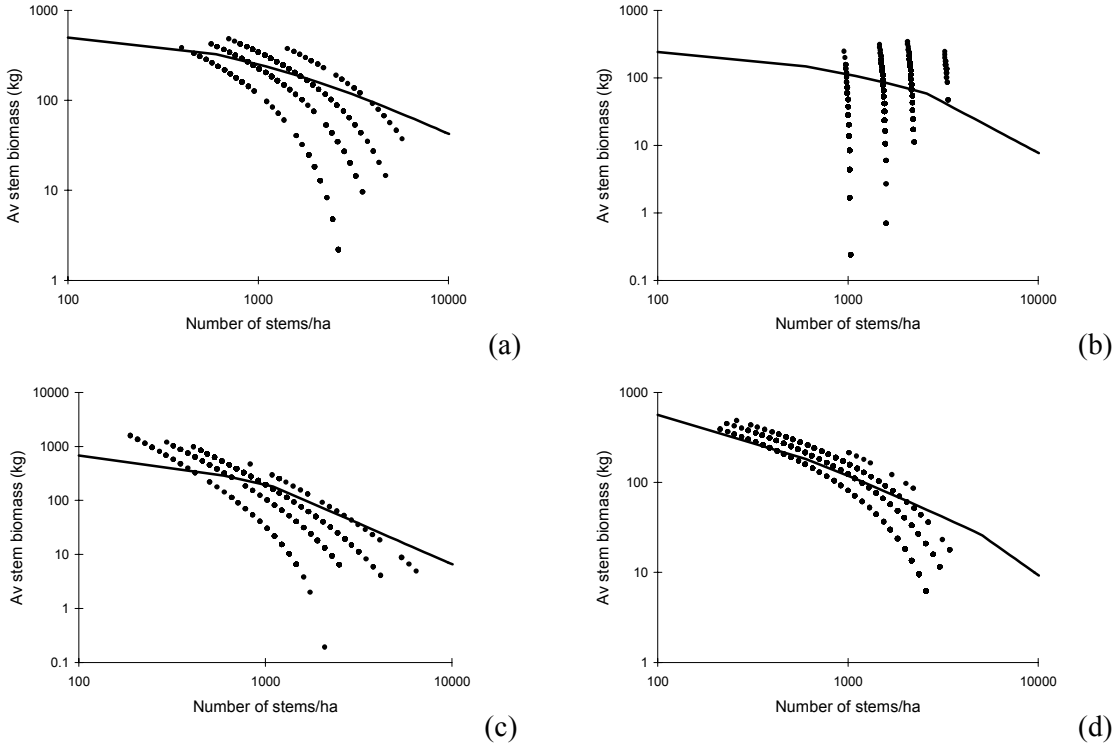

Figure 6.7 Observed relationships in the input data between the number of stems per hectare and the aboveground biomass for: (a) lodgepole pine; (b) black spruce, (c) aspen and (d) balsam fir.

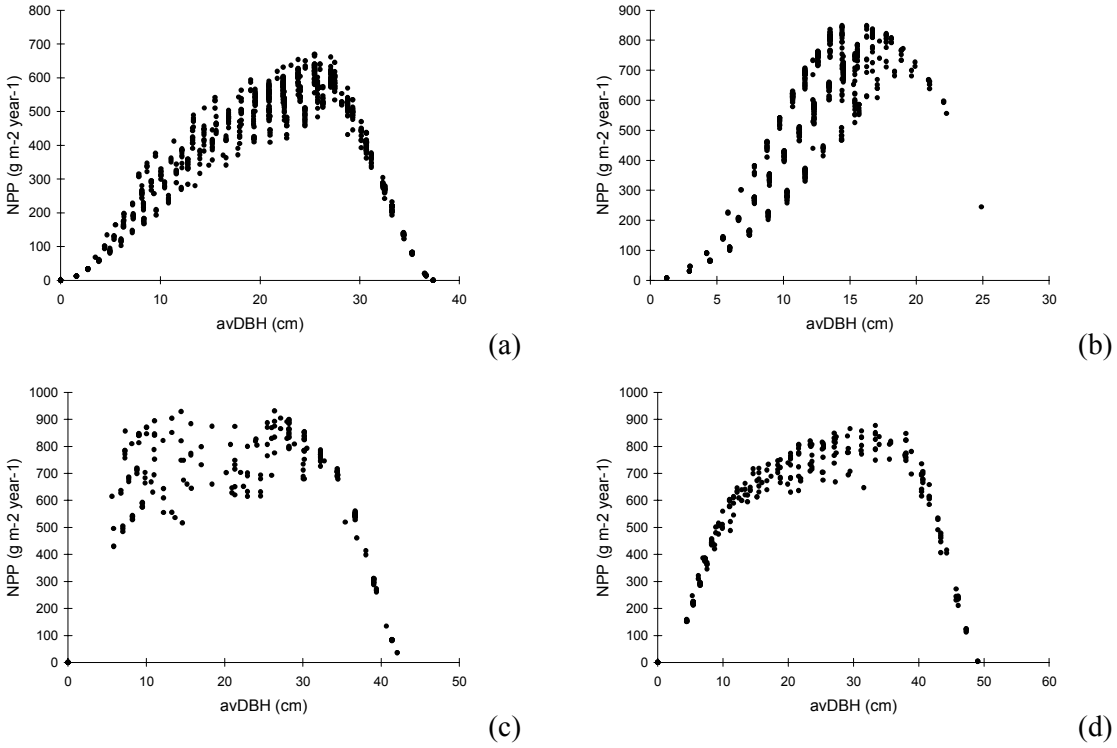

Figure 6.8 Relationship between predicted average diameter at breat height (DBH) and net primary productivity (NPP) for: (a) lodgepole pine (b) black spruce, (c) aspen and (d) balsam fir. The figures were built from the results obtained for a set of 3,000 randomly selected stands.

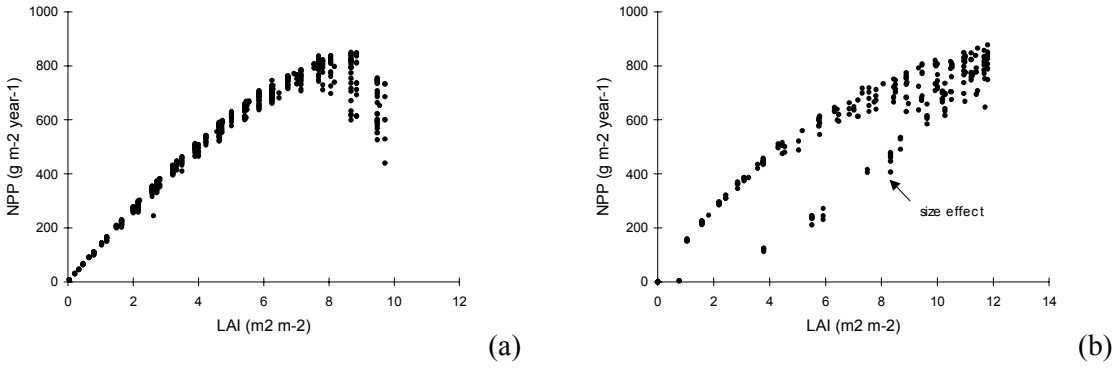

Figure 6.9 Relationship between predicted LAI and NPP for: (a) black spruce and (b) balsam fir (based on a sample of 3,000 stand centroids).

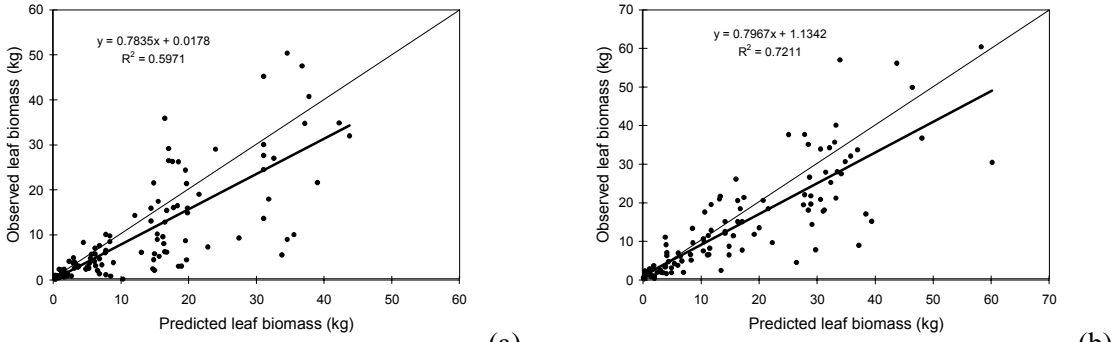

Figure 6.10 Relationship between leaf biomass measured in ENFOR project P-92 (Singh 1982) and the predicted leaf biomass from a model calibrated on data from the ENFOR project P-236 (Ouellet 1983), for: (a) black spruce and (b) white spruce.

6.1.4.3 NPP simulation maps

For both the "real" and "potential" modes, the NPP simulations results at 3,000 randomly selected stand polygons were averaged for each of 36 strata, created in the GIS from a union of four soil types and 12 forest cover types (12 of the 48 possible combinations did not occur). Strata averages were then used to populate the polygons covering the entire study region (approximately 80,000 polygons in total). This allowed the creation of two approximate maps of NPP, simulated using potential and real mode (**Figure 6.11** and **Figure 6.12**, respectively). The simulation in potential mode clearly indicates higher NPP than that obtained from "real" mode, although the relative distributions of simulated NPP are very similar. Furthermore, the ranges of these values are consistent with observations of NPP typical of interior Canadian forest ecosystems.

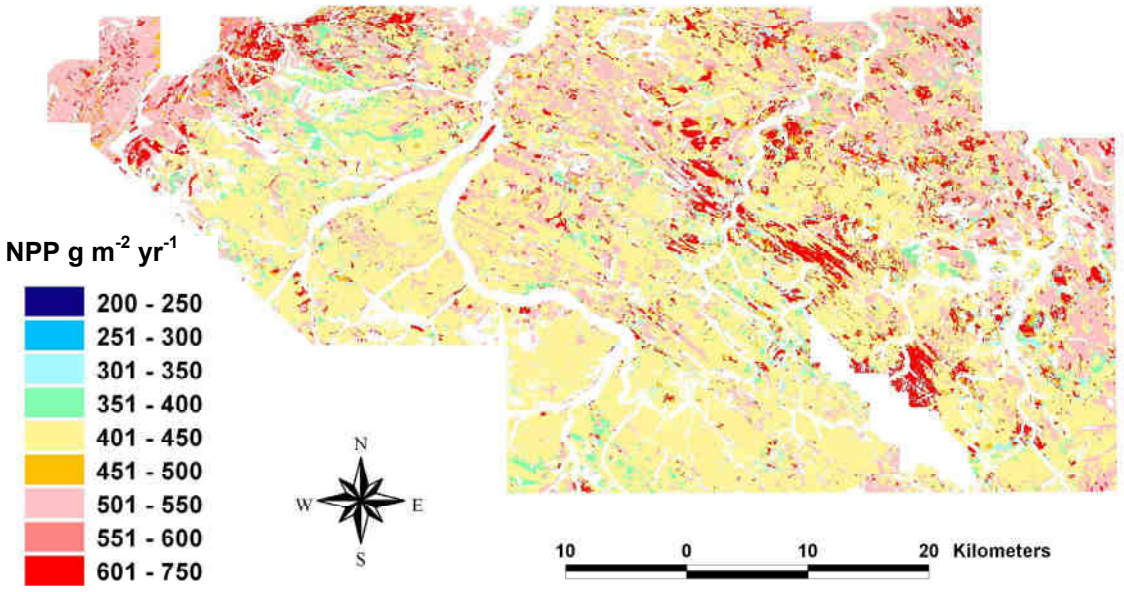

Figure 6.11 Map of net primary productivity estimated for the Alberta study area using StandLEAP in "potential mode".

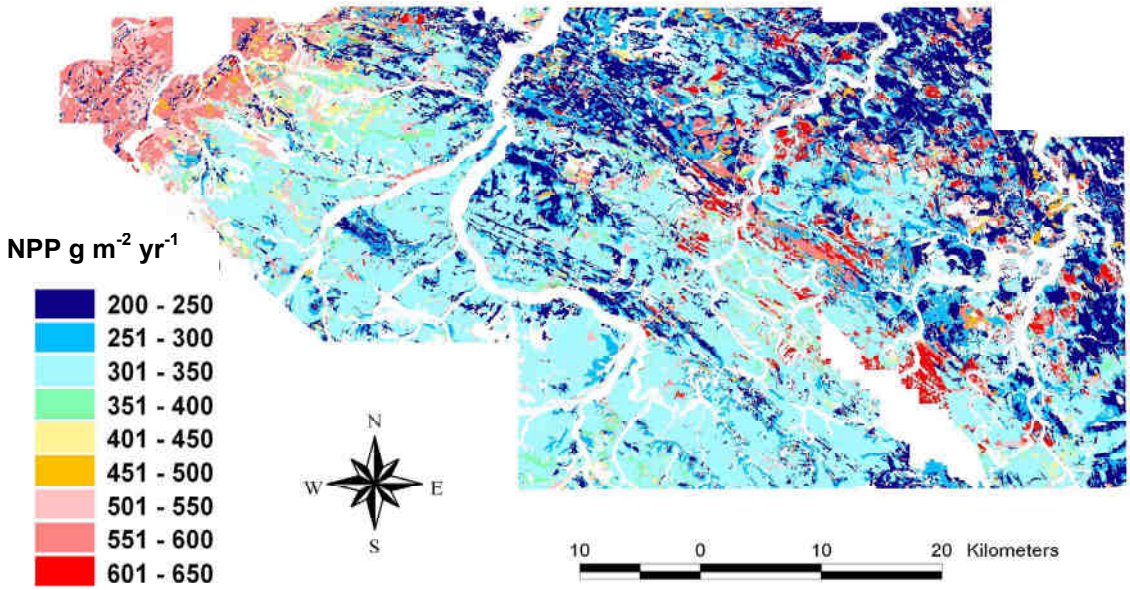

Figure 6.12 Map of net primary productivity estimated for the Alberta study area using StandLEAP in "real mode".

6.2 Stand successional modelling using FORSKA-M

FORSKA-M is a forest gap model of the type originally invented by Botkin et al. (1972), but derived directly from the FORSKA-2 model of Prentice et al. (1993; see also Sykes and Prentice 1995, 1996). The latter model was developed primarily to represent landscape level processes (i.e., disturbance effects) in natural or semi-natural European boreal and cool temperate forests, but FORSKA-M builds on this to represent climate change impacts on forest dynamics in managed forests. Until recently, most of the effort on FORSKA-M had been devoted to forests in Germany and elsewhere in Central Europe (Lindner, 2000; Lasch et al., 1999). It differs from other gap models in its explicit consideration of density effects on tree growth (Lindner et al., 1997) and also features a more detailed multi-layered soil module, which in combination with daily climate input data, yields an improved simulation of drought effects on forest dynamics (Lasch et al., 1998). In common with all gap models, individual species characteristics are parameterized from observed data, reported either from site-level measurement or from published literature. These parameterizations allow different species to respond differently to environmental conditions (availability of light, soil moisture and nutrients) and hence to compete for dominance in a simulated 0.1 ha plots or "patches". In a typical model experiment, 100 or more such patches will be simulated, and the results averaged to account for disturbance effects on the landscape-level age-class structure.

6.2.1 Species parameterization

In previous work, Price et al. (1999a, b; Price and Apps, 1996) developed another variant of FORSKA-2, for application to boreal forest ecosystems along a transect crossing central Saskatchewan and northern Manitoba (Price and Apps, 1995). This work required compiling a set of parameters for North American boreal tree species, using data taken from the literature and other gap models (see Price et al. 1999b). In the latter study, FORSKA-2 was also modified to account for effects of moisture limitations and interannual variations in rainfall in the Canadian boreal—to simulate more realistic responses at sites where significant droughts could occur (see also Bugmann et al., 2002). Hence, the parameter set used by Price et al. (1999) was a useful

starting point for parameterizing FORSKA-M, although in the present study, much greater reliance was placed on the stand-level data available from the Weldwood PGS plot measurements. The modified drought stress functions were also incorporated into FORSKA-M and further adapted to account for model calculations based on daily (in place of monthly) climate data (in particular, setting new values for the drought parameters: d_1= 1.5, d_2=0.55).

Data from 997 PGS plots were carefully surveyed. Species composition was first analysed using the most recent set of PGS plot measurements. The most important forest types were identified, based on species composition and site characteristics (i.e., subregion, ecosite, soil type) of the PGS plots. **Table 6.5** shows the distribution by percentages of PGS plots of nine major forest types in the study area used for parameterizing FORSKA-M. This distribution agrees quite closely with that obtained from the AVI shown in **Table 4.4**.

In an initial analysis, a subset of 45 sites was selected from the 997 PGS plots, to represent the range of forest types on different soil classes in the Upper and Lower Foothills subregions. The Montane and Subalpine subregions were not considered here because: in the Montane there was only a small number of PGS plots; while in the Subalpine, species composition is differs markedly from that in the rest of the study region. Eight of the 45 sites were used to derive parameters for the model and the results were evaluated using data from another 7 validation sites. The overall results of this experiment were very encouraging. The model was able to replicate both the species composition and height-over-DBH relationships observed at most of the test PGS plots satisfactorily, although aspen growth rates were generally overestimated (see also Lindner et al. 2001). In a second more careful assessment, 10 PGS plots were used for species parameter calibration and seven retained for validation. Site selection criteria included the length of the available time series of PGS plot measurements, the age of the stand (both young and mature stands were considered) and a lack of evidence of disturbance due to human or natural causes during the period of plot remeasurements.

Table 6.5 Distribution of nine major forest types found within the FMF Study Region, based on data from 997 Permanent Growth Sample Plots (compare with **Table 4.4**, based on data from the AVI).

Forest Type	Fraction of forest area (%)
Pl	51.6
Sb	20.0
Sw	5.2
Aw	2.5
AwPl	0.6
PlSb	2.8
PlSw	1.6
SbSw	0.30
AwSw	0.10
Total selected forest types	84.7

6.2.2 Validation of FORSKA-M for selected PGS plots

Simulated stand structure and growth performance of different tree size classes have been shown to be very useful indicators of the performance of gap-type and process-based forest models in Europe (Lindner et al., 1997; Sievänen et al., 2000; Mäkelä and Sievänen, 2000). In this study several indicators were used: (1) height/DBH ratio, (2) DBH distribution and related characteristics, (3) volume growth curves, and (4) average biomass. For model calibration and

validation, simulation runs were initialised with the first available PGS plot measurements (collected 1957-1963) and continued until the most recent measurement, covering periods of 32–43 years. Results from earlier work (Lindner et al., 2001, unpublished) showed that productivity at one site (number 167) was greatly overestimated, so the nutrition parameter for this site was reduced for the simulations reported here. It should be emphasized that these model parameters are not finalized, and further adjustments are anticipated as we continue working with the model.

6.2.3 Height/DBH ratio

In general, there was reasonable or good agreement between measured and simulated data relating height to DBH (**Figure 6.13**). The distribution of simulated tree data was smoother than that seen in the PGS plot measurements, which is to be expected in view of site differences and the irregular spatial distribution of trees at individual sites—factors that are not captured by the model.

6.2.4 Stand diameter distributions and related characteristics

Diameter distributions are particularly useful for evaluating simulation results from models such as FORSKA-M, because they integrate simulated physiological tree characteristics as well as intra- and inter-specific competition, and allow the effects to be compared with readily available stand measurement data (**Figure 6.14**).

Figure 6.14 shows observed and simulated diameter distributions for two PGS plots. At site 160, the stand diameter distribution was simulated reasonably well, although growth rate of the fir component was underestimated, as was survival of spruce (71 stems compared to 90 in the PGS plot data). The slow growth of fir resulted from earlier parameter adjustments, which were intended to reduce the biomass of fir obtained when simulations were initialised with bare ground. In the latter case, it appears that abundance of balsam fir in the simulated stand was particularly sensitive to factors such as disturbances and limited seed availability, which are difficult to simulate with a patch model that lacks explicit landscape representation.

Results for site 183 demonstrate that distributions of observed tree diameters can be relatively wide, thus indicating that local site variability and/or spatial competition patterns may lead to significant differences in growth rates of individual trees—another characteristic not captured by the model. In this case, FORSKA-M predicted a much narrower diameter distribution, where smaller tree sizes were lacking (presumably due to them being shaded out by the larger trees in the simulated stand).

As a further evaluation of the model, cumulative diameter distributions (1 cm classes) were generated and compared to observed data (**Figure 6.15**). The Kolmogoroff-Smirnov test (KS) could then be applied to the cumulative diameter distributions to assess statistical differences between simulated and observed data. The KS uses the maximum difference between measured and observed cumulative distributions as a criterion, which usually indicates the deviations for only one or a very few diameter classes (see example above). The distributions can be analysed further, e.g., to check for biases in overall productivity (i.e., if the two distributions have similar shapes but do not overlap).

Average differences between measured and simulated cumulative distributions were analysed for 8 PGS plots, and used to assess implications of parameter changes on this aggregated indicator of model performance. **Figure 6.16** shows that lodgepole pine growth rates were generally simulated well, although they tended to be overestimated for smaller trees at some sites. On the other hand, growth of white spruce was represented poorly (sites 167, 175, 181 and 188), a problem that can likely be resolved only by obtaining more data for this species. The two strikingly large deviations at sites 181 and 188 were both caused by a single white spruce appearing in the simulated mixed stands—both of which died in the simulation runs. Aspen growth was reasonably well-represented on average. At site 160, all major species were slightly under-estimated, which is attributed to underestimation of site fertility.

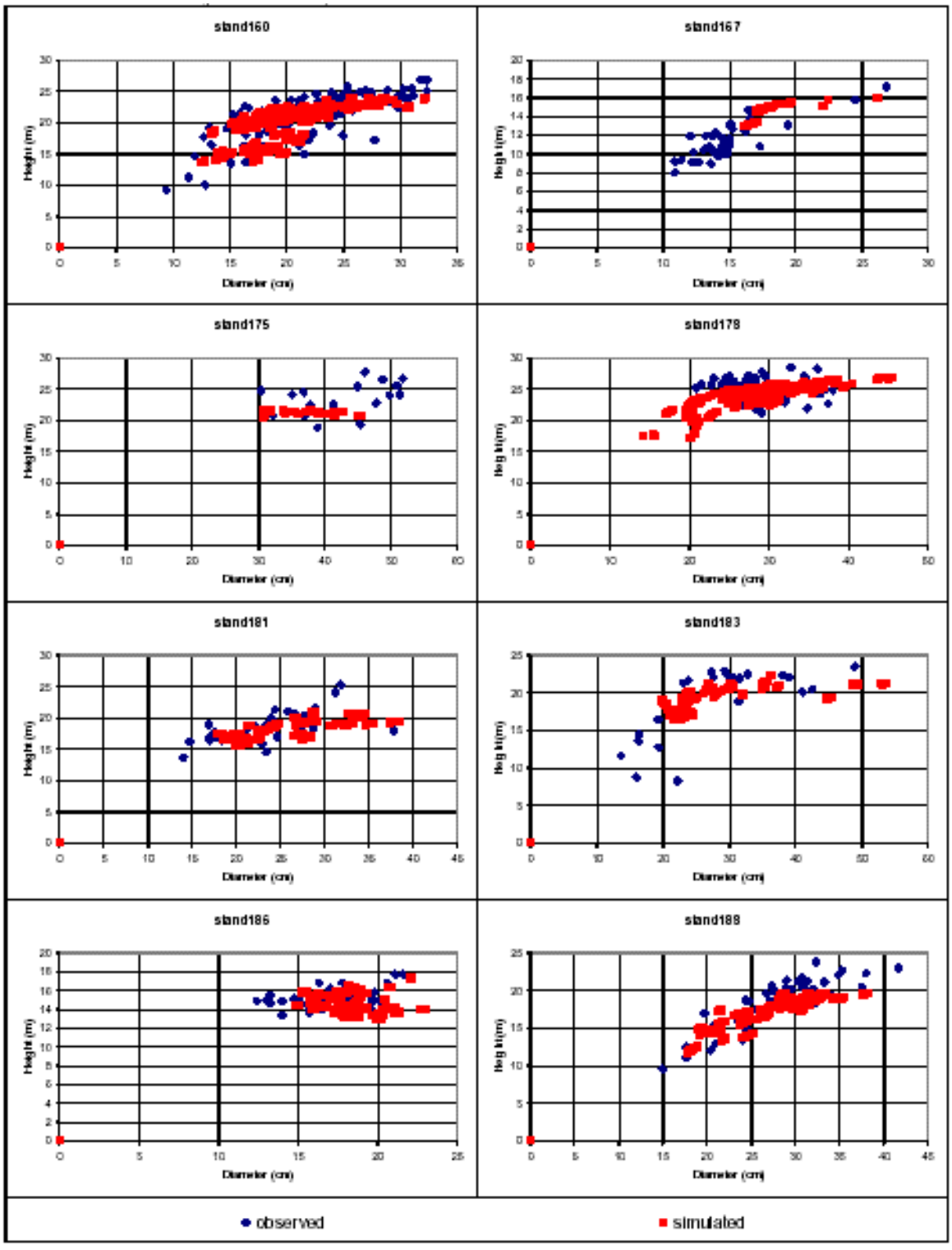

Figure 6.13 Height/DBH relationships for observed and simulated data at the eight calibration PGS plots.

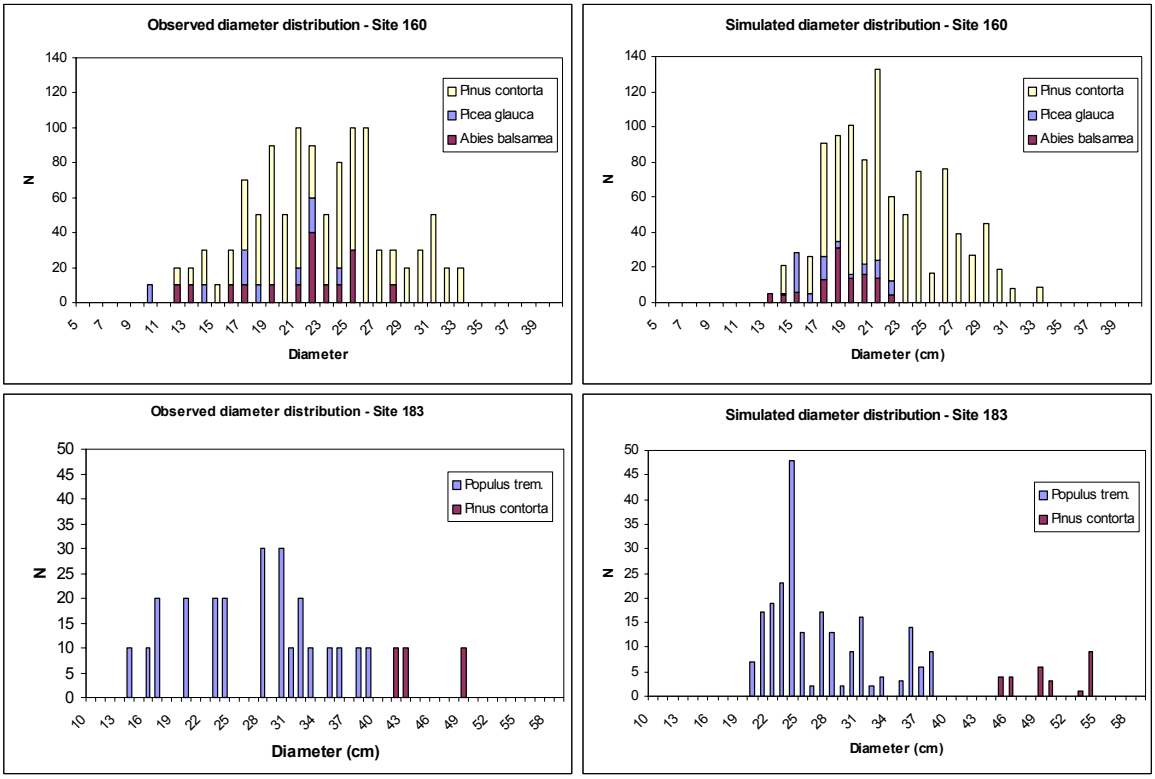

Figure 6.14 Comparison of observed diameter distributions and those simulated by FORSKA-M at two calibration sites in the Alberta study area.

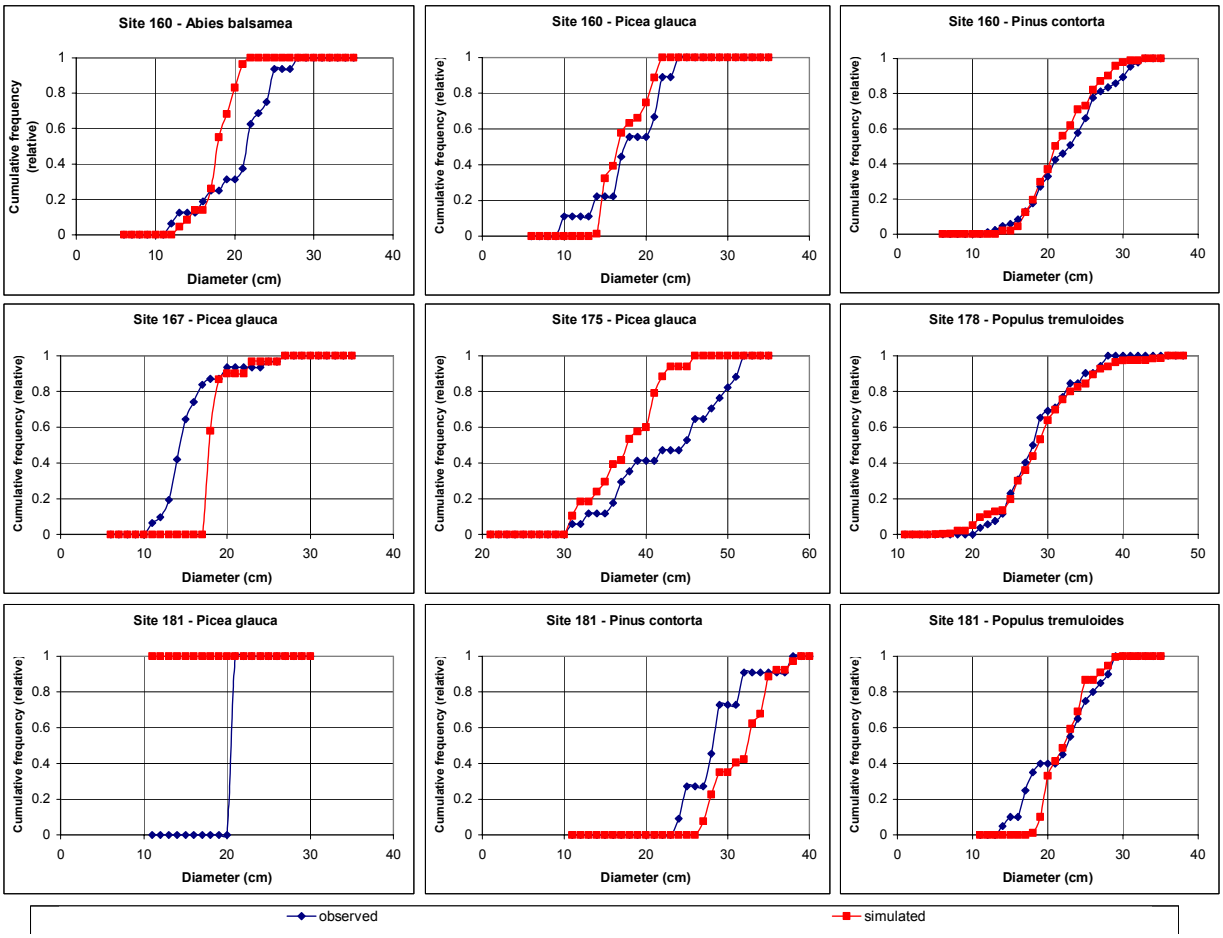

Figure 6.15 Comparison of observed and simulated cumulative diameter distributions for dominant species at selected calibration sites (PGS plot plots 160 to 181).

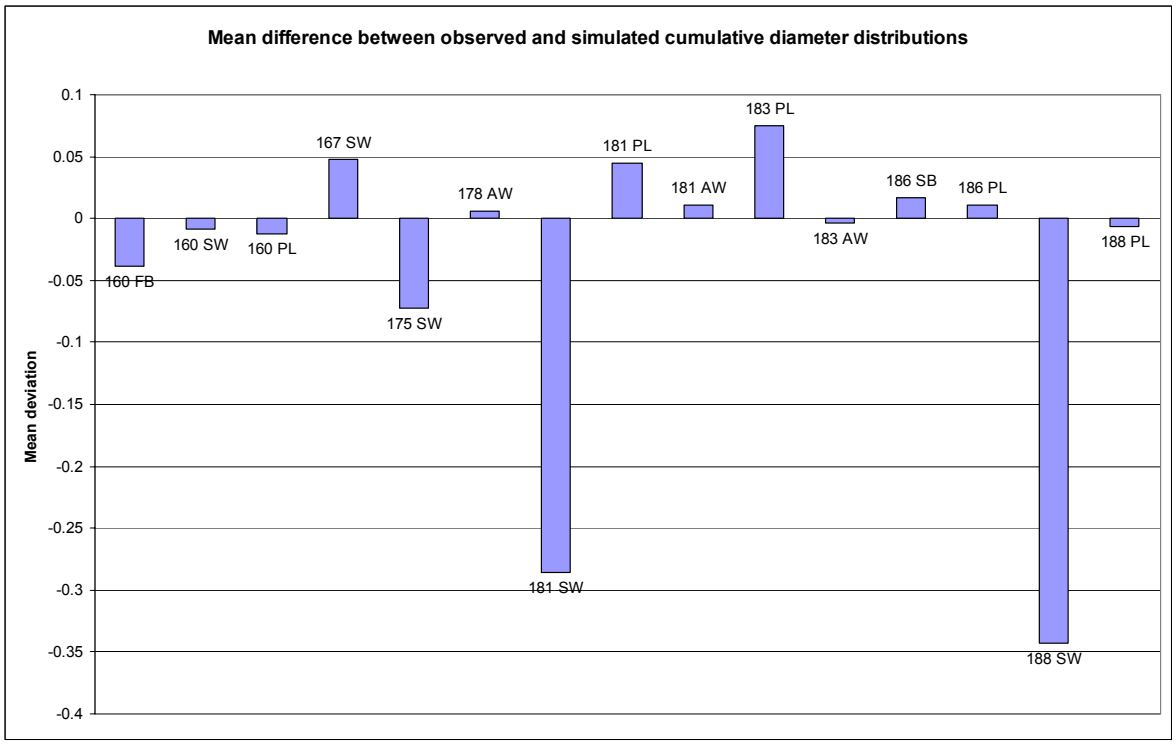

Figure 6.16 Mean differences between observed and simulated stand diameter distributions at calibration sites in the Alberta study area.

6.2.5 Application of FORSKA-M to simulate effects of climate change on stand structure

Using the available soils and simulated climate data described earlier (Sections **4.2** and **4.3**), FORSKA-M was then applied to the 45 representative PGS plots with tree diameter, height, and height of crown base initialized from the most recent measurements. Simulations consisting of 50 replications were run for 100 years for each site under current climate (baseline) and three climate change scenarios (temperature increase of +2 °C with precipitation changes of 0, -10% and +10%). The estimates of biomass density predicted for each scenario were then averaged over the last 20 simulated years, for each of the nine forest types.

In addition, the effects of varying the disturbance rate on stand development and structure were explored. Short disturbance intervals will result in a larger proportion of younger stands in the landscape, and therefore, lower area-weighted average wood volume and aboveground biomass density. Disturbance intervals of 100 years are considered typical for much of the boreal, although there is evidence that in the regions of the Foothills Model Forest, the natural disturbance interval (i.e., in the absence of forest fire suppression) may be significantly shorter (Van Wagner 1978; see also Price et al. 1997). Accordingly, simulations were repeated with disturbance intervals of 50, 100, 150 and 200 years.

The sensitivity of the results obtained when stand conditions were initialized with PGS plot measurements was examined by repeating both sets of experiments (i.e., effects of different climate change scenarios and of varying the disturbance rates), but instead initializing each run at each site with bare ground. This experiment tested the ability of the model to "grow" the correct natural vegetation derived only from the differences among species captured in the species parameters, and driven by the simulated climate and soil conditions.

6.2.6 Results

Figure 6.17 shows the results from all four sets of experiments summarized as area-weighted results for the entire study region. This allows easy comparison of the general trends obtained for differences in climate scenario and disturbance regime, for simulations initialised either from bare ground or from site-level PGS plot measurement data. In addition, the simulation results for all 45 study plots were grouped into forest types based on the species composition reported in the most recent forest inventory (see **Figure 6.18** and **Figure 6.19**).

The growth responses of lodgepole pine to climate dominated all the regional weighted averages (**Figure 6.17**), because the model parameterization was clearly successful in simulating the abundance of this species in the study region. The primary determinant is the relatively low precipitation regime, which favours pine species in general, particularly when the modified drought parameterization (see Section 6.2.1) is adopted (see also Price et al. 1999b and Bugmann et al. 2002).

Balsam fir is parameterized to grow slowly, but the process-based formulation of the growth function in FORSKA-M gives a strong competitive advantage to shade tolerant species wherever they succeed compete successfully and grow.

6.2.6.1 Effects of varying the natural disturbance interval

Figure 6.18 shows the results obtained for each forest type when the simulated forest patches were initialised using measurements taken at the PGS plots., and then subjected to different average disturbance return intervals. These results indicate that average biomass tends to stabilize with a disturbance interval between 100 and 150 years. With shorter disturbance intervals, the mean simulated biomass was much lower, although less frequent disturbances still allowed some further increase in mean biomass (**Figure 6.17**a, c). In general terms, the range of biomass densities estimated by the model were somewhat lower than the area-weighted mean values reported in **Table 5.3**. Average biomass density estimated from AVI stand level data and PGS observations lay in the range 160-190 Mg ha^{-1}, with the exception of the black spruce-dominated systems, where it was approximately 60 Mg ha^{-1}. By comparison, assuming a 100-year return interval, FORSKA-M typically predicted biomass densities of 100 to 150 Mg ha^{-1} (**Figure 6.17** and **Figure 6.18**), although in the specific case of black spruce-dominated systems, FORSKA-M predicted about 60 Mg ha^{-1} (**Figure 6.18**b).

6.2.6.2 Effects of climate change

The different climate change scenarios produced clear differences among sites in the simulated vegetation (**Figure 6.17**c, d; **Figure 6.19**). Increased temperature had mainly positive effects on growth, while a decrease in precipitation produced generally negative impacts. This was not surprising, given the low average annual precipitation in this region. On the wettest sites, however, increasing precipitation reduced growth rates. In some cases, pine growth appeared to benefit even on the drier sites, presumably because other species were able to compete less effectively with increased water stress (see also Price et al. 1999b).

The overall implication is that for changes of the order of a 2 ºC increase in mean temperature and adjustments in annual precipitation of up to ±10%, there should be only minor impacts on average biomass production, with a tendency of species composition to shift towards increased occurrence of pine and aspen and reduced abundance of spruces and firs. This presupposes, of course, that there would be no impact of climate change on the natural disturbance regime. Based on these simulations, the most sensitive forest types are spruce-dominated, which suggests that pines and aspen should be favoured in long-term management of the more sensitive sites.

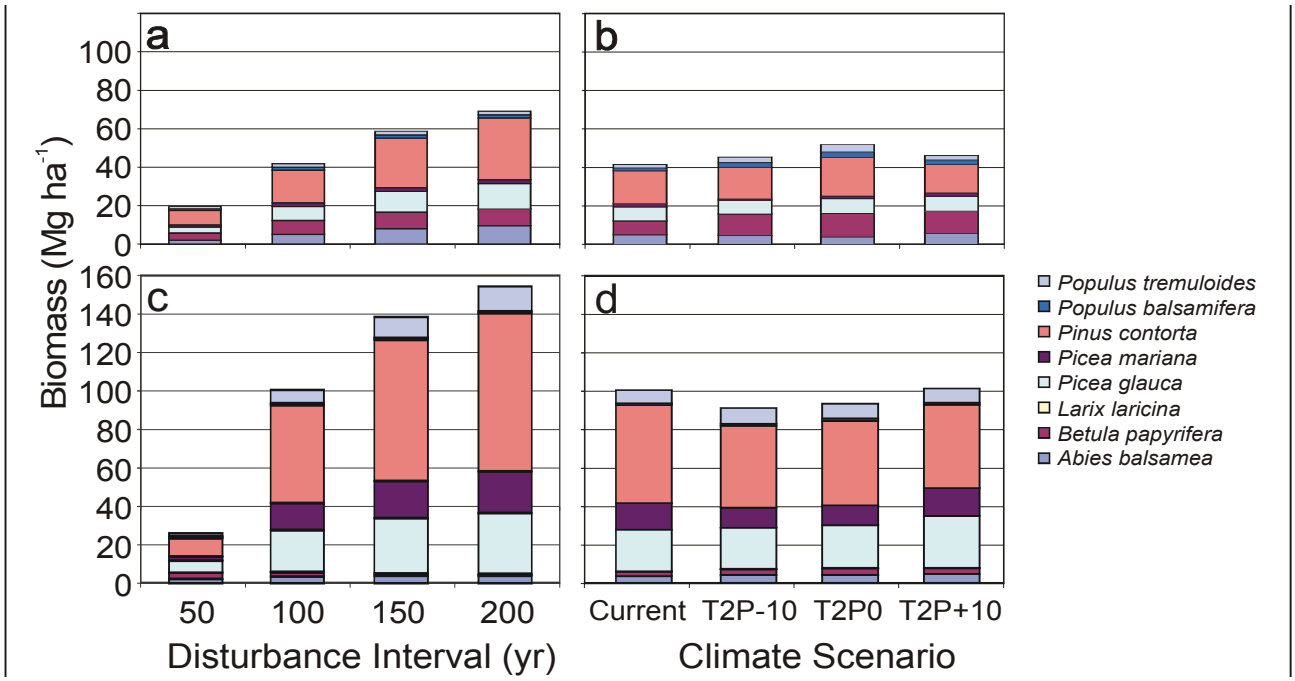

Figure 6.17 Summary of results obtained with FORSKA-M for effects of varying disturbance interval and different climate scenarios on simulated area-weighted average biomass density in the Alberta study region. (a) 600-year simulations under current climate starting from "bare patches"; (b) 600-year simulations under four alternative climate scenarios starting from bare patches; (c) 100-year simulations under current climate with sites initialised from PGS plot measurements; (d) 100-year simulations under four alternative climate scenarios with sites initialised from PGS plot measurements.

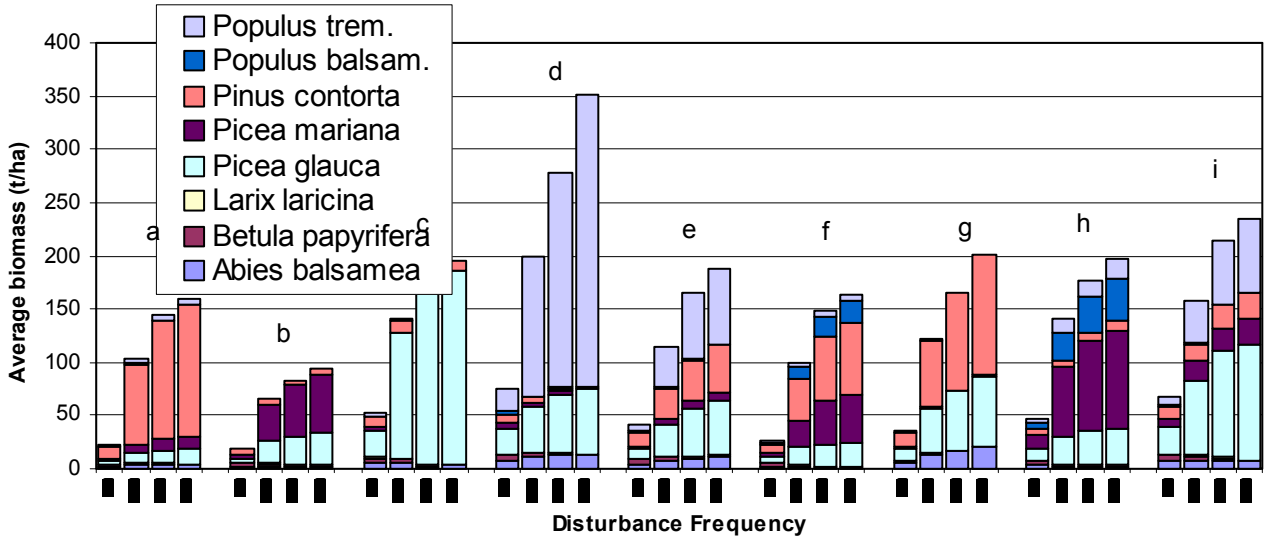

Figure 6.18 Effect of varying the disturbance interval on biomass density simulated by FORSKA-M for the major forest types in the Alberta study region. The four disturbance regimes are expressed in terms of the mean return interval: (left to right) 50 years, 100 years, 150 years and 200 years. Climate regime was derived from 1961-90 normals. Species groups are (a) lodgepole pine; (b) black spruce; (c) white spruce; (d) aspen; (e) aspen-pine; (f) black spruce-pine; (g) pine-white spruce; (h) black spruce-white spruce; (i) aspen-white spruce.

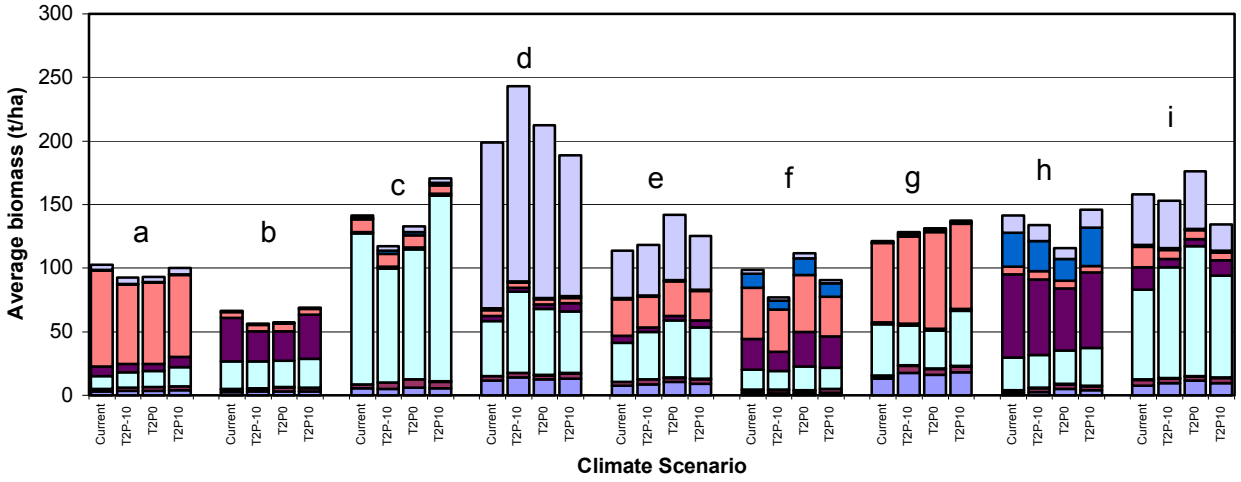

Figure 6.19 Biomass density simulated by FORSKA-M for the major forest types in the Alberta study region, under current climate and three alternative scenarios of future climate.The four climate scenarios are (left to right) current (based on 1961-90 climate normals); normals with 2 ºC increase in temperature and 10% reduction in average precipitation (T2P-10); normals with 2 ºC increase in temperature and no change in average precipitation (T2P0); and 2 ºC increase in temperature and 10% increase in average precipitation (T2P+10). Disturbances were set to a 100-year return interval for all simulations. Species groups as in **Figure 6.18**.

6.2.6.3 Model limitations

When the patches were instead initialised from bare ground, FORSKA-M predicted that white spruce and balsam fir should grow on most sites, while black spruce was under-represented. These results were likely caused by the assumption of uniform seed availability, and/or by the very generalized soils mapping, which does not adequately capture the wetter areas that favour black spruce. Both factors are certainly important, although the spatial variability in past fire occurrence probably explains why the assumption of uniform seed availability fails.

These simulations have therefore exposed some major weaknesses in the model. The simulations of present natural vegetation (PNV) differ very much between a long disturbance interval (say 200 years) and "zero" disturbance (2,000 years of simulation). Intuitively, it would seem that a 200-year interval should be close to zero disturbance, but the simulations revealed a significant difference. Comparison of observed data with simulation results indicated that biomass was much closer to reality when generated from the 2,000-year, zero disturbance simulation. Moreover, the species composition showed distinct differences both between 200 and 2000 year disturbance frequency and between observations and either simulation experiment. This strongly suggests there is a problem with the regeneration module and the assumption of general availability of seed of all species in FORSKA-M (and other gap models) in a disturbance driven landscape. On the other hand, an additional factor is the relatively rare occurrence of sites with sufficient soil moisture to allow drought-intolerant species to survive. Clearly, seed of shade-tolerant species like firs and spruces will not be widely available for regeneration following fire, given the patchy distribution of sites populated by these species. It should be noted, however, that currently the model is not capable of simulating water-saturated soils. Thus typical black spruce ecosites are currently missing—which causes an over-representation of the dry and mesic forest types in the study area. Finally, the observed species composition shows that almost pure stands dominated by lodgepole pine, black or white spruce, or aspen are quite frequent in the

Foothills Model Forest. The simulation results, in the other hand, generate mainly mixed stands of lodgepole pine, spruce and fir. This suggests that the species-specific parameters of the main species are not differentiated enough. Another—perhaps more likely—explanation could be that species composition in the study area is not primarily influenced by site conditions and climate, but rather by disturbance history and dynamically changing landscape patterns of forest types.

6.2.7 Further work

An option available for FORSKA-M is the so-called "natural regeneration management routine", which is designed to favour regeneration of those species that were present in the stand prior to harvest or disturbance and allows only limited immigration of new species from surrounding sites. Hence, an additional experiment would be to run a set of simulations for 600 years initialized from PGS plot level measurements. The objective would be to see whether the model could maintain the initial landscape pattern of stands over the length of the simulation. If it can, then it would suggest that the model should be able to adequately represent the relative importance of seed availability, disturbance effects and soil conditions.

This page intentionally blank.

7 Discussion

This study proved to be an ambitious project with very challenging objectives. We believe it is the first attempt at developing comprehensive and spatially detailed data sets that can be used to drive small-scale models of forest processes over extensive regions. Such a project would have been almost inconceivable a decade ago, and even today, many of the individual steps in data analysis were constrained by available computing resources. Nevertheless, we have substantially succeeded in achieving our primary objectives:

1. by creating spatial data sets needed to develop and test process models of forest productivity and species succession, and
2. by performing simulations with different models of forest responses to climate.

In addition, the data archive will provide valuable input and validation data sets for current and future spatial modelling exercises because they provide a rigorous basis both for simulating the spatial variability and for validating model predictions over an extensive region—which we hope will attract a variety of research groups. Wider access to the data is something that remains to be resolved with our collaborators and partners, but we are optimistic that the "value-added" data products created in this study will not be cause for commercial or political concern.

Not all objectives were achieved: in particular, calibration, testing and validation of both the models used in the study, StandLEAP and FORSKA-M, took far more effort than anticipated, and to date only limited explorations of the impacts of climate change on productivity and succession have been completed.

The work also revealed several weaknesses in our ability to model, even at a relatively coarse resolution, specific processes linked to forest productivity, and the impact of environmental factors on these processes. Interactions with soil-related processes such as nutrition and, more importantly, drainage, were poorly represented both in the available spatial data and in the ensuing simulation of processes. These are likely to have decreased our ability to represent the spatial variability in forest productivity over the landscape.

7.1 Data sets

In addition to the effort invested in process modelling, several major datasets have been developed during the course of this study, including GIS coverages of forest biomass, stand density, leaf area, digital elevation and climatology. Of these, the two requiring the most significant effort were the biomass and leaf area products.

7.1.1 Biomass

Using allometric relationships applied to individual tree measurements taken from Permanent Growth Sample (PGS) plots, it proved possible to derive a credible map of forest biomass density from AVI data for the Alberta study area (**Figure 5.6**). Moreover, while there were certainly problems with estimation errors and even a bias towards significant underestimation for high biomass sites, the modelled variations were in general not statistically different from those in the observations, with the notable exception of black spruce stands. These results suggest that the methods developed here are worth considering for wider application when the alternative is to carry out more intensive ground-based measurements.

Clearly, if accurate assessment of forest biomass over extensive regions is to be achieved, e.g., for carbon accounting purposes, then statistical modelling methods similar to those used in this study will be needed. Reducing the uncertainty in these large-scale estimates will be a major concern. Based on the results from this study, the most significant improvements would be obtained by:

1. More regional studies of allometric relationships for individual species to replace the generalized relationships derived from the work of Singh (1982, 1984) and Manning et al. (1984). That is, more intensive, regionally-based studies of the allometry of individual species would likely be the most useful method of improving regional estimates. At the same time, such studies would allow a more careful assessment of the errors resulting from the use of the generalized relationships.
2. More rigorous validation of tree and stand level biomass functions, using larger validation samples, combined with boot-strapping procedures or other methods.
3. Stand structure information obtained at finer levels of definition to facilitate stand-level modeling, e.g., classification of crown closure to more than four classes (perhaps as many as 10?). In particular, more accurate stand height measurements, reported to within 1 m, would greatly improve prediction of forest biomass density at the stand-level
4. More detailed exploration of physiographic factors (slope, aspect, elevation), and site factors (soil texture, nutrient status, moisture regime, climatology) to determine which are the most important and to develop more detailed statistical predictions of biomass from empirical data.

7.1.2 Leaf Area Index (LAI)

Obtaining meaningful estimates of LAI over extensive forested regions is a challenging problem, which requires both plot-based field measurements using the best available optical methods (Chen et al. 1997), and scaling-up of the plot-level relationships using remote sensing data. The estimates obtained in this study seem generally consistent with other values, but relatively poor correlation and small sample size suggests that the ground-based relationships could be improved with more measurements. In particular, the available allometric data lacked any local measurements of tree leaf area (or leaf mass and specific leaf area, $m^2\ kg^{-1}$) related to stem diameter and other single-tree measurements. There is a clear need for such data to improve regional estimates of LAI, which ideally would be obtained for each of the major tree species in each of the ecoregions. At the same time, some measurements of understorey vegetation foliage area would facilitate improvements to the vegetation indices derived from remote sensing data (Section 5.4.2.5).

More ground-based optical measurements, i.e., both at sites where allometric measurements were made and at other locations across the region of interest, would serve both to reduce the error and provide a clearer assessment of the inherent variability in LAI of forest canopies. This in turn would improve the data used for modeling and model validation in the mapping of LAI by satellite.

The ongoing grizzly bear research project is currently (summer 2002) performing additional field-based optical LAI measurements in the Foothills Model Forest. These additional data could be combined with existing data and used to refine the present LAI map (**Figure 5.12**). The map, perhaps extended over the entire FMF region, would be of great value for a number of applications including habitat assessment, and improvements to land-cover classification, as well as biomass and productivity modelling.

7.1.3 Soils

As discussed in the next section (7.2.1), a strong limitation in the capacity of the StandLEAP model to provide correct estimates of productivity appears to result from the relatively poor representation of the distribution of soil characteristics across the study region. Soil texture data were taken from modal profiles described for polygons in the soil survey of Dumanski et al. (1972). Undoubtedly these data were hard-won and the survey was a major step forward in mapping large-scale soil variability in the region. However, for detailed simulations of forest processes to succeed, it is almost essential that better, finer-scale estimates of the variations in texture and depth are used, given that these are major determinants of soil water (and hence

nutrient) availability. Moreover, in the Foothills region, the majority of forested sites are moisture-limited due to the combined effects of low average annual precipitation and relatively high mid-summer temperatures driving evapotranspiration. Such conditions are likely to become more extreme if the climate warms as projected, so the impacts of soil conditions can only become more important in determining future productivity.

With these considerations in mind, some effort was invested in considering how local soils data could be improved. During the study, as familiarity with the available data increased, the limitations of the existing CanSIS-based soil polygon data became more apparent and the idea developed to use statistical methods, such as multi-variate regression models and neural network analysis, to relate observed soil profiles to topographic and elevational factors. The latter can be mapped at high resolution relatively easily, and high resolution datasets should become widely available from satellite-borne active sensor measurements in the near future. Four potential soil profile datasets were located, each with their own strengths and limitations. So far, these data have been collated, in some cases requiring digitizing and validation, and located on regional maps (**Appendix III**). A review of the research literature showed that statistical modelling techniques have been developed and used successfully to predict soil physical characteristics from topographic and climatic data. We are now prepared to apply some of these methods using the DEM data and soil profile information that have been compiled.

7.1.4 Relevance of Alberta results to other regions

The techniques and experience developed in this study should be relevant to other forest regions in Canada. In particular, the estimation of biomass from vegetation inventory data and growth sample plot data is a direct contribution to the EOSD project. Moreover, early indications are that this method was relatively successful, when compared to some other studies in other regions. Part of the reason for this success must lie in the enormously valuable dataset of tree measurements derived from the network of Permanent Growth Sample (PGS) plots located across the Weldwood FMA. Availability of the Alberta Vegetation Inventory (AVI) data for the study region was another major factor in this success. To our knowledge, such a comprehensive linkage of PGS plot data to the AVI has never been attempted before, and it is unlikely that there are many other regions where similar studies can be carried out.

This raises an important question: Given the relatively unusual availability of data sets, are the results of this study useful in other regions? The answer is likely to be that, in line with the objectives of EOSD, the study region forms an important site for validating other estimates of forest biomass distribution derived ultimately from remote sensing data. The future of forest biomass mapping across large regions such as Canada and elsewhere in the world lies in the development of algorithms to estimate biomass density from a range of remote sensing information. This approach is likely to be problematic, not least because biomass cannot be expected to correlate directly with reflectance data, and active (radar-based) sensors are likely to fail when biomass densities are high. Hence, extensive spatial biomass data sets derived from ground based measurements, such as the biomass data set developed here, are essential for validation of other methods applied elsewhere.

7.2 Models

7.2.1 StandLEAP

The absolute values of net primary productivity (NPP) generated by StandLEAP in both modes were generally plausible, although an independent validation would be desirable. At first sight, however, the correspondence between the maps (**Figure 6.11** and **Figure 6.12**), and the map of biomass-over-age (**Figure 5.8**) seems disappointingly poor. The biomass-over-age map also confirms local field observations of productivity, which suggest stands in the eastern portion of the study region are generally more productive (higher mean merchantable wood volume per

hectare) than those in the west and closer to the Rocky Mountains. There are, however, a number of important points that must be made.

First, the data presented in **Figure 5.8** can only be considered an approximate guide to bioproductivity, based as they are on the biomass map (**Figure 5.6**). In particular, the biomass map evidently underestimates in the high density regions, as discussed in Section 7.1.1, which would imply a tendency to underestimate the biomass-over-age ratio in these regions as well. The ratio of biomass to age is notoriously affected by stand age, with high values typically occurring at mid-rotation and lower values being generated for younger and older stands. Direct comparison with NPP is therefore likely to produce relatively low agreement. The problem here is one of *allocation*. As trees develop, the allocation of photosynthate (i.e., the material produced in NPP), adjusts to meet their individual requirements, as intra- and inter-specific competition for light, water and nutrients influence the need for additional investments in foliage, roots or stemwood (to increase height and physical strength). At the same time, some losses of NPP to insect (and vertebrate?) herbivory, and to litterfall and root turnover, will inevitably occur, all of which contribute to changes in the standing biomass. Although StandLEAP does account for allocation of photosynthate, it does not presently vary this with age. Hence it is likely that estimates of NPP for young and old stands will differ to some extent from the values predicted for typical stands represented by the PGS plots.

Second, although the distribution of biomass-over-age in **Figure 5.8** shows distinctly higher values towards the east, the trend is not uniform and in fact the central regions, particularly those north of the mine area, have the highest values, and further east, towards the study area boundary, they decrease. Further confirmation of these trends is seen in stand height (**Figure 4.6**), and crown closure densities (**Figure 4.7**) and in the distribution of dominant species (**Figure 4.9**). The NPP maps of **Figure 6.11** and **Figure 6.12** tend to parallel this distribution with higher values in the central areas, and lower values in the east and western portions. The NPP values, particularly those estimated by StandLEAP running in "real" mode, in these areas are entirely plausible. The major differences in the distributions of *relative* values occur, in the northwest and northeast corners, where NPP seems too high and too low, respectively. The northwestern portion is dominated by white spruce of relatively low height and open canopy structure, growing on predominantly coarser sandy and sandy-loam soils (**Figure 4.4**), with relatively steep slopes. In contrast, the northeastern area is dominated by relatively tall black spruce stands, some with relatively high crown-closure, established on sandy-loam soils.

The reasons for these contradictions are almost certainly related to two important environmental factors that so far have not been considered adequately. These are, firstly, the poor spatial resolution of existing soils data. Soil texture and depth affect nutrient and water limitations across the region, and thus highlight a major need that we are keen to remedy. Shallower, coarse-textured soils would be expected on the mountain slopes at the west while deeper more developed soils, and even impervious basins forming wetland areas, would be more common in the flatter regions of the east. Secondly, there is the related problem of the regional hydrology. Climate data interpolations suggest that the Rocky Mountains cast a rain shadow, such that precipitation increases slightly towards the eastern edge of the study area. Furthermore, water draining rapidly from the stands growing on the coarse-textured soils in the western areas (the Subalpine and Montane natural regions), will increase summer water deficits, whereas much of the remaining area, though certainly drought prone, will tend to receive more rain and store it for longer. Drainage is a common problem in spatial modelling because its impact is highly non-linear in time and in space, and its control rests largely on features that are difficult to simulate and poorly captured in numerical databases.

The objective of such modelling is to provide a mechanistic basis for assessing the impacts of climate and projected climate changes on spatially varying estimates of productivity. To achieve this objective, the model does not need to be exact on a point-by-point basis, but ideally, it should be no less exact than competing methods of landscape-level estimation of

productivity. Bearing in mind the caveats already discussed, the results indicated in **Figure 6.11** and **Figure 6.12** suggest a very poor point-by-point fit, but overall they demonstrate that the model can predict biomass increment in a largely unbiased way over the study area.

In summary, we have established the potential of StandLEAP to predict forest productivity at the regional scale from physical data and biological principles, but further work is required, both to improve the quality of the input data, particularly soils and hydrology, and to improve the estimation of NPP allocation to biomass and wood volume.

7.2.2 FORSKA-M

Gap models in general are very dependent upon the tuning of species parameters and FORSKA-M is no exception. Initially the parameter set was based on previous work by Price et al. (1999a), but these parameters needed to be adjusted as a result of much more rigorous calibration and validation procedures. In this regard, the model was successfully calibrated for a complete range of local site conditions.

FORSKA-M was successful in predicting the occurrence of the dominant species, but it was much more successful when the stand structure and composition was initialized from PGS plot data. When runs were initialized with bare patches, it was generally unable to predict the relative abundances of the less common species (i.e., those other than lodgepole pine). This raises important questions about the model assumptions and/or the parameters used to define species differences. A particular question is whether the spatial distribution of species composition in the study area is due to differences in site characteristics that are not captured by the model (or not present in the soils data). Alternatively, is the poor representation of the real forest distribution due to the assumption in the model that seeds of all species are present at all sites? The latter is a common criticism of gap models and may be quite inappropriate for boreal ecosystems where extensive fires are a frequent occurrence in the natural landscape.

The responses of the model to simulated disturbance regimes were generally consistent with reality when initialized from PGS plot data: i.e., they predicted total biomass densities for individual species at levels reasonably consistent with observations. The results for the simulations initialized from bare patches were less successful: biomass densities were lower and the allocation among species was less realistic. The responses to simulated changes in climate were also contradictory. For runs initialized with bare ground, a 2 ºC increase in mean annual temperature produced slight increases in biomass density, relative to current climate, with the greatest increase occurring when future precipitation was assumed to be the same as the 1961-90 mean value. When the runs were initialized with PGS plot data, however, the general response compared to current climate was a reduction in biomass density. Further work is needed to understand these responses and to explore ways of resolving the differences between simulations from bare ground and those initialized from PGS data.

This page intentionally blank.

8 Concluding remarks

There is increasing evidence that over the next 50-100 years, there will be significant changes in mean climate (certainly warmer, probably drier) in the region of the Prairie Provinces. Clearly, an important component of maintaining future forest sustainability in this region is to be able to account and compensate for the impacts of projected climate change on survival and productivity of the region's forests.

We believe that recent and ongoing developments in Geographic Information Systems (GIS), climate data interpolation and remote sensing, can provide much of the data needed to drive detailed process models and make useful predictions of future growth trends. The utility of such an approach lies in the potential to project *relative responses* of present-day forests to a range of plausible climate scenarios. This should provide increased awareness of the possible impacts and allow adaptation strategies to be developed.

At the same time, the continuing development and testing of process-based models of forest succession and productivity must be pursued. There can be little doubt that environmental changes are occurring, whether they are natural or the results of human activities. As our understanding of the causes of these changes improves, so also does our ability to predict their effects. The need to investigate and predict potential impacts is particularly important in the case of forest management, because it is a long-term (multi-decadal) activity, where the investment (i.e, in initial stand establishment) must be carried out in the expectation that environmental changes will occur. Based on our preliminary findings in this study, climate change may affect growth rates positively, but this benefit must be balanced against the likelihood that losses due to fire and other natural disturbances could increase. Obtaining more wood out of shorter rotations may be the most logical objective for forest management in the 21st century!

The present study is an important attempt to document the biophysical characteristics of extensive regions by providing coherent layers of complementary and spatially continuous data. These data can the be used to support a variety of process modelling, to explore the effects of environmental changes and potentially the effects of management strategies intended to mitigate the negative impacts or capitalize on the benefits.

In combination with similar studies carried out in other regions across Canada, there is the potential to develop a network of sites to test models over greater ranges and to provide additional validation of larger-scale models being tested at the national and global scales.

This page intentionally blank.

9 Acknowledgements

This work would not have been possible without the major contributions of cash and in-kind resources received from: Prairie Adaptation Research Cooperative (PARC), the Foothills Model Forest, the Sustainable Forest Management Network Center of Excellence (SFM-NCE) based at the University of Alberta, and the Earth Observation for Sustainable Development research initiative funded by the Canadian Space Agency. In addition the moral and in-kind support from Weldwood Canada (Hinton Division), the Prince Albert Model Forest and Weyerhaeuser Canada (Prince Albert Woodlands Division) are all greatly appreciated. Deserving particular mention are: Mark Johnston, Hugh Lougheed, Mark Storie and Brian Christensen. Ott Naelapea provided some important assistance in the initial exploration for data at the Prince Albert Model Forest.

Within the Canadian Forest Service, important contributions were provided at various stages by the late Ian Corns, Deb Klita, Yonghe Wang, Debbie Mucha, and Zoran Stanojevic, of Northern Forestry Centre in Edmonton, and by Richard Fournier, Luc Guindon, and Rémi St-Amant at the Laurentian Forestry Centre in Ste Foy, Québec. Doug Allan at NoFC, Don Pluth formerly of University of Alberta and Glen Padbury at University of Saskatchewan have all provided assistance in the search for soil profile data.

This page intentionally blank.

10 References

Aber J.D., Ollinger S.V., Federer C.A., Reich P.B., Goulden M.L., Kicklighter D.W., Melillo J.M. and Lathrop R.G. Jr. 1995. Predicting the effects of climate change on water yield and forest production in the northeastern United States. Clim. Res. 5: 207-222.

Agren G.I. and Axelsson B. 1980. Population respiration: a theoretical approach. Ecol. Mod. 11: 39-54.

Beckingham J.D., Corns I.G.W. and Archibald J.H. 1996. Field guide to ecosites of West-Central Alberta. Spec. Rep. 9. Can. For. Serv., North. For. Cent., Edmonton, AB.

Bernier P.Y., Bréda N., Granier A., Raulier F. and Mathieu F. 2001a. Validation of a canopy gas exchange model and derivation of a soil water modifier for transpiration for sugar maple (*Acer saccharum* Marsh.) using sap flow density measurements. For. Ecol. Manage., in press.

Bernier P.Y., Fournier R.A., Ung C.H., Robitaille G., Larocque G.R., Lavigne M.B., Boutin R., Raulier F., Paré D., Beaubien J. and Delisle C. 1999. Linking ecophysiology and forest productivity: an overview of the ECOLEAP project. For. Chron. 75: 417-421.

Bernier P.Y., Raulier F., Stenberg P. and Ung C-H. 2001b. The importance of needle age and shoot structure on canopy net photosynthesis of Balsam fir (*Abies balsamea*): a spatially-inexplicit modelling analysis. Tree Physiol. 21: 815-830

Bonan G.B. 1993. Physiological controls of the carbon balance of boreal forest ecosystems. Can. J. For. Res. 23: 1453-1471.

Bonner, G.M. 1986. Inventory of Forest Biomass in Canada. Forestry Canada, Nat. For. Inst., Petawawa, Ont. Canada.

Brown L., Chen J.M., Leblanc S.G., and Cihlar J. 2000. A shortwave infrared modification to the simple ratio for LAI retrieval in boreal forests: an image and model analysis. Remote Sense. Environ. 71: 16-25.

Bugmann H.K.M., Wullschleger S.D., Price D.T., Ogle K., Clark D.F. and Solomon A.M. 2002. Comparing the performance of forest gap models in North America. Clim. Change 51: 349-388.

Burton P.J. and Cumming S.G. 1995. Potential effects of climatic change on some western Canadian forests, based on phenological enhancements to a patch model of forest succession. Water, Air and Soil Pollution 82: 401-414.

Chen J.M. 1996. Optically-based methods for measuring seasonal variation of leaf area index in boreal conifer stands. Agric. For. Meteorol. 80: 135-163.

Chen J.M. and Black T.A. 1992. Defining leaf area for non-flat leaves. Plant Cell Environ. 15: 421-429.

Chen J.M.and Cihlar J. 1995. Plant canopy gap size analysis theory for improving optical measurements of leaf area index. Appl. Opt. 34: 6211-6222.

Chen J.M., Rich P.M., Gower S.T., Norman J.M., and Plummer S. 1997. Leaf Area Index of boreal forests: theory, techniques, and measurements. J Geophys. Res. 102: 29429-29443.

Cieszewski C.J. and Bella I.E. 1989. Polymorphic height and site index curves for lodgepole pine in Alberta. Can. J. For. Res. 19: 1151-1160.

Comeau P.G. and Kimmins J.P. 1989. Above- and below-ground biomass and production of lodgepole pine on sites with differing soil moisture regimes. Can. J. For. Res. 19: 447-454.

Crow T.R. and Schlaegel B.E. 1988. A guide to using regression equations for estimating tree biomass. North. J. Appl. For. 5: 15-22.

Dang Q.-L., Margolis H.A. and Collatz G.J. 1998. Parameterization and testing of a coupled photosynthesis-stomatal conductance model for boreal trees. Tree Physiol. 18: 141-153.

Dean T.J. and Long J.N. 1986. Variation in sapwood area – leaf area relations within two stands of lodgepole pine. Forest Sci. 32: 749-758.

Dewar R.C. 1997. A simple model of light and water use evaluated for *Pinus radiata*. Tree Physiol. 17: 259-265.

Dumanski J., Macyk T.M., Veauvy C.F., and Lindsay J.D. 1972. Soil survey and land evaluation of the Hinton-Edson area, Alberta. Alberta Soil Survey Report No. S-72-31. Alberta Institute of Pedology, Research Council of Alberta.

Environment Canada, 1994. Canadian Monthly Climate Data and 1961–90 Normals on CD-ROM, Version 3.0E.

ESRI on-line help 1994. (TOPOGRID command).

Fahey T.J. 1983. Nutrient dynamics of aboveground detritus in lodgepole pine (*Pinus contorta* spp. *latifolia*) ecosystems, southeastern Wyoming. Ecol. Mon. 53: 51-72.

Farquhar G.D., von Caemmerer S. and Berry J.A. 1980. A biochemical model of photosynthetic CO_2 assimilation in leaves of C_3 species. Planta 149: 78-90.

Farrar J.L. 1995. Trees in Canada. Co-published by Fitzhenry and Whiteside Limited, Markham, ON and the Canadian Forest Service, Natural Resources Canada, Ottawa, ON, in cooperation with the Canada Communication Group – Publishing, Supply and Services Canada. 502 pages.

Fournier R.A., Guindon L., Bernier P.Y., Ung C-H. and Raulier F. 2000. Spatial implementation of models in forestry. For. Chron. 76: 929-940.

Fournier R.A., Rich P.M. and Landry R. 1997. Hierarchical characterization of canopy architecture for boreal forest. J. Geophys. Res. 102 (D24): 29445-29454.

Frolking S., Goulden M.L., Wofsy S.C., Fan S.-M., Sutton D.J., Munger J.W., Bazzaz A.M., Daube B.C., Crill P.M., Aber J.D., Band L.E., Wang X., Savage K., Moore T., Harriss R.C. 1996. Modelling temporal variability in the carbon balance of a spruce/moss boreal forest. Global Change Biology 2: 343-366.

Gholz H.L. 1982. Environmental limits on aboveground net primary production, leaf area, and biomass in vegetation zones of the Pacific Northwest. Ecology 63: 469-481.

Goetz S.J. and Prince S.D. 1998. Variability in carbon exchange and light utilization among boreal forest stands: implications for remote sensing of net primary production. Can. J. For. Res. 28: 375-389.

Goudriaan J. and van Laar H.H. 1994. Modelling potential crop growth processes. Textbook with exercises. Kluwer Academic Publishers, Dordrecht, NL, 238 pp.

Gower S.T. and Norman J.M. 1991. Rapid estimation of Leaf Area Index in conifer and broad-leaf plantations. Ecology 72: 1896-1900.

Gower S.T., Grier C.C., Vogt D.J. and Vogt K.A. 1987. Allometric relations of deciduous (*Larix occidentalis*) and evergreen conifers (*Pinus contorta* and *Pseudotsuga menziesii*) of the Cascade Mountains in central Washington. Can. J. For. Res. 17: 630-634.

Gower S.T., Vogel J.G., Norman J.M., Kucharik C.J., Steele S.J. and Stow T.K. 1997. Carbon distribution and aboveground net primary production for aspen, jack pine, and black spruce stands in Saskatchewan and Manitoba, Canada. J. Geophysical Res. 102: 29029–29041.

Harrell P.A., Bourgeau-Chavez L.L., Kasischke E.S., French N.H.F., and. Christensen Jr. N.L. 1995. Sensitivity of ERS-1 and JERS-1 RADAR data to biomass and stand structure in Alaskan boreal forest. Remote Sensing Environ. 54: 247-260.

Hogg E.H. 1999. Simulation of interannual responses of trembling aspen stands to climatic variations and insect defoliation in western Canada. Ecol. Model. 114: 175-193.

Huang S., Titus S.J., Lakusta T.W. and Held R.J. 1994. Ecologically based individual tree height-diameter models for major Alberta tree species. *Report #2*, Alberta Environmental Protection, Land and Forest Services, Forest Management Division, Edomonton, AB.

Hungerford R.D. 1987. Estimation of foliage area in dense Montana lodgepole pine stands. Can. J. For. Res. 17: 320–324.

Hutchinson MF. 1989. A new method for gridding elevation and stream line data with automatic removal of pits. J. Hydrol. 106: 211-232.

Hutchinson M.F. and Dowling T.I. 1991. A continental hydrological assessment of a new gridbased digital elevation model of Australia. Hydrological Processes 5: 45-58.

Kaufmann M.R. and Troendle C.A. 1981. The relationship of leaf area and foliage biomass to sapwood conducting area in four subalpine forest tree species. For. Sci. 27: 477-482.

Keane M.G. and Weetman G.F. 1987. Leaf area – sapwood cross-sectional area relationships in repressed stands of lodgepole pine. Can. J. For. Res. 17: 205-209.

Kimball J.S., Keyser A.R., Running S.W. and Saatchi S.S. 2000. Regional assessment of boreal forest productivity using an ecological process model and remote sensing parameter maps. Tree Physiol. 20: 761-775.

Kurz W.A. and Apps M.J. 1999. A 70-year retrospective analysis of carbon fluxes in the Canadian forest sector. Ecol. Appl. 9: 526-547.

Landsberg J.J. and Ludlow M.M. 1970. A technique for determining resistance to mass transfer through the boundary layers of plants with complex structure. J. Appl. Ecol. 7: 187-192.

Landsberg J.J. and Waring R.H. 1997. A generalised model of forest productivity using simplified concepts of radiation-use efficiency, carbon balance and partitioning. For. Ecol. Manag. 95: 209-228.

Lasch P., Suckow F., Bürger G. and Lindner M. 1998. Sensitivity analysis of a forest gap model concerning current and future climate variability. *In* Beniston M. and Innes J.L. (eds). The Impacts of Climate Variability on Forests. Berlin, Springer-Verlag 74: 273-288.

Lasch P., Lindner M. Ebert B., Flechsig M., Gerstengarbe F.-W., Suckow F. and Werner P.C. 1999. Regional impact analysis of climate change on natural and managed forests in the Federal State of Brandenburg, Germany. Environmental Modelling and Assessment 4(4): 273-286.

Lavigne M.B. and Ryan M.G. 1997. Growth and maintenance respiration rates of aspen, black spruce and jack pine stems at northern and southern BOREAS sites. Tree Physiol. 17: 543-551.

Leuning R. 1995. A critical appraisal of a combined stomatal-photosynthesis model for C_3 plants. Plant Cell Environ. 18: 339-355.

Leuning R., Kelliher F.M., De Pury D.G.G. and Schulze E.-D. 1995. Leaf nitrogen, photosynthesis, conductance and transpiration: scaling from leaves to canopies. Plant Cell Environ. 18: 1183-1200.

LI-COR Inc. 1991. LAI-2000 Plant Canopy Analyzer Operating Manual. LI-COR Inc., Nebraska, USA.

Lindner M., Sievänen R. and Pretzsch H. 1997. Improving the simulation of stand structure in a forest gap model. For. Ecol. Manage. 95: 183-195.

Liu J., Chen J.M., Cihlar J. and Park W.M. 1997. A process-based boreal ecosystem productivity simulator using remote sensing inputs. Remote Sens. Environ. 62: 158-175.

Loechel S.E., Walthall C.L., Brown de Colstoun E., Chen J., Markham B.L. and Miller J. 1997. Variability of boreal forest reflectances as measured from a helicopter platform. J. Geophys. Res. 102 (D24): 29495-29504.

Long, J.N. and Smith F. W. 1988. Leaf area – sapwood area relations of lodgepole pine as influenced by stand density and site index. Can. J. For. Res. 18: 247-250.

Luther, J.E., Fournier R.A., Hall R.J., Ung C-H., Guindon L., Lambert M.-C. and Beaudoin A.. 2002. A strategy for mapping Canada's forest biomass with Landsat TM imagery. Proceedings, International Geoscience and Remote Sensing Symposium (IGARSS '02), Toronto, Canada.

Manning, G.H., Massie M.R.C., and Rudd J. 1984. Metric single-tree weight tables for the Yukon Territory. Env. Can., Can. For. Serv., Pac. For. Res. Cen., Victoria, BC. Inf. Rep. BC-X-250

Marchand, P.J. 1984. Sapwood area as an estimator of foliage biomass and projected leaf area for Abies balsamea and Picea rubens. Can. J. For. Res. 14: 85-87.

McCree K.J. 1970. An equation for the rate of respiration of white clover plants grown under controlled conditions. In: Prediction and measurement of photosynthetic productivity, Proceedings of the IBP/PP Technical Meeting, Trebon, 14-21 September 1969, PUDOC, Wageningen, pp. 221-229.

Middleton E.M., Sullivan J.H., Boward B.D., Deluca A.J., Chan S.S. and Cannon T.A. 1997. Seasonal variability in foliar characteristics and physiology for boreal forest species at the five Saskatchewan tower sites during the 1994 Boreal Ecosystem-Atmosphere Study. J. Geophys. Res. 102 (D24): 28831-28844.

Monserud, R.A. and Marshall J.D. 1999. Allometric crown relations in three northern Idaho conifer species. Can. J. For. Res. 29: 521–535.

Nemani R., Pierce L., Running S. and Band L. 1993. Forest ecosystem processes at the watershed scale: sensitivity to remotely-sensed Leaf Area Index estimates. Int. J. Remote Sens. 13: 2519-2434

Newcomer J., Landis D., Conrad S., Curd S., Huemmrich K., Knapp D., Morell A., Nickeson J., Papagno A., Rinker D., Strub R., Twine T., Hall F. and Sellers P. 2000. Collected data on the Boreal Ecosystem-Atmosphere Study. NASA. CD-ROM.

Oker-Blom P., Kaufmann M.R. and Ryan M.G. 1991. Performance of a canopy light interception model for conifer shoots, trees and stands. Tree Physiol. 9: 227-243.

Ouellet D. 1983. Equations de prédiction de la biomasse de douze essences commerciales du Québec. Rapport d'information LAU-X-62, Forêts Canada, Région du Québec.

Parresol, B.R. 1999. Assessing tree and stand biomass: a review with examples and critical comparisons. For. Sci. 45: 573-593.

Pastor J. and Bockheim J.G. 1984. Distribution and cycling of nutrients in an aspen-mixed-hardwood-spodosol ecosystem in northern Wisconsin. Ecology 65: 339-353.

Payendeh B. 1981. Choosing regression models for biomass prediction equations. For. Chron. 57: 229-232.

Pearson J.A., Knight D.H. and Fahey T.J. 1987. Biomass and nutrient accumulation during stand development in Wyoming lodgepole pine forests. Ecology 68: 1966-1973.

Pearson, J.A., Fahey T.J. and Knight D.H. 1984. Biomass and leaf area in contrasting lodgepole pine forests. Can. J. For. Res. 14: 259-265

Penner, M., Power K., Muhairwe C., Tellier R. and Wang Y. 1997. Canada's forest biomass resources: Deriving estimates from Canada's forest inventory. Nat. Resour. Can., Can. For. Serv., Pac. For. Cen., Victoria, BC, Inf. Rep. BC-X-370.

Perala D.A. and Alban D.H. 1994. Allometric biomass estimators for aspen-dominated ecosystems in the upper Great Lakes. U.S.D.A. For. Serv., North Central For. Exp. Stn., Res. Pap. NC-314. 38 p.

Peterson, E.B. and Peterson, N.M. 1992. Ecology, management, and use of aspen and balsam poplar in the Prairie Provinces, Canada. Special Report 1. Forestry Canada, Northwest Region, Northern Forestry Centre, Edmonton, Alberta. 252 pages.

Pierce L.L. and Running S.W. 1988. Rapid estmation of coniferous forest Leaf Area Index using a portable integrating radiometer. Ecology 69: 1762-1767.

Pothier D. and Savard F. 1998. Actualisation des tables de production pour les principales essences forestières du Québec. Ministère des Ressources naturelles du Québec, Direction de la recherche forestière. RN98-3054, 183 p.

Prentice I.C., Sykes M.T. and Cramer W.A. 1993. A simulation model for the transient effects of climatic change on forest landscapes. Ecol. Modelling 65: 51-70.

Prescott C.E., Corbin J.P. and Parkinson D. 1989. Biomass, productivity, and nutrient-use efficiency of aboveground vegetation in four Rocky Mountain coniferous forests. Can. J. For. Res. 19: 309-317.

Price D.T. and Apps M.J. 1995. The Boreal Forest Transect Case Study: Global change effects on ecosystem processes and carbon dynamics in Canada. Water, Air, Soil Pollut. 82: 203-214.

Price D.T. and Apps M.J. 1996. Boreal forest responses to climate change scenarios along an ecoclimatic transect in central Canada. Clim. Change 34: 179-190.

Price D.T., Halliwell D.H., Apps M.J and Peng C.H. 1999a. Adapting a patch model to simulate the sensitivity of Central-Canadian boreal ecosystems to climate variability. J. Biogeography 26: 1101–1113.

Price, D.T. D.W. McKenney, D. Caya, M.D. Flannigan and H. Côté. 2001. Transient climate change scenarios for high resolution assessment of impacts on Canada’s forest ecosystems.

Final report to Climate Change Action Fund, June 2001. http://www.cics.uvic.ca/scenarios/index.cgi?Other_Data#transienthighres.

Price D.T., Peng, C.H. Apps M.J. and Halliwell D.H. 1999b. Simulating effects of climate change on boreal ecosystem carbon pools in central Canada. J. Biogeography 26: 1237–1248.

Price D.T., Halliwell D.H., Apps M.J., Kurz W.A. and Curry S.R. 1997. Comprehensive assessment of carbon stocks and fluxes in a boreal forest management unit. Can. J. Forest Research 27: 2005–2016.

Raulier F., Bernier P.Y. and Ung C-H. 2000. Modeling the influence of temperature on monthly gross primary productivity in a sugar maple stand. Tree Physiol. 20: 333-345.

Régnière J., Cooke B. and Bergeron V. 2001 BioSIM: A computer-based decision support tool for seasonal planning of pest management activities USER'S MANUAL. CFS-Quebec; Information Report LAU-X-116.

Régnière J. and St-Amant R. 2002. Statistical simulation of daily weather from normals: temperature, precipitation and solar radiation. Agric. Forest Meteorol. *in prep*.

Running S.W. and Coughlan J.C. 1988. A general model of forest ecosystem processes for regional applications, I. Hydrological balance, canopy gas exchange, and primary production processes. Ecol. Modelling 42: 125-154.

Running S.W. and Hunt E.R. 1993. Generalization of a forest ecosystem process model for other biomes, BIOME-BGC, and an application for global scale models. *In* J.R. Ehleringer and C.B. Field (eds.) Scaling Physiological Processes: Leaf to Globe. Academic Press, San Diego, pp. 141-158.

Ryan M.G. 1989. Sapwood volume for three subalpine conifers: predictive equations and ecological implications. Can. J. For. Res., 19: 1397-1401.

Ryan M.G. 1991. Effects of climate change on plant respiration. Ecological Applications 1: 157-167.

Ryan M.G. and Yoder B.Y. 1997. Hydraulic limits to tree height and tree growth. BioScience 47: 235-242.

Ryan T.P. 1997. Modern Regression Methods. John Wiley and Sons, Inc. 515 pp.

Sampson D.A. and Smith F.W. 1993. Influence of canopy architecture on light penetration in lodgepole pine (*Pinus contorta* var. *latifolia*) forests. Agric. For. Meteorol. 64: 63-79.

Schoettle A.W. 1994. Influence of tree size on shoot structure and physiology of *Pinus contorta* and *Pinus aristata*. Tree Physiol. 14: 1055-1068.

Sellers P.J., Hall F.G., Collatz G.J., Kelly R.D., Black A., Baldocchi D., Berry J., Ryan M., Ranson K.J., Crill P.M., Lettenmaier D.P., Margolis H., Cihlar J., Newcomer J., Fitzjarrald D., Jarvis P.G., Gower S.T., Halliwell D., Williams D., Goodison B., Wickland D.E. and Guertin F.E. 1997. BOREAS in 1997: Experiment overview, scientific results, and future directions. J. Geophys. Res. 102 (D24): 28731-28769.

Shinozaki K., Yoda K., Hozumi K. and Kira T. 1964. A quantitative analysis of plant form - the pipe model theory. I. Basic analyses. Jap. J. Ecol. 14(3): 97-105.

Shinozaki K., Yoda K., Hozumi K. and Kira T. 1964. A quantitative analysis of plant form - the pipe model theory. II. Further evidence of the theory and its application in forest ecology. Jap. J. Ecol. 14(3): 133-139.

Singh T. 1982. Biomass equations for ten major tree species of the Prairie provinces. Environ. Can., Can. For. Serv., North. For. Res. Cen., Edmonton, AB. Inf. Rep. NOR-X-242.

Singh, T. 1984. Biomass equations for six major tree species of the Northwest Territories. Environ. Can., Can. For. Serv., North. For. Res. Cen., Edmonton, AB. Inf. Rep. NOR-257.

Smith F.W. and Resh S.C. 1999. Age-related changes in production and below-ground carbon allocation in Pinus contorta forests. For. Sci. 45: 333-341.

Smith W.K. 1980. Importance of aerodynamic resistance to water use efficiency in three conifers under field conditions. Plant Physiol. 65: 132-135.

Steele S.J., Gower S.T., Vogel J.G. and Norman J.M. 1997. Root mass, net primary production and turnover in aspen, jack pine and black spruce forests in Saskatchewan and Manitoba, Canada. Tree Physiol. 17: 577-587.

Stump L.M. and Binkley D. 1993. Relationships between litter quality and nitrogen availability in Rocky Mountain forests. Can. J. For. Res. 23: 492-502.

Sykes M.T. and Prentice I.C. 1995. Boreal forest futures – modeling the controls on tree species range limits and transient responses to climate change. Water, Air, Soil Pollut. 82: 415-428.

Sykes M.T. and Prentice I.C. 1996. Climate change, tree species distributions and forest dynamics: A case study in the mixed conifer northern hardwoods zone of northern Europe. Clim. Change 34: 161-177.

Van Wagner C. 1978. Age-class distribution and the forest fire cycle. *Can. J. For. Res.* 8: 220–227.

Waring, R.H., Schroeder P.E. and Oren R.. 1982. Application of the pipe model theory to predict canopy leaf area. Can. J. For. Res. 12: 556-560.

Welles J. 1990. Some indirect methods of estimating canopy structure. *In* J. Norman and N. Goel (eds.) Instrumentation for Studying Vegetation Canopies for Remote Sensing in Optical and Thermal Infrared Regions. Harwood Academic Publishers GmbH, London. pp. 31-43.

White, J.D., Running S.W., Nemani R., Keane R.E. and Ryan K.C. 1997. Measurement and remote sensing of LAI in Rocky Mountain ecosystems. Can. J. For. Res. 27: 1714 – 1727.

Wood, J.W., Gillis M., Goodenough D.G., Hall R.J., Leckie D.G., Luther J.E. and Wulder M.A.. 2002. Earth observation for sustainable development of forests: project overview, Proceedings, International Geoscience and Remote Sensing Symposium (IGARSS ’02), Toronto, Ont. Canada.

This page intentionally blank.

Appendix I: EOSD Site Descriptions

I.1 Alberta Pilot Region (Foothills Model Forest)

The ECOLEAP-West pilot region in west-central Alberta covers about 2700 km^2, with corners located approximately at 53.38ºN, 116.50ºW, on the northeast and at 53.00ºN, 117.83ºW, on the southwest. This area is located within the Foothills Model Forest and lies immediately south of the town of Hinton (285 km west of Edmonton, and 85 km east of the Jasper townsite). Four ecoregions are represented: Upper Boreal-Cordilleran (or Upper Foothills), Lower Boreal-Cordilleran (Lower Foothills), Subalpine and Montane, comprising 68%, 21%, 10% and 1% of the total area, respectively. The terrain ranges from gently undulating to rolling moraines typical of the Lower Foothills to highly dissected, strongly rolling and hilly topography typical of the Upper Foothills. Elevations range from 1070 m asl in the east to 1725 m at the extreme west. The forest stands in this region are dominated by lodgepole pine (*Pinus contorta* Dougl. Var. *latifolia* Engelm.) and white spruce (*Picea glauca* (Moench) Voss). In the Lower Foothills, pure or mixed stands of trembling aspen (*Populus tremuloides* Michx.) and balsam poplar (*Populus balsamifera* L.) are interspersed with lodgepole pine and white spruce, respectively, while black spruce (*Picea mariana* (Mill.) B.S.P.) and tamarack (*Larix laricina* (Du Roi) K. Koch) dominate in poorly drained areas. Local Meteorological Service of Canada (MSC) weather stations are located at Jasper, Hinton, Edson and Robb. Data interpolated from 30-year MSC normals for 1961-1990 indicate mean monthly temperatures ranging from approximately –13.0 ºC (January) to +14.5 ºC (July). Total annual precipitation reaches 540 mm with yearly averages of around 385 mm rainfall and 155 mm snowfall. Average growing season is about 1050 growing degree days (5 ºC base), with about 740 during June, July and August. The study site was selected for its diversity in ecoregions, range of topography and the colocation of other study initiatives including the carbon stocks project, National Forest Inventory pilot project and pilot region for the Alberta Biodiversity Monitoring Program.

I.2 Saskatchewan Pilot Region (Prince Albert Model Forest, BERMS Study Area)

The ECOLEAP-West pilot region in Saskatchewan extends over some 6,000 km^2 with corners located approximately at 54.42 ºN, 104.55 ºW, on the northeast and at 53.7 ºN, 106.50 ºW, on the southwest. The region is located in central Saskatchewan, and includes much of the Prince Albert Model Forest, portions of Prince Albert National Park and the Weyerhaeuser forest management area as well as several of the Boreal Ecosystem Research and Monitoring Study (BERMS) surface flux-measurement sites. The southern boundary lies about 27 km north of Prince Albert. The area is located predominantly in the Mid-Boreal Upland ecoregion where physiography is characterized by rolling uplands and gently undulating plains formed from hummocky moraines at higher elevations on the uplands, and glaciofluvial deposits in the intervening plains. Elevations range from 380 to 850 m asl. Pure and mixed forest stands in this region are dominated by the following species: trembling aspen (*Populus tremuloides* Michx.), jack pine (*Pinus banksiana* Lamb.), black spruce (*Picea mariana* (Mill.) B.S.P.), white spruce (*Picea glauca* (Moench) Voss), and balsam poplar (*Populus balsamifera* L.) in order of dominance. White birch (*Betula papyrifera* Marsh.) and balsam fir (*Abies balsamea* (L.) Mill.) are also present, but not abundant. Meteorological Service of Canada (MSC) weather stations are located at Waskesiu Lake, Northside and Snowden as well as at Prince Albert. Data interpolated from 30-year MSC normals for 1961-1990 indicate mean monthly temperatures ranging from approximately –21.4 ºC (January) to +16.7.0 ºC (July). Total annual precipitation can reach 450 mm with approximately 310 mm rainfall and 140 mm snowfall. Average growing season heat

sum is about 1350 growing degree days (5 ºC base), with about 970 during June, July and August. The study site was selected for the significance and size of this ecoregion in Saskatchewan and the location of the BERMS sites.

Appendix II: Database Description and Metadata

II.1 Introduction

Metadata is information that characterizes data, and is used to provide documentation for data products (Federal Geographic Data Committee (FGDC) 2000; United States Geological Survey (USGS) 2002). Some typical examples of metadata include: documenting the purpose of the data, the names of the creator and the distributor, and spatial referencing, i.e., map projection, and coordinate system.

Continued documentation of both spatial and non-spatial metadata is extremely important, because digital data archives are becoming both increasingly common and increasingly large. Other benefits of metadata include facilitation of technical support; making data accessible to a wider community, data browsing, and data transfer. Metadata help users make informed decisions about data suitability and quality (Hart and Phillips 2002). Good metadata practices also help to reduce the risk of losing knowledge contained in the data when the creators or developers of the dataset retire, move or die (Hart and Phillips 2002).

To date, the following steps have been taken in the development of a data and metadata archive for the ECOLEAP-West study:

1. Assessment of standards for metadata definition and documentation
2. Assessment of available tools for spatial and non-spatial metadata creation
3. Creation of an ECOLEAP-West data archive
4. Metadata creation for a portion of the spatial and non-spatial data layers

II.2 FGDC Metadata Standard

The *Content Standard for Digital Geospatial Metadata* (CSDGM) is a metadata standard developed by the FGDC to "provide a common set of terminology and definitions for the documentation of digital geospatial data" (see http://www.fgdc.gov/metadata/contstan.html). This standard has been widely adopted for geospatial metadata creation and is being used for ECOLEAP-West.

II.3 Metadata Tools

Numerous tools are available for creation and documentation of geospatial metadata. In researching the available tools, several criteria were identified for choosing the tool most suitable for ECOLEAP-West data sets.

- Is it straightforward to use?
- Are the full range of metadata descriptors incorporated in the tool?
- Does it support different operating platforms?
- Is it FGDC-compliant?
- Does it create any metadata automatically?
- Will it be continually improved/updated?
- Does it have user support/help?
- Do we currently have it available?

The metadata tools examined were:

- *Spatial Metadata Management System* (SMSS)
- *Tkme* 2.8.15 (USGS)

- *Corpsmet95* v.1.3
- *MP* (USGS)
- *MetaLite* 1.7.5 (EROS Data Centre)
- *DataLogr*
- *ArcCatalog*

ArcCatalog was the preferred choice because it was readily available as part of *ArcGIS* 8.1—the Canadian Forest Service's standard GIS software, and has been used extensively for ECOLEAP-West spatial data analysis. Further, *ArcCatalog* automatically creates a portion of the metadata because it is already linked with the spatial dataset in the GIS. This makes metadata creation more consistent and less time-consuming. All the remaining metadata tools required "data-entry", with no automatic metadata creation capability.

ArcCatalog provides a metadata editor that adheres to the necessary FGDC standard guidelines. Using *ArcCatalog*, metadata can meet basic FGDC compliance simply by completing "required" FGDC fields, which are highlighted in red in the metadata template (**Figure II.1**).

The most important feature is the automatic association of metadata with all geographic datasets. *ArcCatalog* has been designed to create metadata for any dataset supported by *ArcInfo*, as well as any other dataset identified and catalogued by the user (e.g. text, CAD files, scripts, images). Within the *ArcCatalog* environment, two types of metadata are distinguished. These are *inherent properties* and *documentation*. Inherent *properties* are metadata that can be generated automatically from the data. Examples of inherent metadata are: dataset name, the number of objects it contains, feature types and attributes, the geographic extent and the projection. Documentation is descriptive metadata, to be provided by the user, including items such as names of individuals (or organizations) who collected the data, quality assessments and information on data retrieval. The metadata are stored with the spatial data as XML documents, which travel with the data if the coverage is moved or copied elsewhere. Users can view the metadata in any XML-aware environment.

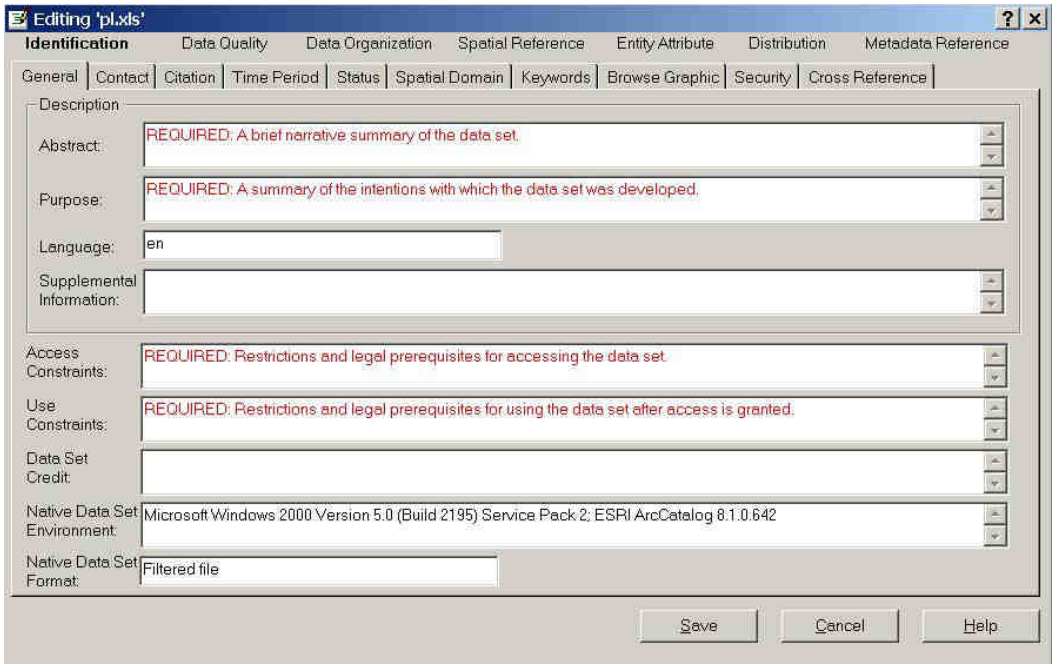

Figure II.1 *ArcCatalog* input screen: required FGDC metadata inputs are highlighted in red to ensure that minimum metadata standards are properly met.

ArcCatalog is also being used to create metadata for (mainly non-spatial) data external to the *ArcInfo* GIS, including spreadsheets, *Access* databases, images, *PowerPoint* presentations, and word processing documents. Currently, there is no commonly accepted standard for non-spatial data. To maintain consistency and ease of use, therefore, the FGDC standard has also been adopted for non-spatial data. Therefore, some spatial fields will remain blank for these data (e.g., coordinate system information).

One metadata file will be created for each group of related, non-spatial datasets or files.

II.4 Ecoleap West Data Archive

A database has been established to organize all the data obtained and developed for the ECOLEAP-West project (Figure II.2), including spatial and non-spatial data for both the Alberta and Saskatchewan Study Areas.

Currently, the "Work Files" directory contains data, graphics, presentations, etc. for ECOLEAP-West sub-projects that are in progress or undergoing modification. When a given file or dataset is finalized, it is copied into an appropriate folder in the "Incoming" directory and metadata are created. These files or datasets are then reviewed for consistency by a data coordinator, responsible for maintenance of the project data archive. Once approved, the data are added to the "Archive" directory where they can be accessed with read-only privileges by the ECOLEAP-West team members. The "Archive" directory is similar in organization to the "Incoming" directory, but is further subdivided into folders for the various sub-projects and components of ECOLEAP-West (Figure II.2). Once the datasets are finalized, the intention is to make selected parts of the archive available for public use on CD-ROM and/or via a CFS website.

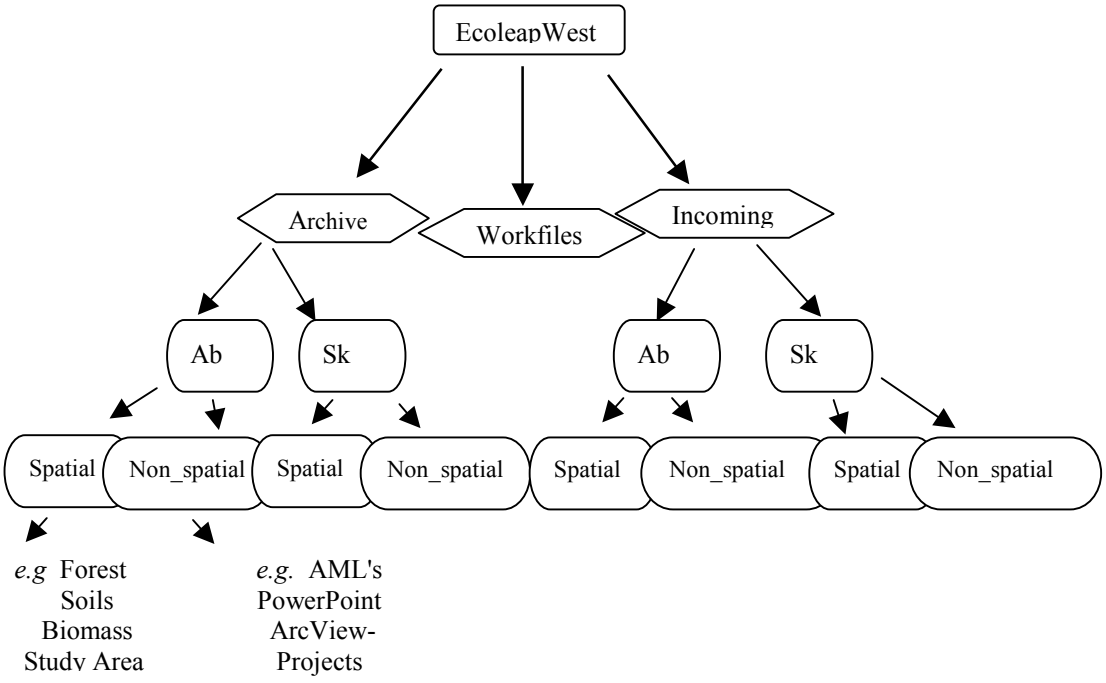

Figure II.2 The structure of the Ecoleap West digital data archive.

II.5 Current and Future Tasks

To date, approximately 70 % of the spatial and non-spatial data has been archived with appropriate metadata. The intent is to finalise the data archive by 31 December 2002.

II.6 References

Federal Geographic Data Committee (FGDC). 2000. Content Standard for Digital Geospatial Metadata Workbook Version 2.0. Federal Geographic Data Committee. Washington, D.C.

Hart D. and Phillips H. April, 2002. Metadata primer – A "how to" guide on metadata implementation. NSGIC website: http://www.lic.wisc.edu/metadata/metaprim.htm

United States Geological Survey. 2002. Tools for the creation of formal metadata - frequently asked questions on FGDC metadata. USGS website: http://geology.usgs.gov/tools/metadata/tools/doc/faq.html#1.1 February 15, 2002.

Appendix III: Outline Approach to Spatial Modelling of Soil Physical Properties

III.1 Problem statement

The major objective of ECOLEAP-West is to be able to apply process models of forest productivity and succession over extensive regions. In order for process models to succeed, they necessarily require spatial data sets that capture the important environmental constraints on the processes being simulated. For terrestrial ecosystems in general, and for forests in particular, a major source of spatial variability—probably the single most important factor—is soils. The problem, of course, is that the same spatial variability that imposes significant variation in forest productivity and species competition, is also singularly difficult to map, either by field work alone or in combination with aerial photography or some other form of remote sensing.

For spatial application, many process-based ecosystem models require a range of spatial input layers, typically including soil depth and often some horizon-based texture classification. These properties (often defined as soil water holding capacity) are critical determinants of soil moisture regime, and hence influence availability of water and nutrients to plants, as well as the thermal environment that strongly affects respiration rates of roots and microbes

In the initial stages of the ECOLEAP-West modelling effort, a digitized version of the local soil survey map prepared by Dumanski et al. (1972) was obtained from Weldwood. This map was used extensively in classifying ecotypes and to allocate modal soil characteristics to relatively large polygons. Like many digital soil maps, it presents broad-level interpretations of geology, climate, vegetation, and topography, reflecting only generalized soil property information extrapolated over a relatively large area. It is not based on detailed soil profile data and does not present small scale (stand-level) variations in physical properties. While such soil maps are useful as indicators of overall forest growth potential, they contain only minimal, coarse-resolution soil property data that are generally unsatisfactory as input to stand-level process-based models.

The initial results of spatial productivity modelling for the Alberta study region using StandLEAP were contrary to both the experience of people familiar with the area and contrary to our estimates derived directly from the Alberta Vegetation Inventory (AVI) (see report Section 4.4.1). The most likely explanation for this is that deeper and finer textured soils are more prevalent in the eastern part of the study area—improving moisture and nutrient availability compared to the western end, which lies in the shallow coarse soils and screes of the eastern slopes of the Rocky Mountains. This general distribution of soil texture and depth across the study area was not available to StandLEAP from the soils data set, and hence caused it to fail.

While it is clear that more accurate maps of soil physical properties, ideally plotted at a stand-level resolution (~ 1:10,000 map scale), are required, it is much less clear how to achieve this. We are developing a research project to investigate the possibility of using available soil profile data and the existing digital data sets for the Alberta study area to model profile distributions from statistical relationships observed at the profile locations. We hope that if successful, the approach can be extended to other regions where profile data are lacking. The objectives of this report are to:

(1) suggest an approach for modelling select soil properties;
(2) describe available datasets;
(3) present an overview of progress to date and anticipated future outcomes.

III.2 Approach

At a given location, a soil's development and its related soil properties, both chemical and physical, are largely influenced by six main driving factors: climate, geology, topography, vegetation, disturbance, and time (Jenny 1980, Gerrard 1981).

Although interrelationships among soils and driving factors are complex, results from recent soil-landscape modelling studies indicate that a substantial amount of spatial variability in soil properties can be accounted for using statistical models that correlate point-specific soil measurements to independent environmental data sampled at those points (e.g. Moore et al. 1993; Bell et al. 1994; Skidmore et al. 1996; Ryan et al. 2000). Maps produced from such modelling efforts are often far more accurate than traditional soil maps (Bell et al. 1994; McKenzie and Ryan 1999). These empirical models are also explicitly quantitative, providing new and useful knowledge about soil-landscape processes and allowing for better portability to other landscapes.

The ability to accurately model and map soils across a given landscape will therefore depend on the availability, scale, accuracy, and spatial extent of both the soil property data and the environmental data known to drive the distribution of these properties. Ryan et al. (2000) point out that datasets used in soils modelling are usually of contrasting scales, from fine (soil horizon attributes) to coarse (local climate/geology), making the identification and scaling-up of predictive relationships difficult. However, employing combinations of environmental predictors at varying scales increases the probability that the most influential driving factors will be identified.

In this study, we will explore the development of statistical models to predict the distribution of several crucial soil properties using a range of environmental correlates. The soil properties of greatest interest are (but not limited to) soil depth and soil texture since these have the largest impact on soil water availability and nutrient status. It should also be possible to predict the occurrence of wetland areas based on stream-flows and the existence of "basins" in the DEM data, although the net accumulation of peat will require additional information and more sophisticated models. In general, this modelling effort will involve: the collation and organization of available soils data; identification, creation, and/or organization of other environmental data layers, many of which we have already acquired; and statistical modelling using a number of techniques. Most importantly, some soil profiles must be selected at random and withheld from the data set used to develop the models. These profiles will then be used as a validation data set, to allow a rigorous statistical assessment of model error.

III.3 Available datasets

Approximately 4,500 soil sample plots are available from four main databases, covering a large geographical extent (**Figure III.1**). Although a large proportion of plots fall outside the ECOLEAP-West study area, they still fall largely within the limits of the Lower and Upper Foothills natural subregions, which are the major subregions within the study area.

The four available soils datasets are the Weldwood PGS plot, ESIS, MSE, and Pluth databases, described below. **Table III.1** provides an overview of the soil attributes contained in each dataset.

ESIS (Ecological Site Information System) Database

This database comprises approximately 670 plots with a complete range of descriptive soil attributes (**Table III.1**). This dataset is derived from sampling efforts carried out from the mid-1970s to early 1990s, ostensibly used in the creation of the Ecological Classification manuals for Alberta. The Ecological Land Survey Site Description Manual (Alberta Environmental Protection, 1994) outlines the sampling methodologies used in ESIS data collection, in addition to describing the data collected.

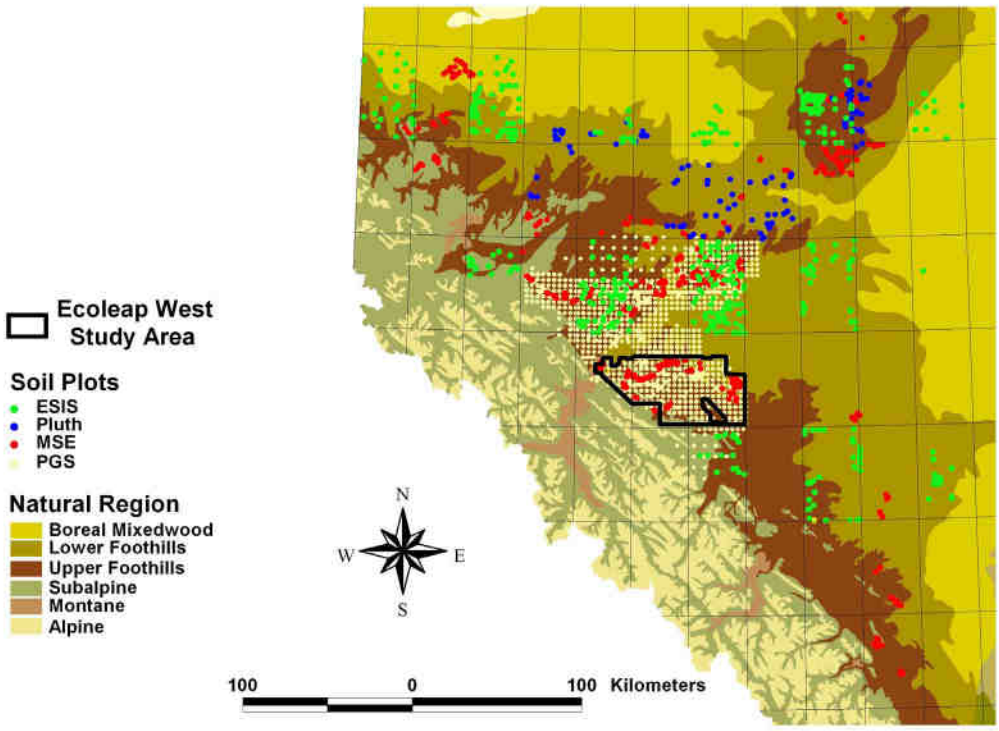

Figure III.1 Distribution of soil profile data available for use in the ECOLEAP-West soils modelling study.

Weldwood PGS plot Database

Comprising approximately 3,200 permanent growth sample plots (PGS plot), this dataset contains vegetation, tree mensuration, and ecological attributes including soils information. The ecological data table within the database contains data collected as part of an ecological site classification for the sample plots and contains a range of descriptive soils information based on ESIS sampling methodologies. These soils data are therefore somewhat subjective and in particular, lack detailed information on soil texture.

MSE (Managed Stand Ecosites) Database

This database contains data for 485 plots, established during 1996-1998, used to create a ecological classification field manual for stands, less than forty years of age, regenerated following clear-cutting. As an extension of previous ecological classification work in Alberta, the types of data collected and the methodology of field collection are comparable to those available from the ESIS dataset.

Pluth Database

This dataset, obtained from D. Pluth of the University of Alberta, contains soils and vegetation data for 152 sample plots. Data were collected during 1984/85 as part of study examining plant community classification and forest site quality (La Roi et al., 1988).

Table III.1 Attributes of the four available soil profile databases.

		Dataset name			
Data type	**Attribute**	**PGS plot**	**ESIS**	**MSE**	**Pluth**
Soil Profile	Horizon Soil Classification	Y	Y	Y	Y
	Horizon Texture Class	Y	Y	Y	Y
	Horizon Particle Sizes	N	N	N	Y
	Horizon Coarse Fragments	Y	Y	Y	Y
	Horizon Boundary	Y	Y	Y	Y
	Horizon Thickness	Y	Y	Y	Y
	Effective Rooting Depth	Y	Y	Y	Y
	Soil Structure	N	Y	Y	Y
	Humus Form	Y	Partial	Y	N
	Soil Colour Data	N	Y	Y	Y
	Mottle Description	N	Y	Y	Y
	Depth to Mottles	Y	Y	N	Y
	Depth to Water Table	Y	Y	Y	N
	Depth to Bedrock	Y	Y	Y	N
	Depth to Carbonates	Y	Y	Y	N
Site/Plot	Location	GPS (Deg/Min/Sec)	Map (Deg/Min)	GPS (Deg/Min/Sec)	Map (Deg/Min)
	Parent Material	N	Y	Partial	Y
	Surface Expression	Y	Y	Y	Y
	Elevation	N	Y	N	Y
	Slope Position	Y	Y	Y	
	Slope Gradient (%)	Y	Y	Y	Y
	Aspect	Y	Y	Y	Y
	Natural Region	AB Natural Subregions	AB Natural Subregions	AB Natural Subregions	Bioclimatic Zones
	Ecosite Designation	Y	Y	Y	
	Soil Moisture Regime	Y	Y	Y	Y
	Soil Nutrient Regime	Y	Y	Y	Y
	Drainage Class	N	Y	Y	Y
Chemical/ Physical	Soil Nutrients	N	N	N	Partial
	Soil Carbon	N	N	N	Y
	Bulk Density	N	N	N	Y
	pH	N	Partial	Y	Y
Vegetation	Overstory Description	Y	Y	Y	Y
	Understory Description	Y	Y	Y	Y

Environmental Correlate Data

Raster-based Digital Elevation Models (DEM) within a GIS will be employed in this study to automatically derive a range of terrain-related variables that aim to characterize dominant processes, including those related to geomorphology (e.g., elevation, slope gradient, aspect, slope plan curvature, slope profile curvature, erosion index). In addition, digital elevation data will be used with the available information on climatology (see Section 4.3 of this report) and hydrology (e.g., upslope drainage area, compound wetness index). The resolution of these attributes will directly reflect the resolution of the DEM, which is being created from 1:50,000 NTS digital map-sheet data. The resultant pixel resolution is estimated to be between 50 and 100 metres. Additionally, digital spatial data on climate normals, bedrock geology, soil parent material, and dominant vegetation cover will be used to supplement terrain-based environmental predictors. These spatial layers will be sampled to obtain correlate values for each soil sample location to use in statistical modelling.

III.4 Statistical modelling, and validation

The four combined datasets will be combined and 70% of the randomly-selected plots used in development of statistical models. The remaining 30% will be used for model validation.

The majority of the soils and site data are categorical (i.e., discontinuous), mainly because they are based on qualitative soil pit and site descriptions. For example, soils in each profile horizon have been assigned a soil texture class based on several "feel" tests performed in the field. Although the approximate fractions of sand, silt and clay are implicit in each texture class, the data are nonetheless categorical and must be treated as such statistically. Several statistical analysis techniques that can use categorical data, such as logistic regression, regression trees, and neural network analyses, will be explored.

The most difficult challenge in this study will be to determine the optimal environmental predictor variables that may account for variation in fine-scale soil property distributions. Natural subregion, bedrock geology, soil parent material, and/or vegetation cover type are broad variables that strongly influence or reflect spatial soil pattern. Hence, initial stratification of the landscape by these factors will be carried out to attempt to reduce overall spatial variability in the soils data.

Soil property predictions using the developed models will then be tested against the independent validation data set to determine overall model prediction accuracy.

III.5 Progress

To date, the following steps have been achieved:

- collation and organisation of soil datasets into a coherent and usable modelling database
- research of methods for creation of DEMs from available digital (NTDB) 1:50,000 contour mapsheets
- research of methods for creation of required terrain indices from DEM
- creation of climate surfaces to derive climate predictors

We will be working to finish the creation of DEMs and derived indices during August, 2002. Additionally, we are hoping to obtain bedrock and surficial geology maps from the Alberta Geological Survey. Subsequently, we will proceed with statistical modelling and validation in early Autumn, 2002.

III.6 References

Alberta Environmental Protection. 1994. Ecological Land Survey Site Description Manual. Finance, Land Information and Program Support Services, Resource Information Division, Edmonton, AB, Canada.

Bell, J.C., R.L. Cunningham, and M.W. Havens. 1994. Soil drainage class probability mapping using a soil-landscape model. Soil Sci. Soc. Am. J. 58: 464-470.

Dumanski, J., Macyk, T.M., Veauvy, C.F., and J.D. Lindsay. 1972. Soil survey and land evaluation of the Hinton-Edson area, Alberta. Alberta Soil Survey Report No. S-72-31. Alberta Institute of Pedology, Research Council of Alberta.

Gerrard, A.J. 1981. Soils and landforms: an integration of geomorphology and pedology. George Allen and Unwin Publishers Ltd., London, U.K. 219 pages.

Jenny, H. 1980. The soil resource: origin and behaviour. Ecol. Stud. 37. Springer-Verlag, New York.

La Roi, G.H., W.L. Strong, and D.J. Pluth. 1988. Understory plant community classifications as predictors of forest site quality for lodgepole pine and white spruce in west-central Alberta. Can. J. For. Res. 18: 875-887.

McKenzie N.J. and P.J. Ryan. 1999. Spatial prediction of soil properties using environmental correlation. Geoderma. 89: 67-94.

Moore, I.D., P.E. Gessler, G.A. Nielsen, and G.A. Petereson. 1993. Soil attribute prediction using terrain analysis. Soil Sci. Am. J. 57: 443-452.

Ryan, P.J., N.J. McKenzie, D. O'Connell, A.N. Loughhead, P.M. Leppert, D. Jacquier, and L. Ashton. 2000. Integrating forest soils information across scales: spatial prediction of soil properties under Australian forests. For. Ecol. Manage. 138: 139-157.

Skidmore, A.K., F. Watford, P. Luckananurug and P.J. Ryan. 1996. An operational GIS expert system for mapping forest soils. Photo. Eng. Remote Sens. 62: 501-511.